



Application of organic petrography in North American shale petroleum systems: A review



Paul C. Hackley^a, Brian J. Cardott^b

^a U.S. Geological Survey, MS 956 National Center, 12201 Sunrise Valley Dr, Reston, VA 20192, USA

^b Oklahoma Geological Survey, 100 E. Boyd St., Rm. N-131, Norman, OK 73019-0628, USA

ARTICLE INFO

Article history:

Received 13 April 2016

Received in revised form 10 June 2016

Accepted 13 June 2016

Available online 16 June 2016

Keywords:

Organic petrology

Thermal maturity

Shale petroleum systems

Unconventional resources

Vitrinite reflectance

Shale gas

Tight oil

Solid bitumen

ABSTRACT

Organic petrography via incident light microscopy has broad application to shale petroleum systems, including delineation of thermal maturity windows and determination of organo-facies. Incident light microscopy allows practitioners the ability to identify various types of organic components and demonstrates that solid bitumen is the dominant organic matter occurring in shale plays of peak oil and gas window thermal maturity, whereas oil-prone Type I/II kerogens have converted to hydrocarbons and are not present. High magnification SEM observation of an interconnected organic porosity occurring in the solid bitumen of thermally mature shale reservoirs has enabled major advances in our understanding of hydrocarbon migration and storage in shale, but suffers from inability to confirm the type of organic matter present. Herein we review organic petrography applications in the North American shale plays through discussion of incident light photographic examples. In the first part of the manuscript we provide basic practical information on the measurement of organic reflectance and outline fluorescence microscopy and other petrographic approaches to the determination of thermal maturity. In the second half of the paper we discuss applications of organic petrography and SEM in all of the major shale petroleum systems in North America including tight oil plays such as the Bakken, Eagle Ford and Niobrara, and shale gas and condensate plays including the Barnett, Duvernay, Haynesville–Bossier, Marcellus, Utica, and Woodford, among others. Our review suggests systematic research employing correlative high resolution imaging techniques and in situ geochemical probing is needed to better document hydrocarbon storage, migration and wettability properties of solid bitumen at the pressure and temperature conditions of shale reservoirs.

Published by Elsevier B.V. This is an open access article under the CC BY license (<http://creativecommons.org/licenses/by/4.0/>).

Contents

1.	Introduction	9
2.	Measurement of vitrinite reflectance	13
2.1.	Microscope systems — state-of-the-art	14
2.2.	Advantages of vitrinite reflectance measurement	14
2.3.	Sources of error in reflectance analysis of shales	14
2.4.	Atypical reflectance values.	16
3.	Scanning electron microscopy (SEM) of organic matter in shale	16
4.	Secondary optical thermal maturity parameters	18
4.1.	Fluorescence	18
4.2.	Thermal alteration index (TAI)	18
4.3.	Conodont alteration index (CAI)	19
4.4.	Reflectance of other macerals	19
4.4.1.	Inertinite vs. vitrinite	19
4.4.2.	Solid bitumen reflectance	19
4.4.3.	Zooecial reflectance.	20
4.5.	Comparison to geochemical thermal maturity parameters	20
5.	North American shale petroleum systems	21
5.1.	Tight oil	24

E-mail addresses: phackley@usgs.gov (P.C. Hackley), bcardott@ou.edu (B.J. Cardott).

<http://dx.doi.org/10.1016/j.coal.2016.06.010>

0166-5162/Published by Elsevier B.V. This is an open access article under the CC BY license (<http://creativecommons.org/licenses/by/4.0/>).

5.1.1.	Bakken Formation	24
5.1.2.	Eagle Ford Formation.	27
5.1.3.	Niobrara Formation	29
5.1.4.	Tuscaloosa marine shale	29
5.1.5.	Other tight oil systems	30
5.2.	Shale condensate and dry gas	32
5.2.1.	Barnett Shale	32
5.2.2.	Duvernay Formation	35
5.2.3.	Haynesville-Bossier formations	36
5.2.4.	Marcellus Formation	37
5.2.5.	Utica Shale	39
5.2.6.	Woodford Shale	40
5.2.7.	Other shale gas systems	41
6.	Summary and conclusions.	43
	Acknowledgements	44
	References	44

1. Introduction

The importance of shale petroleum systems in North America cannot be understated, where the Bakken and Eagle Ford tight oil fields and the Marcellus, Barnett and Haynesville shale gas fields rank among the largest in proved reserves (Energy Information Administration, 2015a). Hydrocarbon production from these and other ‘tight’ petroleum systems (Fig. 1) discussed herein is responsible for the ranking of the United States as the world’s leading producer of oil and gas since 2013 (Energy Information Administration, 2015b), and has impacted every sector of the energy industry (Bazilian et al., 2014). This recent growth in shale hydrocarbon production has resulted in numerous technical publications on the petroleum geology of shale (e.g., Breyer, 2012; Chatellier and Jarvie, 2013; Rezaee, 2015; Ma and Holditch, 2015), launch of new trade magazines (e.g., *Unconventional Oil & Gas Report*), research journals (e.g., *Journal of Unconventional Oil and Gas Resources*), and technical conferences (e.g., *Unconventional Resources Technology Conference*), and has provided the motivation for development of this review paper as a resource to those seeking information on organic petrology of the North American shale plays.

In keeping with its widely acknowledged position as the most common sedimentary rock, shale is widespread in the energy basins of North America and is present throughout the stratigraphic column. Fig. 2 relates the spatial and temporal distribution of current shale development in the widely dispersed basins of the United States and Canada. For example, in the Appalachian foreland basin, shale activity

primarily occurs in the Ordovician Utica Shale and Devonian Marcellus Formation. In the Gulf Coast passive margin basin, hydrocarbons are produced from shales in the Upper Cretaceous Eagle Ford and Jurassic Haynesville-Bossier Formations, among others. The Upper Devonian-Mississippian Bakken Formation tight oil play is developed in the Williston intracratonic sag basin which straddles the United States-Canada border. Although not currently developed, industry has tested unconventional development in the Miocene Monterey Formation in the forearc-transform basins of southern California. In this manuscript, we will discuss applications of organic petrography in these and other shale plays.

Organic petrography is widely regarded as the study of solid organic matter in sedimentary rocks mainly via incident light microscopy (Suárez-Ruiz et al., 2012), and has long been the domain of coal petrographers. However, the advent of the ‘shale revolution’ in North America since about 2005 has shifted primary focus of organic petrology in many laboratories to ‘tight’ clastic and carbonate hydrocarbon source rocks which have retained some proportion of their generated hydrocarbons, and petrographers have adopted their skills and knowledge to working in this arena. Determination of thermal maturity in shale petroleum systems is critical to hydrocarbon prospecting and the petrographic approach of vitrinite reflectance (symbolized R_o herein) generally is regarded as the most robust analytical approach to maturity determination (Hackley et al., 2015). Therefore, reflectance analysis is a primary effort for shale organic petrography and will be described in detail herein. Determination of organic facies is equally important to shale

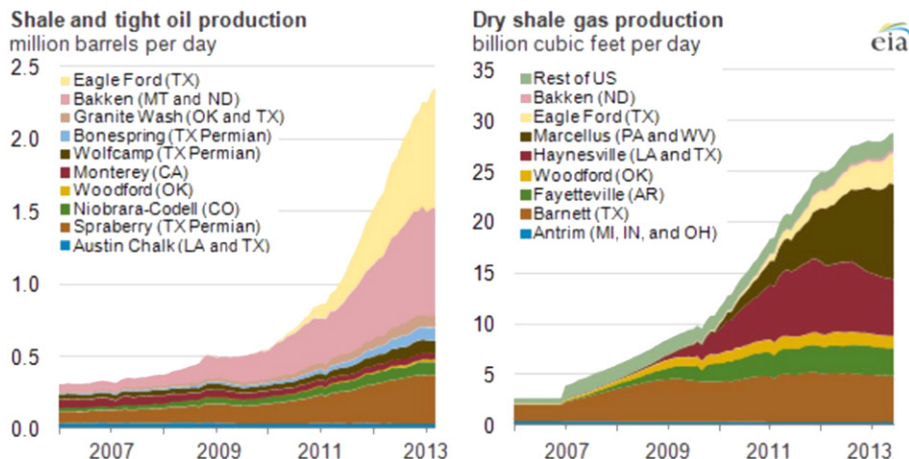


Fig. 1. Plots of shale and tight oil production and shale gas production, 2006–2013. (Source: From Energy Information Administration (2013)).

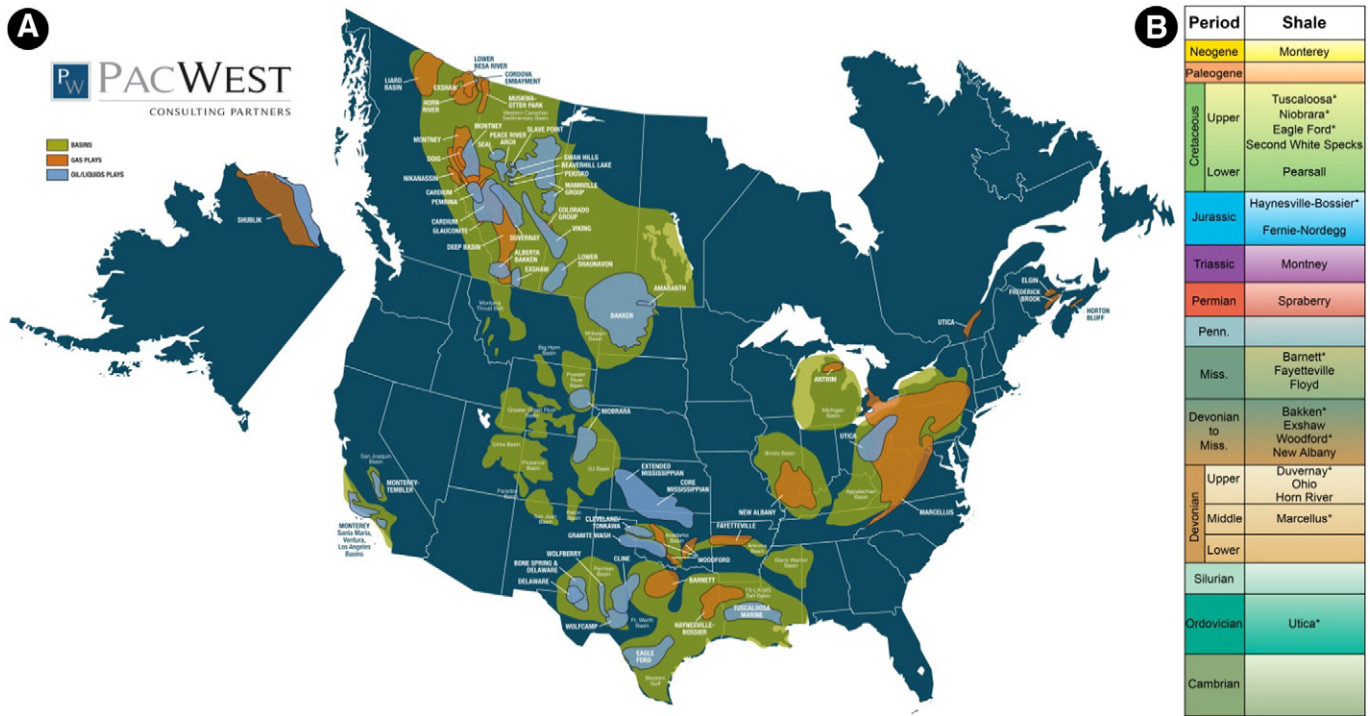


Fig. 2. A. Map of North American shale plays. From PacWest Consulting Partners (2016). B. Stratigraphic column showing relative ages of shale plays discussed in the text. Units marked with an asterisk are presented in detail. (Source: A is reproduced with permission of Nilesh Daval, PacWest Consulting Partners and IHS Energy).

petroleum system evaluation (e.g., Tyson, 1995; Ercegovac and Kostić, 2006) and petrographic approaches are complementary and sometimes superior to bulk analyses for geochemical screening, [i.e., the organic petrography tells what the total organic carbon (TOC) and kerogen type determined from programmed pyrolysis consists of, e.g., the relative proportions of oil-prone, gas-prone or inert kerogen and/or solid bitumen]. As will be seen below, organic petrography reveals that solid bitumen is the dominant organic constituent of most thermally mature (postpeak oil generation) North American shale plays. Here, we provide

practical information on organic petrography methods and the determination of shale thermal maturity through reflectance analysis, and review organic petrology applications in most of the major North American shale plays, including the recent development of scanning electron microscopy (SEM) as a complement to standard optical microscopy (e.g., Camp et al., 2013). We also provide photomicrograph examples of typical organic matter in North American shales (listed in Table 1), based on work by U.S. Geological Survey (USGS) to develop an online atlas of organic matter in shale (Valentine et al., 2013; and

Table 1
Samples imaged in this study.

USGS sample ID	Formation	Age	Location	County	Sample type	Collector
111211-1	Woodford	Devonian-Mississippian	Oklahoma	Carter Co., OK	Outcrop	Mike Lewan, USGS ret.
1-23-49-25W4 5882'	Duvernay	Devonian	Alberta	Alberta, Canada	Core	Raphael Wüst, Trican
6-14-37-7W5 11955'	Duvernay	Devonian	Alberta	Alberta, Canada	Core	Raphael Wüst, Trican
Clarion resources 1-20 Fleckton 7652'	Bakken (Upper)	Devonian-Mississippian	North Dakota	Ward Co., ND	Core	Paul Hackley, USGS
Whiting BN 1-23H 10353.1'	Bakken (Upper)	Devonian-Mississippian	North Dakota	Billings Co., ND	Core	Terry Huber, USGS
Amoco No. 1 Rebecca K. Bounds 591'	Niobrara (Smoky Hill Chalk)	Upper Cretaceous	Kansas	Greeley Co., KS	Core	Paul Hackley, USGS
Cemex 3	Niobrara B	Upper Cretaceous	Colorado	Boulder Co., CO	Outcrop	Paul Hackley, USGS
Monterey KG-17	Monterey	Miocene	California	Santa Barbara Co., CA	Outcrop	Paul Lillis, USGS
Chevron Prudential 1-A 1435.8'	Utica	Ordovician	Ohio	Marion Co., OH	Core	Matt Erenpreiss, OGS
Houston Oil & Minerals Walker D-1-1 1256'	Barnett	Mississippian	Texas	San Saba Co., TX	Core	James Donnelly, BEG
Blakeley No. 1 7223'	Barnett	Mississippian	Texas	Wise Co., TX	Core	James Donnelly, BEG
RTC 1 13,027'	Woodford	Devonian-Mississippian	Texas	Pecos Co., TX	Core	Stephen Ruppel, BEG
Shell 1 Leppard 13,671'	Eagle Ford	Upper Cretaceous	Texas	Bee Co., TX	Core	Stephen Ruppel, BEG
WT-1	Skull Creek	Lower Cretaceous	Colorado	Jefferson Co., CO	Outcrop	Dan Jarvie, WWG
Samedan No. 2 C.W. Andrews 11,068'	Tuscaloosa marine shale	Upper Cretaceous	Mississippi	Amite Co., MS	Core	Paul Hackley, USGS
BP A-8H T.W. George 11,366-11,366.2'	Haynesville	Jurassic	Texas	Harrison Co., TX	Core	James Donnelly, BEG
IN-08-06B	New Albany (Clegg Creek)	Devonian-Mississippian	Indiana	Clark Co., IN	Outcrop	Peter Warwick, USGS
OH-4 Core 2839 1342-1343'	Marcellus	Devonian	Ohio	Ashtabula Co., OH	Core	Bob Ryder, USGS ret.
WV-6 MERC No. 1 7440.7'	Marcellus	Devonian	WV	Monongalia Co., WV	Core	John Repetski, USGS

see <http://energy.usgs.gov/Coal/OrganicPetrology/PhotomicrographAtlas.aspx>.

Solid bitumen is the term organic petrographers use to describe an organic maceral representing the secondary product of hydrocarbon generation from kerogen (pre-oil solid bitumen terminology in genetic classification of Curiale, 1986). This term does not correspond exactly to the geochemist’s definition of bitumen, which is the organic material removed from rock samples by typical organic solvents such as pentane or dichloromethane (e.g., Durand, 1980; Vandembroucke and Largeau, 2007). Nevertheless, the terms describe the same material in part, for what is extractable from thermally mature (peak oil window and beyond) shales by organic solvents primarily is extracted from solid bitumen. Fig. 3A relates a conceptual model showing that the dominant petrographically observable organic matter occurring (present-day) in

thermally mature shales is solid bitumen (although partly insoluble), from which the extractable organic matter (the geochemist’s bitumen) is sourced. In thermally mature and postmature shale systems, such as the Barnett Shale of Texas, the dominant organic matter visible to organic petrographers is solid bitumen (Fig. 3B). Pre- and post-Soxhlet extraction programmed pyrolysis S1 values (Han et al., 2015) on aliquots of the same thermally mature Barnett Shale sample (Fig. 3C) confirm that the extractable organic material is sourced from the solid bitumen identified by organic petrographers. Similar reductions were observed in S2 and TOC contents. Petrographic comparison of pre- and post-extracted samples reveals little visible change in solid bitumen via optical microscopy; however, the maximum resolutions available to optical microscopy (generally 400–1500×) may be insufficient to detect major physical changes. Recent work by Reeder et al. (2016) used correlative

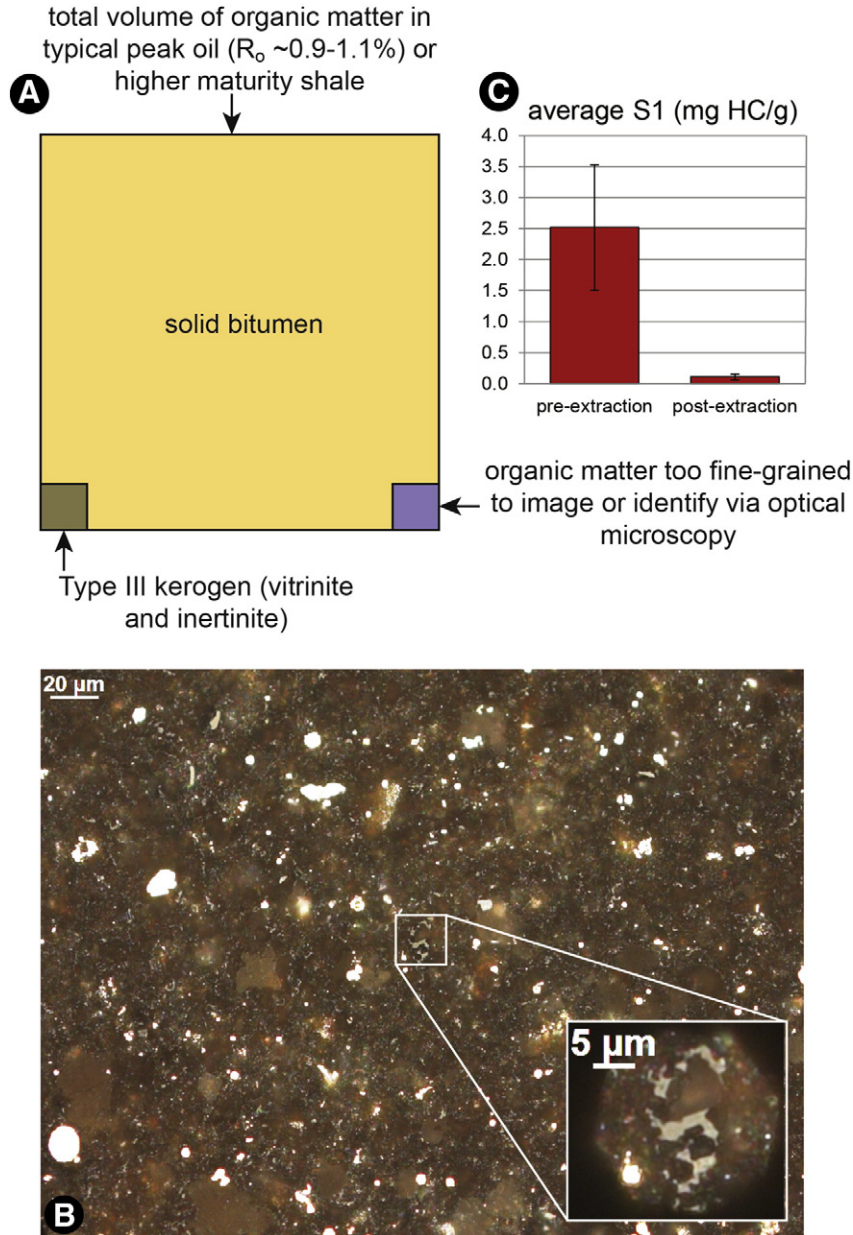


Fig. 3. A. Conceptual representation of petrographically observable organic matter in thermally mature shale showing relative proportions of organic matter types. Oil-prone Type I/II organic matter (algal material and bacterial biomass) is converted to hydrocarbons and not present as kerogen in thermally mature shales (although some of the heavier conversion products presumably are retained in solid bitumen). Refractory Type III/IV kerogens (vitrinite and inertinite) are retained with little change but represent only a small portion of the total organic matter, which is dominated by solid bitumen. A portion of the organic matter labeled ‘organic matter too fine-grained to image or identify via optical microscopy’ may be liquid or gaseous hydrocarbons. B. Thermally mature (~1.54% R_o) organic-rich (~3.0 wt.% TOC) Barnett Shale showing a network of solid bitumen which constitutes the dominant organic matter. C. Removal of some soluble solid bitumen from thermally mature (~1.0% R_o) Barnett Shale as documented via pre- and post-extraction S1 values from pyrolysis (data from Han et al., 2015). Similar reductions were observed in S2 values and TOC content.

SEM imaging of the same location on a pre- and post-extracted sample to document opening of an organic porosity via partial removal of solid bitumen(?), although this research identified the soluble extracted organic matter as bitumen and the remainder as insoluble kerogen according to the geochemist's definitions. [Barker et al. \(2007\)](#) compared reflectance measurements of pre- and post-extracted shales and coals, finding overall a slight decrease in reflectance for post-extracted samples. For shales, this observation suggests removal of the more mature saturate and aromatic portions of the solid bitumen, leaving a lower reflectance polar-rich residue. However, the [Barker et al. \(2007\)](#) study was directed primarily at measuring vitrinite reflectance in coal; in 13 shale samples where reflectance measurements could be interpreted to have been made on solid bitumen there was no systematic increase or decrease in the R_o value between pre- and post-extracted samples. Nevertheless, studies using gas adsorption and high-magnification SEM techniques suggest that solvent extraction does open organic porosity in solid bitumen (e.g., [Wei et al., 2014](#); [Löhr et al., 2015](#); [Zargari](#)

[et al., 2015](#); [Xiong et al., 2016](#)). This is particularly important in the oil window where hydrocarbon-filled organic matter pores in solid bitumen may serve as the primary storage and migration mechanism ([Löhr et al., 2015](#)). The nomenclature of solid bitumen is cluttered; for a recent summary of solid bitumen terminology and the origins of solid bitumen types see [Cardott et al. \(2015\)](#). In this text we will use the term 'solid bitumen' for all products of hydrocarbon generation from kerogen (pre-oil solid bitumen per [Curiale, 1986](#)) and for products from alteration of a once-liquid oil (post-oil solid bitumen per [Curiale, 1986](#)). Solid bitumen is recognized in shale reservoirs by fracture-filling, groundmass (enveloping), and void-filling textures (embayment against the euhedral crystal terminations of authigenic minerals). These textures, and the absence of plant structure (cell lumens or walls), help to distinguish solid bitumen from the terrestrial Type III kerogen vitrinite.

The vitrinite maceral is the remains of woody material found in sedimentary rocks, including shale (e.g., [Taylor et al., 1998](#)). The reflectance

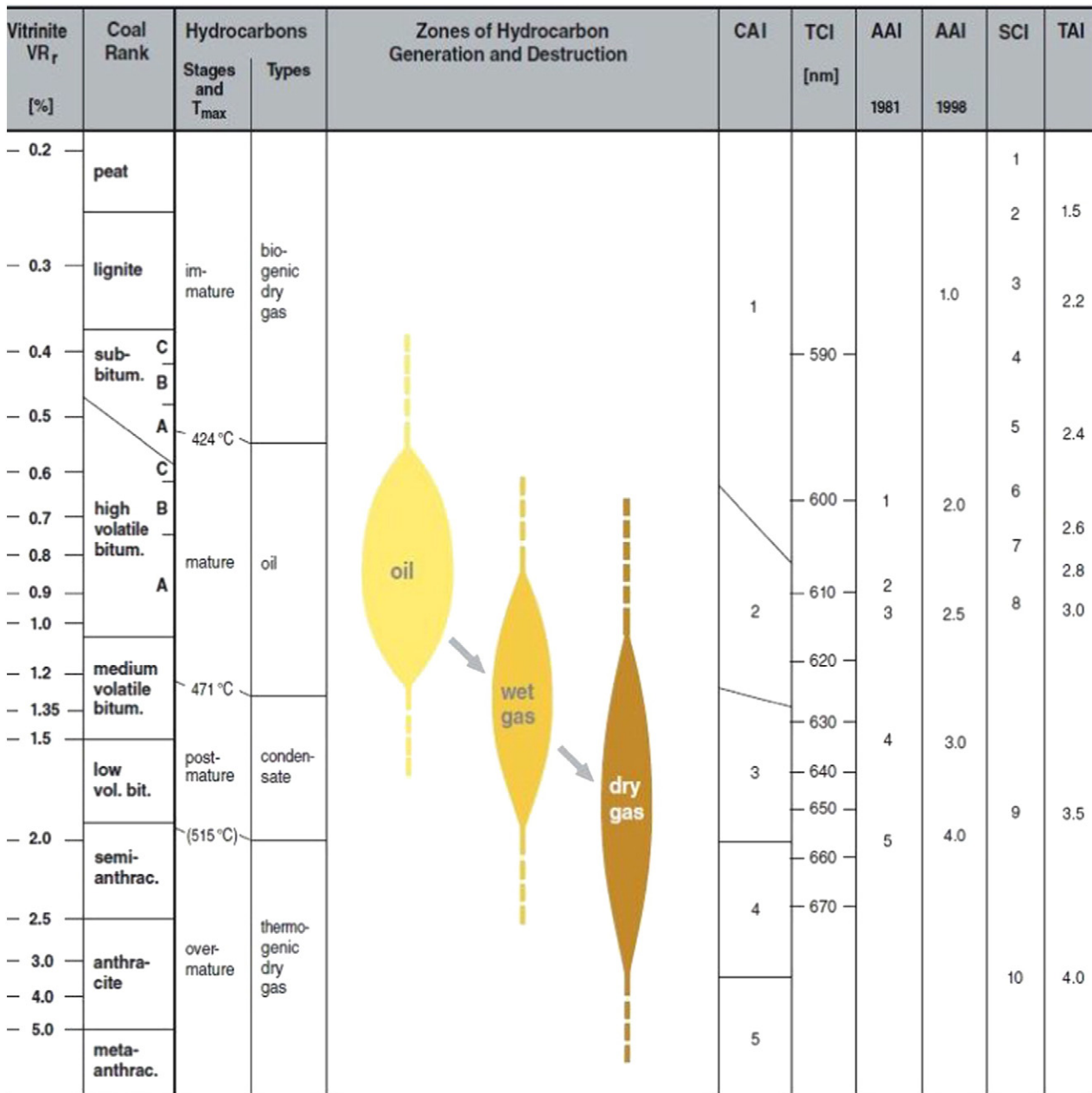


Fig. 4. Optical thermal maturity parameters and zones of hydrocarbon generation. From [Hartkopf-Fröder et al. \(2015\)](#). CAI, conodont alteration index, see [Section 4.3](#); TCI, transmittance color index (not discussed in text); AAI, acritarch alteration index (not discussed in text); SCI, spore color index (not discussed in text); TAI, thermal alteration index, see [Section 4.2](#).

of incident light upon vitrinite in polished rock samples is dependent upon its refractive and absorptive indices, which are a direct function of the degree of aromatization and abundance of delocalized electrons. Vitrinite reflectance increases systematically with increasing maturity, i.e., depth of burial (Dow, 1977) due to increasing aromatization, condensation, and the preferred arrangement of vitrinite molecular structure into the stress field encountered with increasing load pressure (McCartney and Teichmüller, 1972; Levine and Davis, 1984; Carr and Williamson, 1990). Because of this character, vitrinite reflectance is the most robust of many techniques available to determine thermal maturity of rock strata in sedimentary basins, a consideration vital to hydrocarbon exploration (Mukhopadhyay and Dow, 1994). Most evaluation schemes for shale petroleum systems prospectivity consider R_o a key parameter (Curtis, 2002; Miller, 2014; Bernard and Horsfield, 2014; Dembicki and Madren, 2014; De Silva et al., 2015). Solid bitumen reflectance (symbolized BR_o herein) also increases with thermal maturity due to the same chemical reactions that occur in vitrinite.

As general rules of thumb, oil typically is generated from buried organic matter (principally aliphatic H-rich kerogen) in the range of approximately 0.6–1.2% R_o (Fig. 4) whereas gas generation (from humic kerogen or from cracking of oil) generally commences at 1.0% R_o and greater (Tissot and Welte, 1984; Hunt, 1996; Taylor et al., 1998). There are well-known exceptions to these rules of thumb, such as early oil generation from sulfur-rich kerogens at lower R_o values of ~0.4% or less (e.g., Orr, 1986; Baskin and Peters, 1992; Lewan, 1998; Lewan and Ruble, 2002). Jarvie et al. (2005) provided the following guidelines for the Barnett Shale in Texas: immature <0.55% R_o ; oil window 0.55–1.15% R_o ; condensate-wet-gas window 1.15–1.40% R_o ; dry-gas window >1.40% R_o . Thus, vitrinite reflectance in self-sourced shale systems allows prediction of the relative locations and depths at which undiscovered accumulations of oil versus gas are reservoired. The reader is referred to the following monographs and important texts for further information on theory and research of vitrinite reflectance (McCartney and Teichmüller, 1972; Davis, 1978, 1984; Stach et al., 1982, p. 319–332; van Krevelen, 1993, p. 365–377; Mukhopadhyay and Dow, 1994; Taylor et al., 1998, p. 371–397).

Vitrinite reflectance analysis has been applied to rocks other than coal since the 1950s (Teichmüller, 1958; Taylor et al., 1998, p. 501–505); many studies have been designed to determine accuracy and precision and to provide basic guidelines for measurement (e.g., Barker, 1996; Barker and Pawlewicz, 1993; Borrego et al., 2006; Borrego, 2009; ASTM, 2015a). In the two-plus decades following publication of *Vitrinite reflectance as a maturity parameter: applications and limitations* (Mukhopadhyay and Dow, 1994), the state of the art has been advanced significantly by members of the Society for Organic Petrology (TSOP: <http://www.tsop.org/>) and the International Committee for Coal and Organic Petrology (ICCP: <http://www.iccop.org/>). Since the advent of the shale revolution the annual meetings of both societies typically include technical sessions and symposia which include applications of organic petrology to shale systems, and which usually are published as special volumes of the International Journal of Coal Geology. The ICCP also includes several working groups focusing on petrography and reflectance measurement in shale; see for example <http://www.iccop.org/commissions/commission-ii/working-groups-ii/>. The ICCP offers an accreditation program for dispersed organic matter reflectance in shale which currently lists >50 petrographers globally. A description of the ICCP accreditation program and history of its development was given by Cook (2011b). In Section 2 below, we first review basic practical information related to vitrinite reflectance measurement in shale.

2. Measurement of vitrinite reflectance

Macerals are individual components of organic matter with distinctive physical and chemical properties (Spackman, 1958). A classification of dispersed organic macerals in rocks other than coal developed jointly by members of TSOP and ICCP (Stasiuk et al., 2002) is available online

(http://tsop.org/newsletters/1999_2002.pdf) and reproduced in Table 2. Although generally accepted by dispersed organic matter petrographers, this classification is not currently available from a peer-reviewed format. We have provided some commentary in Table 2 that is not included in the official TSOP/ICCP classification (Stasiuk et al., 2002).

In shales, the vitrinite maceral group refers to organic matter derived from the woody tissue of post-Silurian vascular plants (e.g., plants with conducting cells, xylem and phloem), whereas inertinite group macerals have experienced combustion, oxidation or another carbonization process (e.g., desiccation), and liptinite group macerals include primarily algal material (e.g., discrete cysts such as *Tasmanites* or *Leiosphaeridia*) or amorphous organic matter (bituminite) derived from algal or bacterial precursors. Liptinite macerals in lacustrine shales may also commonly include waxy leaf exine (cutinite) and pollen and plant spores (sporinite). ASTM (2015a) provides details of vitrinite reflectance analysis on shale, while ASTM (2015b) provides details of the technique applied to coal. In brief, vitrinite reflectance analysis is the measurement of the percentage of light reflected from the vitrinite maceral at high magnification (400–750×) under oil immersion. The reported vitrinite reflectance value is an average of many measurements (>20 for shales; 100 for coals). Vitrinite reflectance measurements from a single coal sample generally display a normalized distribution over a narrow range, whereas shale reflectance measurements show a broader distribution. Vitrinite reflectance is symbolized as R_o , or R_{max} when the stage or polarizer is rotated (for metallurgical coals), and reported in %. Reflectance analysis can be applied to any of the maceral groups, and all macerals (with the exception of the inertinite group maceral fusinite) increase in reflectance during thermal maturation due to molecular condensation and aromatization. For post-Silurian shales the oil and gas generation windows primarily are correlated to vitrinite reflectance.

Table 2
TSOP/ICCP classification of dispersed organic matter in sedimentary rocks. From Stasiuk et al. (2002).

Group	Maceral	Comment (added herein)
Vitrinite	Telinite	In practice, the individual macerals of the vitrinite group are indistinguishable in fine-grained shales and therefore collectively identified as 'vitrinite'.
	Collotelinite	
	Vitrodetrinite	
	Collodetrinite	
	Gelinite	
Liptinite	Corpogelinite	Occurs as discrete bodies (telalginite) and lamellar masses (lamalginite). Amorphous organic matter. Occurs as a continuum grading from organic-rich (lamalginite) to mineral-rich (mineral bituminous groundmass).
	Alginite	
	Bituminite (amorphinite)	
	Liptodetrinite	
	Sporinite	
	Cutinite	
	Suberinite	
	Resinite	
Inertinite	Chlorophyllinite	Similar to the Vitrinite Group, the individual macerals of the inertinite group generally are not distinguished in practice.
	Fusinite	
	Semifusinite	
	Funginite	
	Secretinite	
	Macrinite	
	Micrinite	
Zooclasts	Inertodetrinite	
	Scolecodont	
	Graptolite	
	Chitinozoa	
	Foram lining	
Secondary products	(Migra)bitumen or solid bitumen	Predominant organic matter component of thermally mature shales Originates from cracking of oil
	Pyrobitumen	
	Oil	

2.1. Microscope systems – state-of-the-art

The evolution of digital capabilities has impacted the organic petrology of shale resulting in recent improvements to vitrinite reflectance measurement systems including the introduction of digital cameras as detection systems (replacing photomultipliers) and LED illumination (replacing tungsten halogen bulbs). These innovations have greatly increased instrument stability and day-to-day reliability in reflectance measurement. Petrographic microscopes for reflectance analysis including these newer systems were reviewed in Cook (2011a). Recent innovations in fluorescence microscopy of shale include introduction of metal halide illumination replacing mercury arc lamps. Advantages include long bulb life and light delivery via fiber optic cable to a collimator which eliminates the alignment necessary for mercury or xenon arc lamps. Confocal laser scanning microscopy has also been applied to the organic petrology of shale systems (e.g., Stasiuk, 1999a,b; Stasiuk and Sanei, 2001; Stasiuk and Fowler, 2004; Xiao et al., 2002; Kus, 2015; Hackley and Kus, 2015) although this technique is not in routine use.

2.2. Advantages of vitrinite reflectance measurement

There are many advantages to using vitrinite reflectance and it is generally regarded as the “gold standard” thermal maturity parameter for shale (e.g., Hackley et al., 2015). For example, vitrinite is ubiquitous in most shale of Upper Paleozoic and younger age and in modern unconsolidated sediments. Therefore, only a small amount of sample is required, sometimes as little as 0.25 g of organic-rich shale, although 5–15 g is preferred. The analysis is inexpensive and reproducible in interlaboratory studies (e.g., Dembicki, 1984; Borrego, 2009; Araujo et al., 2014; Hackley et al., 2015, although see below). Sample preparation is simple, requiring only mounting and polishing of whole rock samples; kerogen concentration requiring acid dissolution of the rock matrix generally is not necessary. Measurement is reported to two decimal places, allowing assignment of thermal maturity to a specific position within a broad possible range. Most important, vitrinite reflectance analysis is applicable to a broad thermal range of materials, ranging from immature sediments to low temperature anchizone-epizone metamorphism (e.g., Mählmann and Frey, 2012). Last, it is a long-standing technique practiced in many laboratories worldwide, going back over fifty years for shales (e.g., Teichmüller, 1958, 1971; Robert, 1971; Castaño and Sparks, 1974; Bostick, 1974).

2.3. Sources of error in reflectance analysis of shales

Vitrinite reflectance analysis was first applied to determine coal rank (Hoffman and Jenkner, 1932; ICCP, 1971; McCartney and Teichmüller, 1972; Stach et al., 1982; Mukhopadhyay, 1994). Vitrinite is abundant in banded bituminous coals, making the selection and reflectance measurement of vitrinite in coal straightforward. However, application of vitrinite reflectance to determination of the thermal maturity of marine and lacustrine shales introduced numerous sources of error (Castaño and Sparks, 1974; Jones and Edison, 1978; Dow and O'Connor, 1982). Unlike coal, vitrinite in shale is sparse, small, and may be altered by physical and chemical weathering during transport to the depositional environment. The focus of vitrinite reflectance analysis of shales is to properly identify indigenous vitrinite by eliminating possible sources of error.

Possible errors begin with the sample itself. Basic sample types include core, outcrop, and well cuttings. Organic matter begins to weather as soon as it is exposed to oxygen. Therefore, organic matter in outcrop samples may be altered by weathering. Typical optical signs of weathering are either darker (tarnished) or brighter (oxidized) rims of organic particles and random micro-fractures (Fig. 5A; Cardott, 1994; Lo and Cardott, 1994). Weathering at outcrop is more of a problem for coal samples than for shale samples where organic matter is

better protected from weathering in a less permeable well-indurated matrix.

The main problem with well cuttings is the potential for contamination from mixing of cuttings from uphole. Caving contamination will dilute quality of hydrocarbon source rock determined by geochemical analysis and lower measured vitrinite reflectance. In addition, well cuttings may contain an organic drilling mud additive such as lignite or walnut hulls. The best way to identify these potential errors is by first looking at variation in lithology of well cuttings and, if possible, hand-picking the selected lithology for vitrinite reflectance analysis. Examination of samples in whole-rock preparations will aid in identification of caving contamination and drilling mud additives under the microscope as these contaminants will occur isolated in the binder matrix. Core samples may not have weathering or caving contamination errors but, like other sample types, may contain organic-matter-sourced errors (described below).

Rock type (e.g., coal, shale, siltstone, sandstone) may impact vitrinite reflectance analysis. Organic richness and low thermal conductivity make coal the benchmark for thermal maturity studies (Bostick and Foster, 1975; Senftle and Landis, 1991; Goodarzi et al., 1993). Fig. 5B illustrates maximum vitrinite reflectance measurements determined on a coal stringer found within a Woodford Shale core where the reflectance range is only 0.20% R_{max} . The reflectance of vitrinite in other lithologies will deviate from the coal benchmark (e.g., Jones et al., 1972; Goodarzi, 1985a). Permeable sandstones are the most problematic due to possibility of alteration of vitrinite from oxidizing fluids. If possible, vitrinite reflectance measurements utilized for basin analysis should be compared between rocks of a single lithology, preferably coal or shale.

Sample handling may affect vitrinite reflectance analysis. Oil-based drilling mud is a problem for chemical analyses of organic matter, but has not been observed to alter vitrinite reflectance due to protection by the mineral matrix in well-indurated shale. Oil-based drilling mud may be cleaned from the surface of well cuttings by rinsing in a sieve with water and dishwashing liquid and air dried. If using a kerogen concentrate, the sample should not be treated with oxidants such as nitric acid (used in palynomorph separation).

Organic matter identification errors occur during microscopic analysis or the interpretation stage. Barker and Pawlewicz (1993) determined a minimum number of 20 measurements accurately define the shape of the reflectance histogram. Fig. 5C illustrates the normal range of data ($\sim 0.3\% R_o$) and shape of the reflectance histogram at a thermal maturity in the oil window. Collecting <20 measurements limits the validity of the calculated average value since there will not be enough data to define a normalized distribution. The objective of the study (e.g., accuracy vs. precision of the oil, condensate, or gas windows) will determine if a quantitative value (≥ 20) or a qualitative value (<20) is needed (ASTM, 2015a). A mean reflectance value and its standard deviation are computed and reported from the total number of measurements.

An inferior quality of the vitrinite clast texture will influence the measured reflectance value (Bostick and Foster, 1975; Dow and O'Connor, 1982). For example, a pitted (e.g., Fig. 5D) or scratched surface texture usually will result in a lower reflectance value. These degraded values should be measured, identified and used as an aid in identifying the lowest reflecting indigenous vitrinite (e.g., low-gray vitrinite of Bostick, 1979) but excluded from the calculation of the mean random vitrinite reflectance value (Fig. 5E).

The size of the measuring spot will determine the minimum size required for the vitrinite clast (i.e., the clast should be significantly larger than the measuring spot). ASTM (2015a) recommends a projected diameter size of 5 μm . Edge effects from being too close to the edge of the clast or the influence of glare from high-reflecting pyrite should be avoided. Sanei et al. (2015a) used the adjustable measuring spot capabilities of the currently available instrumentation to show that larger spot sizes integrate more surface imperfections resulting in lower

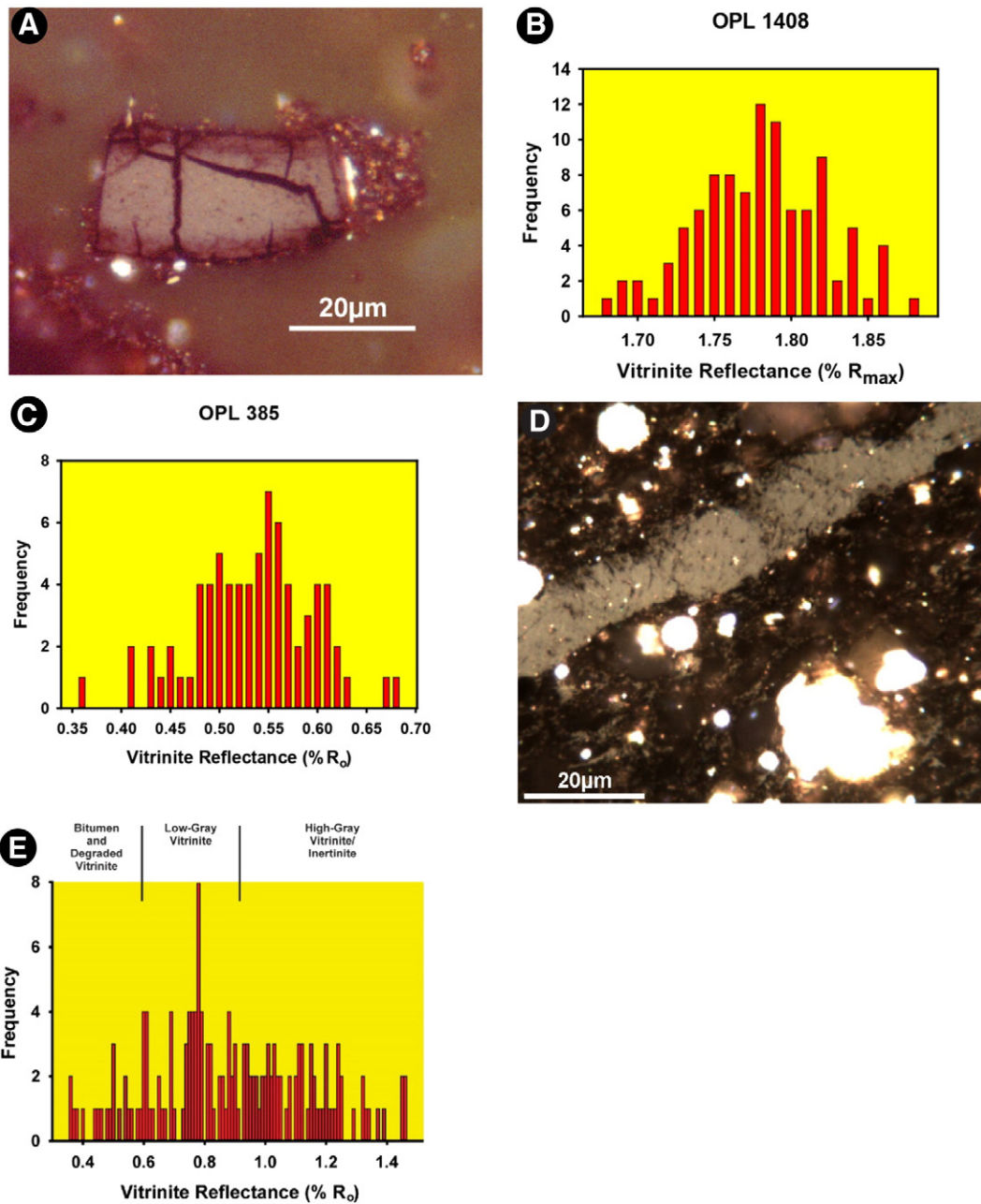


Fig. 5. A. Photomicrograph of weathered vitrinite clast from Johns Valley Shale outcrop sample showing micro-fractures and dark reaction rims (reflected white light; from Cardott, 1994). B. Vitrinite reflectance histogram of a coal stringer in a Woodford Shale core from western Oklahoma showing a narrow range of maximum vitrinite reflectance measurements (OPL 1408; 100 measurements). C. Vitrinite reflectance histogram of a Woodford Shale sample from the Arbuckle Mountains in southern Oklahoma showing the typical range of random vitrinite reflectance measurements in the oil window (OPL 385; 75 measurements). D. Gray reflecting organic matter showing a pitted surface unsuitable for inclusion in calculation of a mean reflectance value. E. Reflectance histogram of Atoka shale sample from the Ouachita Mountains in southeast Oklahoma showing the interpretation of measured bitumen, degraded vitrinite, low-gray vitrinite, and high-gray vitrinite/inertinite reflectance values (from Cardott, 1994).

measured reflectance values. An air bubble attached to the objective will cast a shadow on the field of view and should be recognized and avoided. Likewise, immersion oil should be removed from the objective prior to standard calibration to avoid contamination of the immersion oil on the standard.

Properly identifying vitrinite may be the most important criteria and greatest source of error in vitrinite reflectance analysis. ICCP (1998) described vitrinite types in the vitrinite maceral group occurring in banded bituminous coals (subgroups are telovitrinite, detrovitrinite, gelovitrinite); Potter et al. (1998) compared previously defined vitrinite-maceral terms with these current terms. However, in practice, vitrinite types are not recognizable in the small vitrinite clasts found in shales and all vitrinite macerals are identified as vitrinite (e.g., ASTM,

2015a). At best it should be recognized that some vitrinite macerals (e.g., pseudovitrinite derived from bark sheets) will have slightly higher reflectance than other vitrinite macerals at the same thermal maturity (Kaegi, 1985; Khorasani and Michelsen, 1994).

Additional sources of error may be introduced by polishing equipment and the microscope system. Whole-rock or kerogen concentrate pellets are polished to a relief-free, scratch-free surface and kept in a desiccator overnight prior to the analysis to remove any water in the pores that could dilute the refractive index of the immersion oil. Reflectance standards within the thermal maturity range are used to calibrate the microscope system every 15 to 30 min during analysis in order to eliminate drift. The microscope system should include a stabilized light source and good quality optics. Newer systems, e.g., Hilgers Fossil,

using LED illumination and digital cameras are highly stabilized and do not require frequent re-calibration.

Vitrinite reflectance is measured to a precision of 0.01% R_o . The reported mean random vitrinite reflectance value should also be reported to 0.01% R_o . Any implied higher precision (e.g., 0.001% R_o) due to rounding should be avoided. The best method of recognizing the quality of the data is to look not only at the mean value and number of measurements but also to the shape of the reflectance histogram, spread of values, and photomicrographs of correctly identified vitrinite.

2.4. Atypical reflectance values

Many studies have reported that reflectance of vitrinite appears to be suppressed relative to expected values (e.g., Schito et al., 2016), and, based on empirical studies, several mechanisms have been proposed to explain this 'vitrinite reflectance suppression.' For example, suppressed vitrinite may have atypical maturation kinetics due to a priori enrichment in H or S, or, as a consequence of association with aliphatic, lipid-rich organic materials (liptinite), which exsolve lower reflecting oil or bitumen that migrates into vitrinite and lowers its reflectance (e.g., Jones and Edison, 1978; Hutton and Cook, 1980; Kalkreuth, 1982; Kalkreuth and Macauley, 1987; Corrêa da Silva, 1989; Hao and Chen, 1992; Mastalerz et al., 1993; Petersen and Rosenberg, 1998; Gurba and Ward, 1998; Petersen and Vosgerau, 1999; Ujjié et al., 2004; Ward et al., 2007, among others). Experimental studies (Huang, 1996; Barker et al., 2007) and some empirical data sets (Price and Barker, 1985; Wenger and Baker, 1987; Hao and Chen, 1992) demonstrated bitumen impregnation as an unlikely mechanism although compositional differences occurring due to diagenetic sulfuration of organic matter remains viable for reflectance suppression.

An alternative to reflectance suppression is the retardation of organic matter maturation kinetics by overpressure as a result of impermeable conditions in fine-grained sediments (McTavish, 1978, 1998; Hao et al., 1995, 2007; Carr, 2000). Overpressured conditions (pressures higher than hydrostatic pressure) occur wherever high sedimentation rates prevent equilibrium compaction from occurring (Hunt, 1996). The reduction in vitrinite maturation kinetics due to overpressure is called reflectance retardation, in contrast to reflectance suppression which occurs due to chemical conditions which potentially lower aromaticity. Vitrinite reflectance retardation is thought to develop due to high pore pressures preventing products evolved during the normal maturation of vitrinite from leaving the reaction site (Hao et al., 2007), and this reflectance retardation has been demonstrated through high water pressure pyrolysis experiments (Uguna et al., 2016). Whereas reflectance suppression impacts only vitrinite, retardation of maturation kinetics affects all organic matter, including oil-prone algal material and may thus lower the top of the oil window in settings with thick overpressured sections (e.g., Petersen et al., 2012). However, some studies have documented overpressured conditions that have had no discernable effect on rates of organic matter maturation (Hao et al., 1995; He et al., 2002). Because suppression or retardation of vitrinite reflectance values can have significant impact on thermal history modeling and hydrocarbon exploration programs, some studies have used empirical data sets to help develop correction functions (Wilkins et al., 1992; Lo, 1993; Quick, 1994; Newman, 1997; Wilkins et al., 2002), while others have proposed selection criteria for avoiding suppressed vitrinite during petrographic analysis (Buiskool Toxopeus, 1983). Proper discrimination of vitrinite-like solid bitumen from vitrinite may be the source of some reports of vitrinite reflectance suppression (Hackley et al., 2013). Others have used artificial maturation techniques to document experimental conditions under which vitrinite reflectance suppression/retardation occur (Lewan, 1985; Huang, 1996; Seewald et al., 2000). While we cannot review these issues in detail in this publication, readers should be aware that atypical vitrinite chemistry or

retardation of maturation kinetics may impact reflectance values in shale systems.

3. Scanning electron microscopy (SEM) of organic matter in shale

The presence of an interconnected organic porosity network has emerged as an important control on reservoir permeability and hydrocarbon storage space in shale petroleum systems (e.g., Modica and Lapierre, 2011; Clarkson et al., 2013; Romero-Sarmiento et al., 2014). Imaging of organic porosity in shales dates to the pioneering work of Mann et al. (1994) who interpreted organic-hosted pores in Posidonia Shale as products of retrograde hydrocarbon condensation in solid bitumen during uplift. Application of scanning electron microscopy (SEM) techniques to shale has expanded rapidly since Loucks et al. (2009) imaged organic nanoporosity in the Barnett Shale and examination of Argon ion-milled rock surfaces via SEM has become the standard industry practice for identification of pore systems and mudstone reservoir characterization (e.g., Passey et al., 2010; Sondergeld et al., 2010; Loucks et al., 2010, 2012; Heath et al., 2011; Slatt and O'Brien, 2011; Curtis et al., 2012a; Josh et al., 2012; Klaver et al., 2012, 2015; Camp et al., 2013; Goergen et al., 2014; Jiao et al., 2014; Cardott et al., 2015; Lu et al., 2015, among many others). Most of the recent shale SEM studies have focused on characterization of organic porosity; however some have used this technique to explore inorganic content, e.g., Camp and Wawak (2013) used false color images to enhance information derived from grayscale SEM images, enabling better distinction of silicate phases in samples of Eagle Ford, Haynesville and Marcellus shales. Transmission electron microscopy (TEM) also has been used for organic matter characterization in shale reservoirs (e.g., Bernard et al., 2010, 2012a,b; Dong et al., 2015); however, sample preparation requires expensive and time-consuming milling of ultra-thin (~250 nm) wafers via focused ion beam, limiting widespread application.

There is a general consensus that organic porosity forms as a consequence of advancing thermal maturity and the generation of hydrocarbons from kerogen (e.g., Behar and Vandenbrouke, 1987; Jarvie et al., 2007; Curtis et al. 2012b; Loucks et al., 2009, 2012; Zhang et al., 2012; Bernard et al., 2012a,b; Valenza et al., 2013; Driskill et al., 2013a,b; Chen and Xiao, 2014; Cardott et al., 2015; Romero-Sarmiento et al., 2014; Pommer and Milliken, 2015, among others). For example, Bernard et al. (2012a) documented the development of nanoporosity in pyrobitumen occurring in Barnett Shale samples of gas window maturity, whereas samples at lower maturity did not exhibit significant organic porosity. Another study by this group (Bernard et al., 2012b) also documented formation of irregular nanoporosity at the gas window stage of thermal maturity in the Posidonia Shale. Juliao et al. (2015) showed increased microporosity in oil window mature solid bitumen-rich samples of the La Luna Formation relative to adjacent samples which contained less solid bitumen via picnometry and porosimetry techniques. Chen and Jiang (2016) found little or no organic porosity in immature Duvernay shale but up to >6% porosity in organic-rich overmature samples. However, other studies have found conflicting results or no systematic relationships between organic porosity and thermal maturity (Fishman et al., 2012; Milliken et al., 2013), and there are inconsistencies regarding the thermal regime at the onset of organic porosity development and its development in different organic matter types. Contradictory findings by different studies on samples from the same wells (e.g., Reed et al., 2014) illustrates that development of the SEM approach to characterization of organic matter porosity still is in its early stages. A particular caution is that interpretations from SEM observations may not be representative of the larger, bulk sample due to the small areas imaged at typical high magnifications. Some researchers consider that some organic porosity observed at lower thermal maturity can be an artifact of desiccation, e.g., features such as separation of solid bitumen from adjacent mineral grains, straight cracks through solid bitumen veins or meandering cracks in solid bitumen with complementary shapes on either side all suggest dehydration (Neil Fishman, Hess,

written communication, 2016). Another caution and one of the major difficulties in SEM petrography of organic matter is the inability, in most cases, to distinguish solid bitumen from kerogen, or to differentiate kerogen types. Only in the last several years have some correlative microscopy studies combined organic petrology and SEM imaging techniques to document the type of organic material in which porosity is developed (Bernard et al., 2012b; Chalmers et al., 2012; Fishman et al., 2012; Cardott et al., 2015; Baruch et al., 2015; Löhr et al., 2015; Luo et al., 2016). However, distinction of kerogen from solid bitumen at dry gas window maturity continues to be ignored even in some of these studies. In Fig. 6 we illustrate correlative incident white light oil immersion optical microscopy with SEM imaging in low maturity Bakken shale, showing the benefit of optical microscopy to discern multiple solid bitumen populations in the same field. Until correlative microscopy studies become routine, SEM approaches will continue to suffer from the inability to identify organic matter type.

Some research has combined different in situ probing tools with SEM to further characterize shale organic matter properties. For

example, Emmanuel et al. (2016) used atomic force microscopy with SEM imaging to document high variability of elastic moduli in Eagle Ford Formation kerogen whereas solid bitumen in the same samples had consistent moduli across a range of peak oil to early gas condensate thermal maturities (0.8–1.2% R_o). Neutron scattering experiments and molecular modelling were employed by Bousige et al. (2016) to also claim kerogen stiffening at higher maturity, i.e., a plastic to brittle transition with thermal maturity advance. However, these studies ignored distinctions between kerogen and solid bitumen, considering all organic matter in shale as kerogen even at high maturity (2.2% R_o). This suggests they may have unintentionally compared the mechanical properties of two different types of organic matter. Finally, despite the important findings of organic porosity revealed via SEM petrography of shales, no studies have yet demonstrated that organic nanoporosity is indeed present at reservoir temperatures and pressures. It is therefore possible that the open interconnected porosity observed in some SEM studies of high maturity shales is due simply to volatilization of hydrocarbons from solid bitumen at surface conditions. In Section 5 below we include

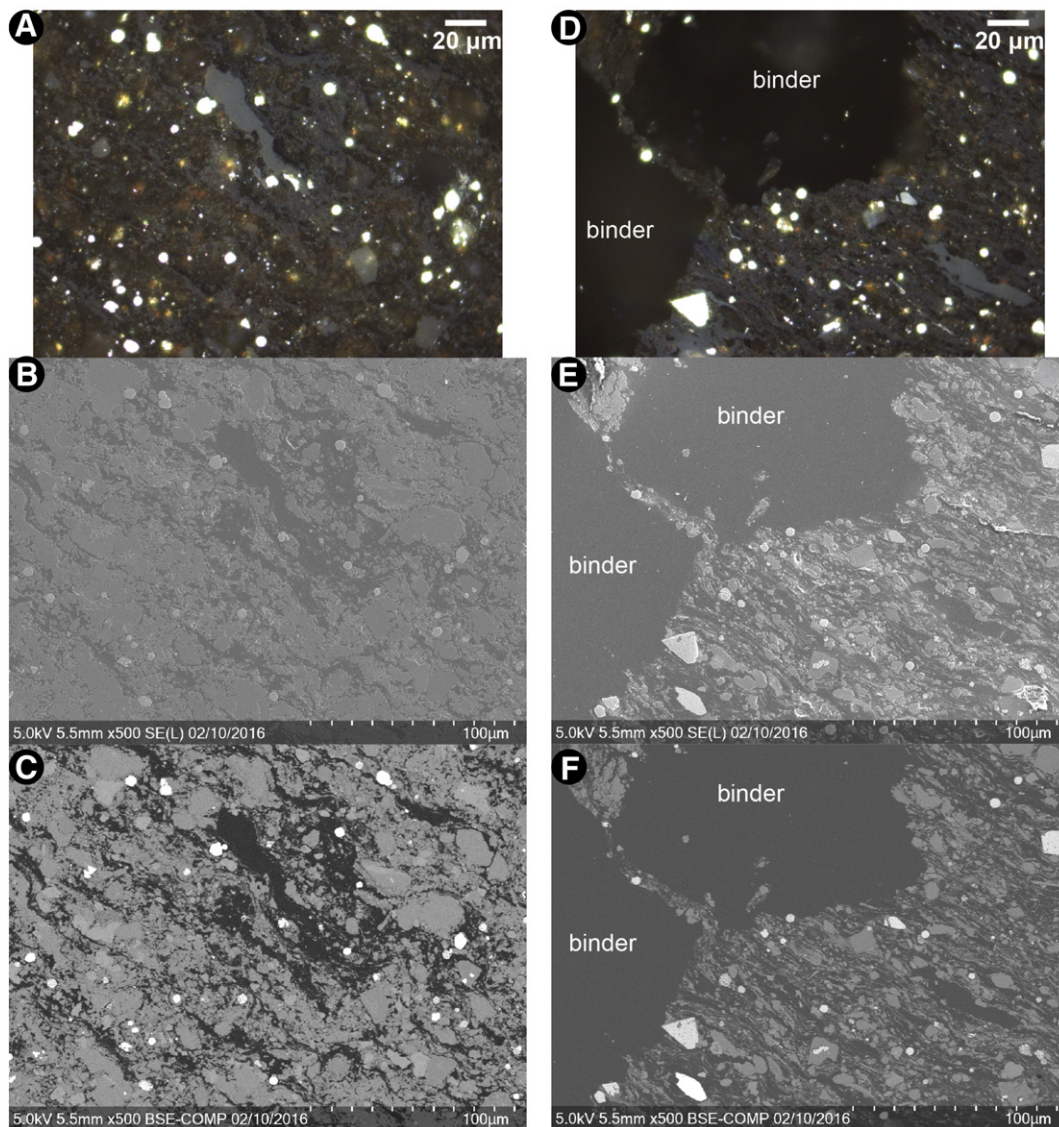


Fig. 6. Correlative optical microscopy-SEM images from a mechanically polished, low maturity (BR_o 0.32%) organic-rich (14.6 wt.% TOC) Bakken shale sample collected at 7652 ft. (2332 m) from the Clarion Resources 1-20 Fleckton well (API 3310100273), Ward Co., North Dakota. A. White incident light, oil immersion photomicrograph showing accumulation of brighter reflectance pre-oil solid bitumen with homogeneous reflecting surface coalesced from darker solid bitumen in groundmass. The formation of pre-oil solid bitumen follows a continuum. We interpret the darker organic matter here as solid bitumen, distinguishable from bituminite, based on gray color in incident white light. B. Secondary electron scanning electron microscopy - (SE-SEM) image of same field as A. C. Back-scattered electron (BSE)-SEM image of same field as A–B. D. White incident light, oil immersion photomicrograph showing accumulation of brighter reflectance solid bitumen with homogeneous reflecting surface coalesced from darker solid bitumen in groundmass. E. SE-SEM image of same field as D. F. BSE-SEM image of same field as D–E. Images courtesy of Brett Valentine, USGS. In the SEM images B–C and E–F organic matter is black. All SEM images are of carbon-coated samples.

a brief discussion of SEM petrography as applied to the organic petrology of North American shale systems, e.g., see Section 5.1.2 on the Eagle Ford Formation.

4. Secondary optical thermal maturity parameters

Vitrinite reflectance is not the only petrographic thermal maturity determinant in shale; fluorescence, thermal alteration index (TAI), conodont alteration index (CAI), and the reflectance of other macerals also are used, although not as commonly as vitrinite reflectance. Here we briefly mention some of these other petrographic thermal maturity approaches applied in shale petroleum systems, comparing each with the utility of vitrinite reflectance measurements. For a recent in-depth review of optical thermal maturity parameters applied to sedimentary rocks, readers are referred to Hartkopf-Fröder et al. (2015).

4.1. Fluorescence

Fluorescence of liptinite macerals, a qualitative thermal maturity indicator, can be used to confirm mean random vitrinite reflectance values of shale samples from immature conditions up to the early to middle oil window (e.g., Jacob, 1965; Ottenjann et al., 1975; Bustin et al., 1985; Araujo et al., 2014). In general, liptinite fluorescence colors change from green to greenish yellow to yellow to orange in reflected blue light before fluorescence is mostly extinguished at an equivalent vitrinite reflectance of about 1.0–1.1% R_o (Teichmüller and Durand, 1983). Decreased organic fluorescence at higher maturities is due to increased molecular aromatization and an increase in fluorophore density, the concentration quenching effect (Bertrand et al., 1986; Lin and Davis, 1988; Pradier et al., 1991). The fluorescence color of organic matter can be quantified by spectrometry (e.g., van Gijzel, 1981) and many researchers have related the spectral parameters of organic fluorescence to equivalent vitrinite reflectance values (reviewed in Suarez-Ruiz et al., 2012). In Devonian shales of the Appalachian Basin, organic fluorescence of *Tasmanites* still is visible at ~0.8% R_o (Hackley et al., 2015) but *Tasmanites* generally is not present at higher thermal maturities after conversion to hydrocarbons (Taylor et al., 1998; Ryder et al., 2013). Hydrous pyrolysis of Devonian shale samples shows *Tasmanites* fluorescence still is present after 72 h at 320 °C (~0.7% R_o) followed by almost complete conversion to hydrocarbons occurring after 72 h at temperatures >325 °C (~1.0% R_o). Recently, studies have applied confocal laser scanning fluorescence microscopy to determination of thermal maturity of organic matter in immature and early oil window mature shale, using a quantitative spectral approach (Hackley and Kus, 2015) similar to conventional fluorescence microscopy. The confocal laser scanning microscope, used primarily in biomedical imaging, has great promise for high resolution 3-D fluorescence microscopy of

sedimentary organic matter in low maturity shales (e.g., Kus, 2015), allowing collection of hyperspectral volumes (a 3-D digital image with spectral information attached to every pixel) and potentially enabling investigation of individual fluorophore moieties (Fig. 7). However, conventional and confocal fluorescence microscopy of shales generally is not possible beyond the middle to peak oil window, limiting the application of this approach as an optical thermal maturity parameter to low maturity systems.

4.2. Thermal alteration index (TAI)

Thermal alteration index (TAI; Fig. 3) refers to a progressive color change developed in pollen grains and spores (palynomorphs) ranging from yellow to black due to thermal maturation advance (e.g., Staplin, 1969, 1982). Palynomorphs are separated from the whole rock via acidification (kerogen concentration) and compared to a color chart. Despite widespread use of this transmitted light optical maturity parameter as a regional evaluation tool for thermal history of sedimentary basins (e.g., Pavluš and Skupien, 2014; Naqishbandi et al., 2015), there are few applications to shale petroleum systems exploration in North America. Scattered examples include the 1970s–1980s Eastern Gas Shales Project where Zielinski and McIver (1982) used TAI to map expected locations of oil, wet and dry gas hydrocarbons reservoirs in Devonian shales of the Appalachian Basin. Laughrey et al. (2004) used TAI to characterize overmature samples of Marcellus Shale from north-central Pennsylvania; however, this work was in the context of researching a conventional natural gas field. More recently, Broadhead and Gillard (2007) used TAI to characterize thermal maturity of the Barnett Shale for hydrocarbon exploration in the Permian Basin. Their study showed TAI values to be generally consistent with Production Index calculations from Rock-Eval pyrolysis (see below), confirming the Barnett as thermally mature for hydrocarbon generation in south-eastern New Mexico. Elgmami et al. (2011) used TAI to characterize shale gas samples from the Utica, Haynesville and Fayetteville shale plays, concluding an inert high maturity kerogen (>1.5–2.5% R_o) was present in all samples, indicative of little remaining source potential. Their study illustrated some of the problems inherent in application of transmitted light organic petrography to characterization of high maturity shale samples. For example, the observed TAI colors of dark brown to black can only indicate that samples are ‘post-mature’, whereas reflectance can provide a specific value corresponding to a position within a broad spectrum of thermal maturation for such rocks (dry gas to overmature). Another problem with application of TAI in their study was inaccurate identification; e.g., ‘structured phytoclasts’ were identified in the Ordovician Utica (deposited before the evolution of woody land plants) and ‘opaques’ were identified rather than the solid bitumen which is obvious in all gas shales via incident light petrography. Finally,

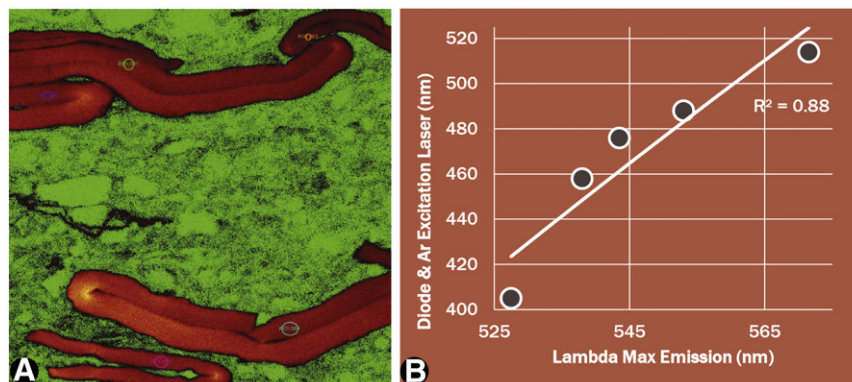


Fig. 7. Fluorescence spectra related to chemical composition (presence of multiple fluorophores) in algal microfossils. A. Confocal spectral image of *Tasmanites* (false colors using red-green lookup table) with regions of interest (ROIs) selected from low quantum yield interior portions of *Tasmanites*. B. Emission spectral maximum as a function of excitation wavelength from ROIs selected in A. Data from confocal experiments conducted by Hackley and Robert C. Burruss (USGS-Reston) during 2013–2015.

Pernia et al. (2015) had difficulty finding palynomorphs for TAI measurements in thermally mature Marcellus and Haynesville shales whereas they were able to measure TAI in immature Barnett and Monterey samples. R_o measurements were obtained for all the samples in their study, illustrating the broader utility of this approach.

4.3. Conodont alteration index (CAI)

Conodonts are Cambrian-Triassic vertebrate remnants composed of carbonate fluoroapatite. Organic material in the fluoroapatite changes color during diagenesis (Epstein et al., 1977; Rejebian et al., 1987) according to a five color scale used to delineate the conodont alteration index (CAI; Fig. 3). This petrographic approach to thermal maturity determination primarily is applied to limestones but some workers have also used CAI in shale and mudstone (e.g., Metcalf and Riley, 2010). Like the TAI described above, CAI studies require separation and concentration of conodont elements from the rock matrix via acidification and hand picking. Large sample sizes (~1 kg) may be required to provide a sufficient number of good quality conodont elements. The CAI is rarely applied for reservoir characterization in the North American shale plays; conodont evaluation is more often applied for regional-scale thermal maturation studies (e.g., Legall et al., 1981; Johnsson et al., 1993; Repetski et al., 2008), or to address specific biostratigraphic correlation issues (e.g., Over, 2007). Repetski et al. (2008) presented a comprehensive evaluation of CAI values throughout the Appalachian Basin in the context of oil and gas resources, including the Marcellus and Utica shales. Their regional CAI map is useful for prediction of thermal maturity in these petroleum systems, showing progressive north-west to southeast increase in thermal maturity towards the Appalachian hinterland, consistent with thermal maturity patterns documented from vitrinite reflectance of overlying Carboniferous coals (Ruppert et al., 2010).

4.4. Reflectance of other macerals

4.4.1. Inertinite vs. vitrinite

Most inertinite is considered a product of vegetation charring or oxidation and a large body of work has been directed at establishing a relationship between its reflectance and the temperatures of wildfire (Scott and Glasspool, 2007; Scott, 2010). Despite that inertinite is 'inert' from carbonization prior to incorporation into sediments, there is some evidence that its reflectance increases during burial maturation (Smith and Cook, 1980) and the Raman spectra of inertinites show systematic change with progressive thermal maturity advance in coal and marine shale (Wilkins et al., 2014, 2015). A full discussion of inertinite reflectance is outside the scope of this paper. However, we consider distinguishing vitrinite from inertinite (which can appear vitrinite-like) as essential in deriving a valid vitrinite reflectance value from shale.

For marine shales there are many opportunities for the woody organic matter to be oxidized along the path from the source terrestrial environment to final depositional marine environment. While considering the potential range from slight to severe oxidation, reflectance values from organic matter that are slightly higher to much higher than that of co-occurring vitrinite are interpreted to be an inertinite maceral such as semifusinite, with or without cell structure. Wide variation in inertinite reflectance generally precludes using inertinite reflectance as a thermal maturity parameter in favor of vitrinite. Irregular particle edges are helpful to distinguish dispersed vitrinite in shales compared to the sharp arcuate edges of inertinite macerals which often also have preserved cell structure.

Higher-reflecting vitrinite and/or inertinite recycled from older eroded rocks, included in the term high-gray vitrinite (Bostick, 1979), may be avoided by knowledge of the tectonic setting and geologic history of the host rock. Applying an expected range of reflectance values beginning with the lowest reflecting properly identified vitrinite allows

for the exclusion of possible oxidized or recycled vitrinite and/or inertinite (Fig. 5D). At $<1\% R_o$, the typical spread of vitrinite reflectance values is $\sim 0.3\% R_o$. Pressure-induced anisotropy (apparent minimum to maximum reflectance) of vitrinite causes a larger spread in random vitrinite reflectance values at thermal maturities $>1.0\% R_o$. Incorporating these ideas into interpretation of reflectance histograms may allow petrographers and data users to discount measurements that are not representative of in situ thermal maturity.

4.4.2. Solid bitumen reflectance

Bitumen is defined by geochemists as organic matter soluble in organic solvents (Tissot and Welte, 1984) whereas organic petrographers refer to solid bitumen as a secondary maceral resulting from hydrocarbon generation from kerogen (ASTM, 2015a). Some low maturity solid bitumen in shale is readily soluble by petrographic immersion oil and/or heat from microscope illumination sources as evident by 'streaming' of the solid bitumen into immersion oil, discoloration of the immersion oil, and etching and/or sloughing of the polished solid bitumen surface. Solid bitumen in shale is visually similar to vitrinite (e.g., vitrinite-like) in reflected white light, occurring as amorphous or void-filling blobs, pods, and accumulations when generated from kerogen in a hydrocarbon source rock. Solid bitumen also occurs as pore- and fracture-filling vein deposits (e.g., asphaltite and asphaltic pyrobitumen; Abraham, 1960) as an alteration product of oil (Taylor et al., 1998). Whole-rock mounts are necessary for differentiation of indigenous vitrinite from solid bitumen because the void-filling textures of solid bitumen are destroyed by kerogen concentration (Senftle and Landis, 1991; Barker, 1996). Solid bitumen which lacks a void-filling texture can be indistinguishable from vitrinite, resulting in reports of a so-called 'vitrinite-like maceral' in rocks which pre-date terrestrial land plants (Buchardt and Lewan, 1990; Xiao et al., 2000; Zdanavičiūtė and Lazauskienė, 2009; Schmidt et al., 2015).

In a genetic solid bitumen classification, Curiale (1986, p. 559) described pre-oil solid bitumen as the "early-generation (immature) products of organic-rich source rocks, probably extruded as very viscous fluids" and post-oil solid bitumen as "products of the alteration of a once-liquid oil, which was generated and migrated from a mature source rock." Lewan (1983) demonstrated that pre-oil solid bitumen, generated from kerogen, is the source of oil.

Several studies have provided regression equations to calculate a vitrinite reflectance equivalent from homogenous bitumen reflectance (BR_o) values (summarized in Suárez-Ruiz et al., 2012; Petersen et al., 2013; Mählmann and Le Bayon, 2016). However, the mobility of solid bitumen at reservoir temperatures (Jacob, 1989) and distinctions between pre- and post-oil and textural types (e.g., homogenous, granular, coked, see Sanei et al., 2015a) complicate correlations. The most frequently cited conversion equations are from studies by Jacob (1989) and Landis and Castaño (1995). Schoenherr et al. (2007) combined data from these two studies to derive an 'improved' calibration equation and Mählmann and Le Bayon (2016) examined correlations in different geodynamic settings. Jacob (1989) found BR_o is lower than co-occurring vitrinite reflectance below $1.0\% R_o$ (see also Robert, 1988; Mählmann and Frey, 2012) and higher than co-occurring vitrinite reflectance above $1.0\% R_o$. Jacob (1989) included post-oil solid bitumen reflectance measurements from fracture-filling vein deposits (e.g., asphaltite and asphaltic pyrobitumen). Landis and Castaño (1995) correlated reflectance of homogenous pre-oil solid bitumen with reflectance of co-occurring indigenous vitrinite and suggested BR_o always is lower than vitrinite reflectance in the same rock. Bertrand and Malo (2001) also provided a correlation equation, however they noted that such correlations probably are specific to the basin they are measured in, owing to local variations in vitrinite and solid bitumen composition. Furthermore, because BR_o generally is lower than co-occurring vitrinite reflectance at lower thermal maturities, some studies have suggested cases of reported 'vitrinite reflectance suppression' may instead be related to misidentification of solid bitumen as vitrinite (Ryder et al., 2013;

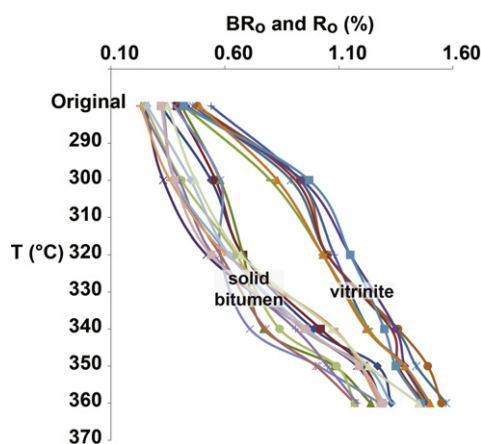


Fig. 8. Vitrinite and solid bitumen reflectance of source rocks and coals ($n = 21$) as a function of hydrous pyrolysis temperature. Data from hydrous pyrolysis experiments on shales and coal conducted by Hackley (USGS-Reston) during 2012–2015.

Hackley et al., 2013). Supporting this assertion, data from hydrous pyrolysis experiments by Hackley at USGS-Reston shows kinetic barriers to solid bitumen maturation are higher than for vitrinite; the effect is more pronounced at lower heating levels (Fig. 8). Moreover, an interlaboratory study found no statistical difference reported between BR_o vs. R_o vs. a mixture of BR_o and R_o values from petrographers analyzing the same shale sample (Hackley et al., 2015). These observations suggest the existing empirical conversion schemes should be treated with caution. Citing problems with the conversion equations, some laboratories have elected to simply report and interpret shale thermal maturity based on BR_o without conversion (Valentine et al., 2014; Zhou et al., 2014), whereas others view BR_o as a poor maturity parameter due to solid bitumen mobility and variety of origin (Petersen et al., 2013). We have compiled some of the more commonly cited expressions to relate solid bitumen reflectance to a vitrinite reflectance equivalent in Table 3. However, we do not advocate converting a measured solid bitumen reflectance value to a vitrinite reflectance equivalent for the reasons cited above. We observe here that petrographic studies are warranted to document mobility of 'solid' bitumens at reservoir temperatures and pressures via heating stage approaches. Similar to the chromatographic migration fractionation effects observed via solvent extraction of rock samples and in produced hydrocarbons (Leythaeuser et al., 1984), we should be able to observe and document migration fractionation effects in solid bitumen reflectance and other properties, e.g., chemical evolution as revealed through μ -FTIR analysis.

4.4.3. Zooclast reflectance

Another common vitrinite-like organic material occurring in shale is zooclasts, including graptolites (in Paleozoic-age rocks), chitinozoa, and scolecodonts (Petersen et al., 2013; ASTM, 2015a; Hartkopf-Fröder et al., 2015). These materials have a gray reflecting surface similar to vitrinite and solid bitumen but can be differentiated (with care) based on their unique morphologies. For instance, graptolite periderms have

arcuate shapes and sharp boundaries with the rock matrix (Cardott and Kidwai, 1991) with fusellar banding best recognized in sections parallel to bedding (Thomas Gentzis, Core Laboratories, written communication, 2016) whereas chitinozoa are shaped like bottles or flasks (Goodarzi, 1985b). Teeth-like scolecodonts can be difficult to distinguish from conodonts although workers have applied micro-spectrometry techniques to show contrasting chemical compositions (Marshall et al., 2013). Although zooclasts increase in reflectance with thermal maturity advance, the trend is not exactly the same as for vitrinite and therefore analysts have devised calibration schemes to relate zooclast reflectance to an equivalent vitrinite reflectance value (e.g., Goodarzi and Norford, 1989; Bertrand, 1990; Petersen et al., 2013, among others). Graptolite reflectance is most commonly used and has been discussed in recent reviews (Suarez-Ruiz et al., 2012; Hartkopf-Fröder et al., 2015). Although zooclast reflectance has been widely applied to highly mature source rocks outside of North America (e.g., Varol et al., 2006; Luo et al., 2016; İnan et al., 2016) it has received little application in the North American shale plays (although zooclast reflectance appears to show thermal maturity consistent with produced hydrocarbon products in the Utica and Marcellus plays; Thomas Gentzis, written communication, 2016). Zooclast reflectance may be underutilized because, apart from the Cambrian Conasauga and Ordovician Utica shales, most North American resource plays are Devonian and younger, thereby allowing the application of vitrinite reflectance to determine thermal maturity. However, in one recent example, Haeri-Ardakani et al. (2015a,b) used reflectance measurements of chitinozoa and graptolites in Ordovician Utica Shale from southern Quebec to show late oil to dry gas window thermal maturity levels were related to present-day burial depth.

4.5. Comparison to geochemical thermal maturity parameters

Basic source rock geochemistry as determined by total organic carbon analysis (TOC) and Rock-Eval or an equivalent programmed pyrolysis method is a key component in assessing source rocks and shale plays (e.g., Barker, 1974; Peters, 1986; Tissot et al., 1987; Peters and Cassa, 1994; McCarthy et al., 2011; Carvajal-Ortiz and Gentzis, 2015; Hart and Steen, 2015; Curiale and Curtis, 2016; Peters et al., 2016). Data from these complementary approaches should be considered in conjunction with information from organic petrography. TOC measurements typically are performed by combustion of acidified samples whereas programmed pyrolysis uses a temperature ramp (typically 25 °C/min) to measure three parameters, termed S1 (vaporized free hydrocarbons or thermal distillate), S2 (cracked kerogens), and S3 (from decomposition of oxygen-containing compounds (Fig. 9A)). S2 and S3 are used to compute hydrogen and oxygen indices (HI: $S2 * 100/TOC$; OI: $S3 * 100/TOC$) which allows for kerogen typing via the widely-used pseudo van Krevelen diagram (Fig. 9B). Fields on the pseudo van Krevelen diagram correspond broadly to different kerogen types: Type I containing primarily long-chain n -alkanes ($>C_{25}$) representative of lacustrine algae, Type II containing shorter chain n -alkanes ($<C_{25}$) with significant cyclization and aromatic moieties representative of typical planktic marine algae, and Type III containing aromatic functions from cellulosic precursors and a small waxy component from plant exine (reviewed in Vandembroucke and Largeau, 2007). Some researchers assign a Type IV kerogen to C-rich materials with little generation potential including terrestrial carbonized wood (e.g., Jaeger, 2013) and high maturity solid bitumen (Hackley, 2012; Valentine et al., 2014). Dembicki (2009) noted that source rocks seldom contain only one kerogen type and their mixtures can give misleading results, complicating interpretation and illustrating the need for complementary organic petrographic information in shale appraisal. A common misconception in the shale literature is that Rock-Eval analysis can identify a 'kerogen' type in high maturity shale systems; however, oil-prone kerogens convert to hydrocarbons which are expelled from the shale or are retained and present as solid bitumen. Therefore, because solid bitumen is the

Table 3

Simple algebraic expressions to relate solid bitumen reflectance to a vitrinite reflectance equivalent. See also Petersen et al. (2013) and Mählmann and Le Bayon (2016).

Expression	Reference
$R_o = 0.618 * BR_o + 0.40$	Jacob (1989)
$R_o = (BR_o + 0.03)/0.96$	Bertrand (1990)
$R_o = (BR_o - 0.13)/0.87$	Bertrand (1993)
$R_o = 0.618 * BR_o + 0.40$ (for $BR_o \leq 0.52\%$); $R_o = 0.277 * BR_o + 0.57$ (for $BR_o > 0.52\%$)	Riediger (1993)
$R_o = (BR_o + 0.41)/1.09$	Landis and Castaño, (1995)
$R_o = (BR_o - 0.059)/0.936$	Bertrand and Malo (2001)
$R_o = (BR_o + 0.2443)/1.0495$	Schoenherr et al. (2007)

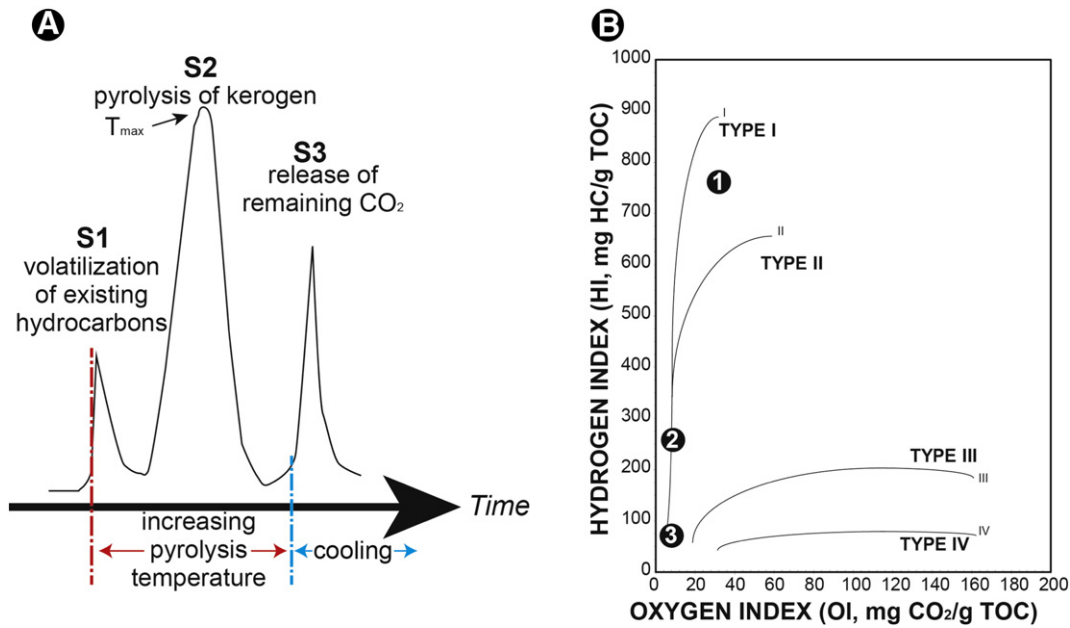


Fig. 9. A. Idealized pyrolysis output showing S1, S2 and S3 peaks. From Laughrey (2014). B. Pseudo van Krevelen kerogen typing diagram used as a screening tool showing evolution pathways for different kerogen types and thermal evolution of Type II kerogen from marine shale: 1. early oil window Type II kerogen (based on petrography) from marine shale (Boquillas Formation, from Hackley et al., 2015), 2. peak oil window mature Type II kerogen from marine shale (Bakken Formation), and 3. dry gas mature Type II kerogen from marine shale (Barnett Shale).

dominant present-day organic matter in thermally mature shale which is analyzed by Rock-Eval and shown in the kerogen typing plot, it is inappropriate to refer to the analysis as representative of a particular 'kerogen' type beyond peak-oil thermal maturity conditions. Rather Rock-Eval is a bulk analytical approach which combines in its output (S1–S3) the total carbon, hydrogen and oxygen occurring in the present-day organic matter (kerogen and/or solid bitumen) of a sample.

The pyrolysis temperature of the Rock-Eval S2 peak (T_{max}) is used as a thermal maturity parameter and can be related to equivalent R_o values from empirical data sets (Jarvie et al., 2001; Laughrey, 2014). Laughrey (2014) provided the equation $R_o(\%) = (0.01867 \pm 0.00063) * T_{max} - (7.306 \pm 0.284)$ for Barnett and Woodford shales (Fig. 10). However, T_{max} values are dependent on organic matter type (e.g., Tissot et al., 1987) and R_o conversions should be applied with caution and only if considering similar lithologies. Even for similar lithologies, R_o – T_{max} correlations may need to be uniquely calibrated. For example, Wüst et al. (2013a) provided a different regression equation of $R_o(\%) = 0.0149 * T_{max} - 5.85$ for the Duvernay Formation of Alberta. The Production Index [$S1/(S1 + S2)$] from Rock-Eval also is used as a thermal maturity parameter with values >0.1 indicating entrance to the oil window.

Carvajal-Ortiz and Gentzis (2015) reviewed application of basic Rock-Eval pyrolysis and TOC data with vitrinite reflectance measurements in the context of recognizing good vs. poor data quality and its impact on shale play appraisal. The discussion below of individual North American shale plays includes reference to kerogen type both as determined through pyrolysis and organic petrography.

5. North American shale petroleum systems

'Shale petroleum systems' refers to a broad set of fine-grained hydrocarbon source rocks, ranging from micrite to mudrock, and the term 'shale' generally is accepted for a variety of lithologies in the context of unconventional hydrocarbon resources. A list of shale properties important for development of successful tight oil and shale gas is compiled in Table 4. This list is not exhaustive nor meant to emphasize certain properties over others. Exploration for shale hydrocarbon resources has occurred in almost every basin in North America where shales with

sufficient organic carbon of oil-gas window thermal maturity occur. Cardott (2008) listed 50+ shales as potential gas exploration targets and the more important units in the conterminous United States are shown in Fig. 11. In the remainder of this paper, we review the application of light and electron microscopy techniques to the organic petrology of the important North American shale plays, beginning with tight oil and concluding with condensate and dry gas. Many of the shale plays are present across a range of thermal maturity windows; presentation in this manuscript is arranged via the dominant hydrocarbon product, which is dependent on other variables besides thermal maturity, including drilling engineering and completion technology, well economics, and production and delivery infrastructure.

While all of the North American shale plays are developed in marine rocks which originally contained a Type II kerogen, organic petrology documents the dominant presence of solid bitumen in thermally mature systems (e.g., Rippen et al., 2013; Kondla et al., 2015; Emmanuel et al., 2016; Van de Wetering et al., 2016). This material constitutes the main component of the measured TOC content in tight oil and shale gas systems as observed via petrography or as demonstrated by comparison of un-extracted vs. solvent-extracted pyrolysis results (e.g., Fishman et al., 2014; Han et al., 2015) or pore measurement results (Valenza et al., 2013; Zargari et al., 2015). As stated earlier, solid bitumen is generated across the full range of shale thermal maturity (immature to overmature) from a broad variety of processes including early generation of hydrocarbons from kerogen in source rocks and from late alteration of liquid oils by devolatilization, water washing and biodegradation.

Some analysts in thermally mature shale systems have interpreted TOC measurements as representative of the original kerogen present, using TOC concentrations to assign depositional facies and conditions of the sedimentary environment (e.g., Loucks and Ruppel, 2007). However, identification of TOC in mature shale systems as derived principally from solid bitumen (e.g., Lan et al., 2015a) suggests that such interpretations are not straightforward, especially considering that solid bitumen can be a mobile phase in subsurface conditions (e.g., Walls and Sinclair, 2011; Sokol et al., 2014; Cardott et al., 2015; Haeri-Ardakani et al., 2015b; Kus et al., 2015). A number of workers have discussed approaches to estimate an original TOC or HI from

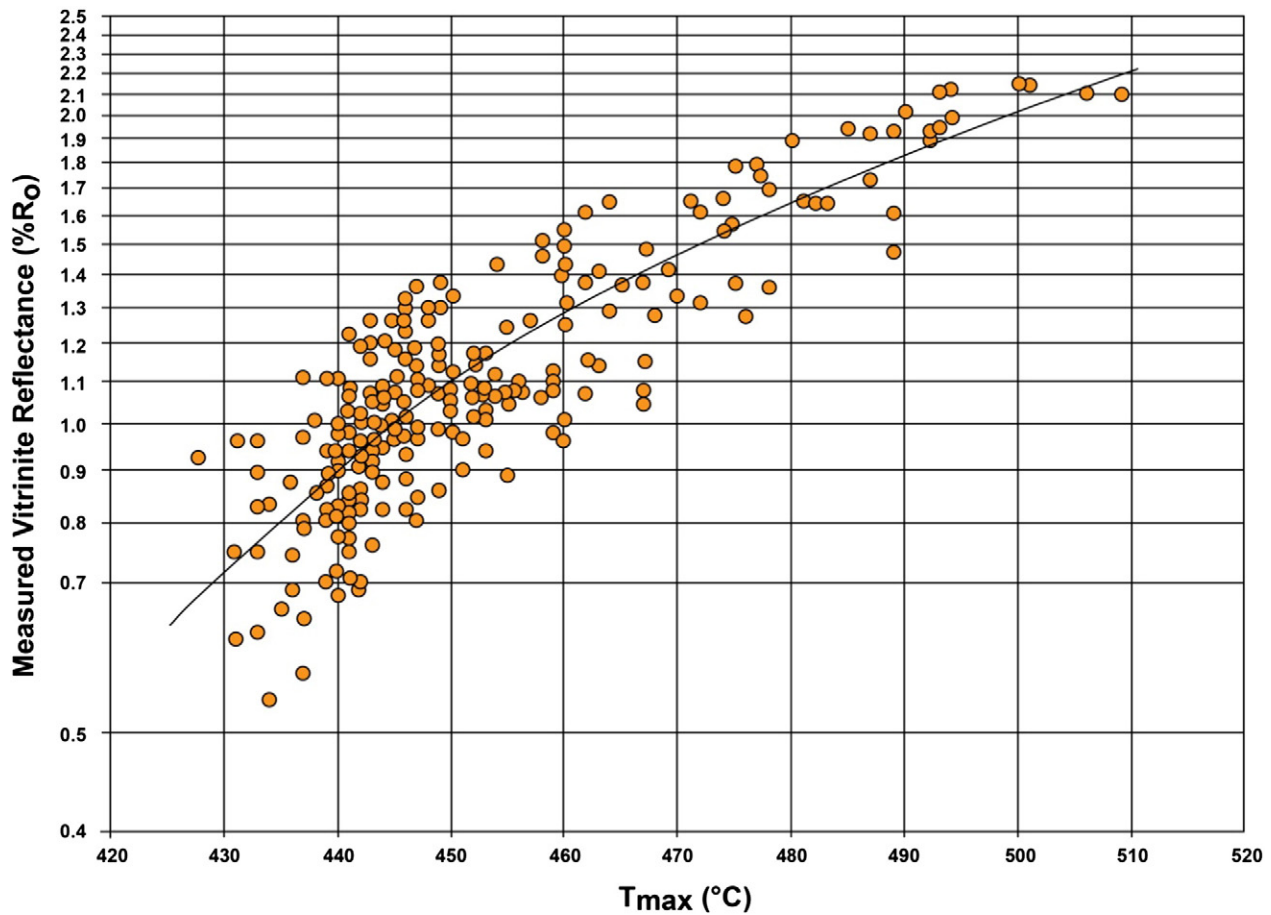


Fig. 10. Measured vitrinite reflectance vs. T_{max} for Woodford and Barnett shale samples. Shown with permission of Richard Drozd, Weatherford Laboratories. From Laughrey (2014). All pyrolysis by Rock-Eval II with samples containing >0.5 mg HC/g TOC ($n = 245$). Relationship shown by best fit line is $R_o(\%) = (0.01867 * T_{max}) - 7.306$.

present-day Rock-Eval properties (e.g., Banerjee et al., 1998; Cornford et al., 1998; Dahl et al., 2004; Jarvie et al., 2007; Romero-Sarmiento et al., 2013) but these approaches rely on assumptions that may be difficult to substantiate. Most workers accept that low permeability of shale systems (nD) prevents complete expulsion of generated hydrocarbons (e.g. Sanei et al., 2015a, and references therein), which may allow interpretation of TOC measurements of solid bitumens in thermally mature systems as partially representative of original kerogen concentrations. Caution is needed and the assumptions that are made must be explicit.

Table 4

Important properties for successful tight oil and shale gas development. From Miller (2014).

Geological properties
Thermal maturity
Organic richness and type
Reservoir thickness
Reservoir pressure
Gas in place/oil in place
Fracture spacing and connectivity
Brittleness (mineralogy)
Matrix permeability
Depth
Stress Field
Fluid compatibility
Other considerations
Exploration and production infrastructure
Service availability
Proximity to market

Work on 'tight' gas systems has observed a negative correlation between solid bitumen abundance, pore throat radius and permeability (Wood et al., 2015), leading to the general conclusion that solid bitumen occludes porosity and degrades reservoir quality (e.g., Jarvie et al., 2007). However, observation of an open organic porosity created by solvent extraction of oil mature shale (Löhr et al., 2015) may imply solid bitumen provides storage capacity and migration pathways for hydrocarbons (e.g., see discussion in Cardott et al., 2015). In fact, wetting experiments show spontaneous imbibition of an oil-phase into Montney Formation shale samples with an interconnected solid bitumen network, and water imbibition instead into Horn River Formation shale samples with poor connectivity of organic matter (Lan et al., 2015b).

Organic petrographers commonly observe solid bitumen embayed against euhedral carbonate crystal faces, an obvious texture which is used to distinguish solid bitumen from vitrinite in shales. This texture is present at all thermal maturities, ranging from immature oil shale to tight oil to shale gas (Fig. 12). Classical concepts of wettability indicate this texture is representative of an oil-wet reservoir (e.g., Donaldson and Alam, 2008) and presumes water-wet conditions existed prior to emplacement of hydrocarbons (Abdullah et al., 2007), allowing growth of carbonate at an interface to which dissolved cations (X^{2+}) and carbonate (CO_3^{2-}) were delivered from formation waters. Concepts of carbonate diagenesis invoke formation of organic acids in shale during kerogen conversion in oil window conditions and their subsequent migration into conventional sandstone and carbonate reservoirs where they control carbonate stability (MacGowan and Surdam, 1990). However, hydrocarbons are present from early diagenesis in shale systems, particularly in sulfur-rich kerogen systems which crack at lower temperatures (Orr, 1986; Lewan, 1998). This observation suggests organic

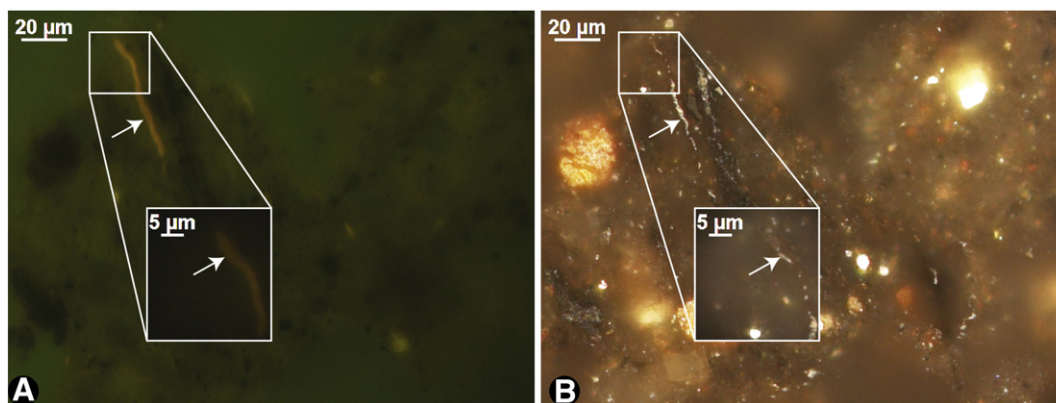


Fig. 13. Lower Cretaceous Skull Creek Shale (Denver–Julesburg Basin, Colorado, $\sim 0.5\%$ R_o) showing fluorescent alginite in the process of kerogen conversion to hydrocarbons and a micrinite residue. A. Blue light fluorescence, oil immersion. Unlabeled arrows point to fluorescent alginite with micrinite residue. B. Same field as A under white incident light.

acid buffering of formation waters can occur at low temperature conditions wherein carbonate phases precipitate from a thin water film separating the crystal surface from contemporaneous early mobile oil. Owing to the prevalence of this texture, heating stage studies which document its low temperature development are warranted in shale systems.

5.1. Tight oil

The term ‘tight oil’ is used herein to indicate a low permeability reservoir where hydraulic fracturing is required to recover economic concentrations of primarily liquid hydrocarbons, e.g., the Bakken or Eagle Ford plays, as opposed to the term ‘shale oil’ which is oil produced from immature kerogen contained in oil shale deposits (Boak, 2012; Reinsalu and Aarna, 2015). Organic petrology is a powerful tool to delineate the oil window (~ 0.6 – 1.2% R_o) in tight oil systems, especially conditions of early, peak, and postoil generation. Organic petrographic approaches to tight oil plays can document the kerogen conversion process wherein oil-prone organic matter is observed in transition to hydrocarbons. For instance, fluorescent alginite in the Lower Cretaceous Skull Creek Formation of Colorado is observed partially converted to a micrinite residue (Fig. 13A–B) in early mature facies ($\sim 0.5\%$ R_o). Stasiuk (1993) noted alginite in the process of thermally- or microbially-induced conversion to bituminite in low maturity Bakken shales of the Williston Basin in Canada. Bertrand and Héroux (1987) described low reflecting solid bitumens evolving from alginite in shallow marine Silurian and Ordovician strata from Anticosti Island, Quebec, Canada. Such observations for evaluation of tight oil systems are only possible with fluorescence microscopy, whereas this approach is not useful in higher maturity shale gas systems where oil-prone kerogens have converted completely to non-fluorescent solid hydrocarbon residues. In the following sections, we document organic petrography applications to several of the more important North American tight oil plays.

5.1.1. Bakken Formation

The USGS estimated undiscovered unconventional oil resources of 7.4 billion barrels in the Devonian–Mississippian Bakken and Three Forks Formations in the USA portion of the Williston Basin (Fig. 14A) (Gaswirth et al., 2013). Almost 90% of oil production in 2010 was from horizontal wells (Energy Information Administration, 2011). Over 5700 horizontal Bakken wells went on production between January 2013 and January 2016 (IHS Energy Group, 2016) and analysis of horizontal well data by McNally and Brandt (2015) resulted in forecast of ~ 1 million barrels (bbls) of oil per day production for the next 20 years. Important hydrocarbon source rocks in the Bakken Formation include upper and lower black, organic-rich mudstones. These two

mudstone members are separated by organic-lean lithologies (LeFever, 1991; LeFever et al., 2011), from which most current unconventional oil production occurs (Fishman et al., 2015). Total organic carbon content in some Bakken shales ranges up to >30 wt.% (Stasiuk, 1993; Lillis, 2013), whereas thermal maturity ranges from immature ($T_{max} < 435$ °C) to late oil window/early wet gas condensate ($T_{max} > 450$ °C) (Nordeng and LeFever, 2009; Jin and Sonnenberg, 2014). Most oil production occurs in western North Dakota in the geographic center of the Williston Basin where thermal maturity is highest (Fig. 14B) (Jin and Sonnenberg, 2012).

Stasiuk (1993) described kerogen in low-maturity Bakken shales from Canada as consisting of two primary components: 1. bituminite, comprised of dark brown fluorescent to non-fluorescent amorphous granular groundmass which forms micro-laminae, and 2. unicellular algae (alginite), which showed textures suggesting it was partially degraded to bituminite. Most organic material was interpreted as originating from the water column during “algal bloom episodes”. Presence of fine-grained, granular, high-reflecting micrinite was interpreted as a microbial breakdown product of bituminite. Later work by Smith and Bustin (1998) supported the interpretation that planktonic organic matter from the surface photic zone was delivered to deep basinal sediments where it was preserved by anoxia, and a regional organo-facies evaluation of Devonian–Mississippian strata in the Western Canada Sedimentary Basin also interpreted Bakken deposition as occurring in deep to intermediate paleo-water depths (Stasiuk and Fowler, 2004). Stasiuk (1994) investigated fluorescence properties of alginite in Bakken shales as a function of thermal maturity, observing a pronounced red shift in wavelength of peak fluorescence intensity coincident with the onset of hydrocarbon generation. Price and Barker (1985) and Jarvie et al. (2011) noted the possibility of vitrinite reflectance suppression in oil window maturity Bakken samples; however, this may result from misidentification of solid bitumen as vitrinite. Newman et al. (2013) applied a vitrinite–inertinite reflectance and fluorescence (VIRF; Newman, 1997) technique to Bakken samples from Parshall Field, concluding vitrinite with suppressed reflectance was present in upper and lower Bakken members and could not be distinguished on the basis of morphology. According to these analysts, suppressed vitrinite reflectance was $\sim 0.3\%$ lower than ‘true’ vitrinite reflectance, which is around 0.85% in the early peak oil window at Parshall. Zargari et al. (2015) used a maturity sequence of ten Bakken samples for a study of pore size distribution, specific surface area and geochemical properties. They found “recovery of the pore system” with successive extractions, suggesting “removal of soluble, oil-like organic material.” Fishman et al. (2015) described amorphous organic matter (AOM) in the Upper Bakken mudstone as present in variable abundance within all facies associations, imparting the dark color to the rock in core and thin section. They interpreted the AOM as a marine-derived kerogen deposited from

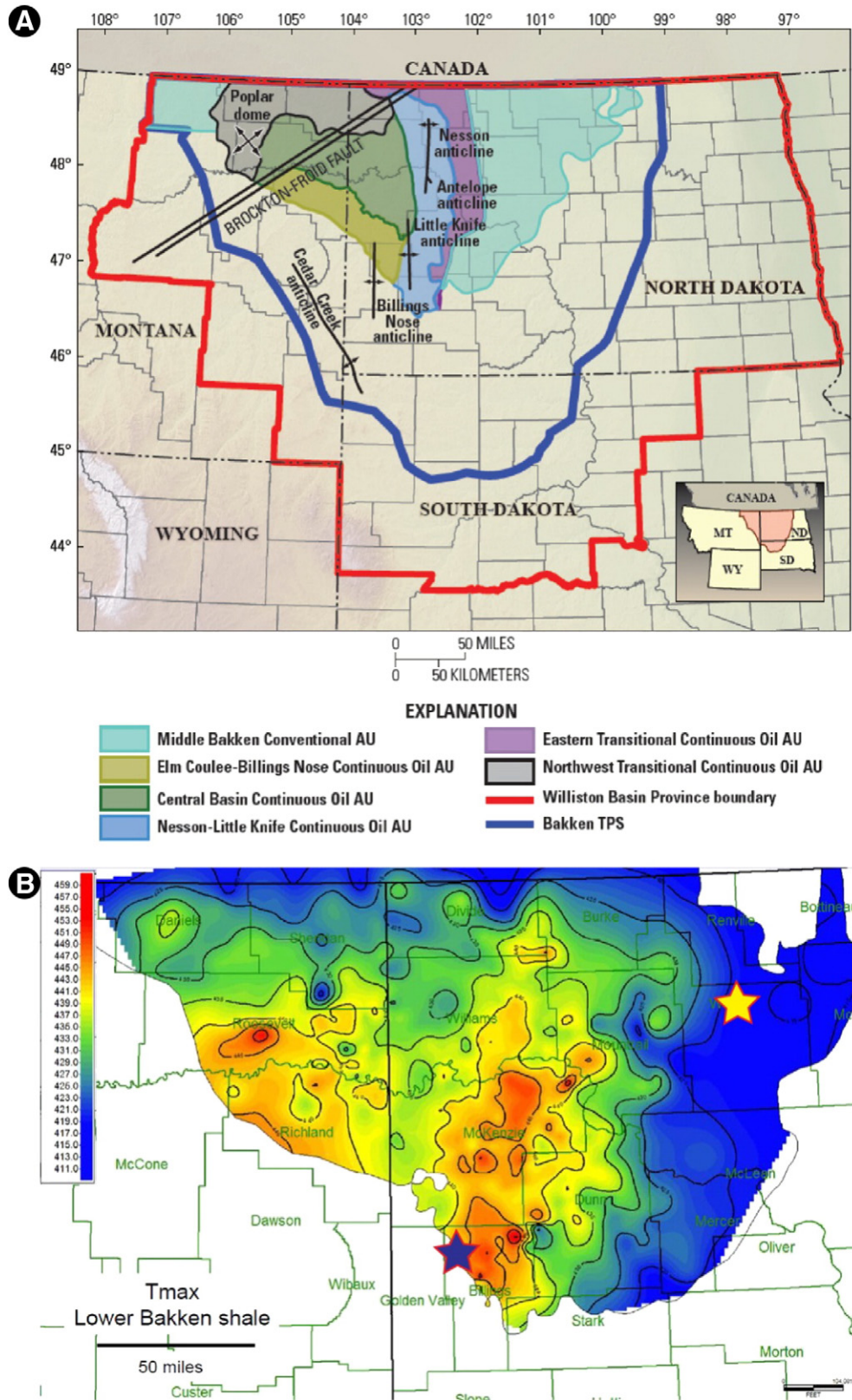


Fig. 14. Maps of the Bakken Formation. A. Assessment units (AU) used by the USGS. From Gaswirth et al. (2013). TPS, total petroleum system. B. Thermal maturity of the Lower Bakken shale from T_{max} . From Jin and Sonnenberg (2012). Yellow star with red border shows location of immature ($\sim 0.32\% BR_0$) Upper Bakken sample in Ward County, North Dakota. Purple star with red border shows location of peak oil window ($\sim 0.90\% BR_0$) Upper Bakken sample in Billings County.

organo-mineral ‘marine snow’ [and noted its intimate association with very fine-grained ($<5 \mu m$) clay minerals, quartz, feldspar, and dolomite].

In an immature (mean $BR_0 \sim 0.32\%$; TOC 14.59 wt.%) Upper Bakken sample from 7652 ft. (2332 m) in the Clarion 1–20 Fleckton well in Ward County, North Dakota (Fig. 14B), most organic matter is finely

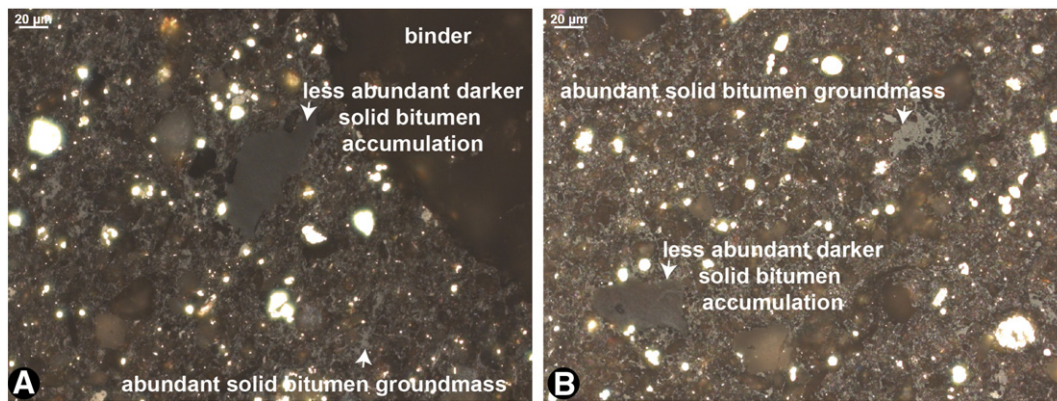


Fig. 15. Photomicrographs (oil immersion, incident white light) of peak oil window Upper Bakken shale from 10,353.1 ft (3156 m) in the Whiting BN 1-23H well in Billings County. A. Dark, less abundant solid bitumen accumulation (sometimes granular) in groundmass of brighter (~0.9% BR_o) solid bitumen. B. A second example of dark, less abundant solid bitumen accumulation (sometimes granular) occurring in groundmass of brighter (~0.9% BR_o) solid bitumen.

comminuted fluorescent and amorphous bituminite. Solid bitumen with groundmass texture (Fig. 6) and variable fluorescence also is abundant and may represent exudate from the bituminite. The solid bitumen (low-gray reflecting surface) typically is associated with brightly reflecting granular micrinite. Some isolated brighter solid bitumen is present locally, possibly representing more mature accumulations that have undergone migration fractionation. Minor discrete telalginite is present, as well as some dispersed inertinite. This description is consistent with description of low maturity Bakken shale samples from the Canadian portion of the Williston Basin (Stasiuk, 1993).

Fig. 15A–B shows photomicrographs of a peak oil window (BR_o ~0.90%; 10.59 wt.% TOC) Upper Bakken sample from the southerly

edge of the play near the depositional limit of the Bakken in the Billings Nose area (Fig. 14A–B). This sample is from 10,353.1 ft. (3156 m) in the Whiting BN 1-23H well in Billings County, the most thermally mature area in the Bakken play with produced hydrocarbon GOR values >6000 (Energy Information Administration, 2011) and T_{max} values >450 °C (Jin and Sonnenberg, 2014). Non-fluorescent groundmass solid bitumen constitutes a large portion of the rock matrix with some fine-grained inertinite (wind-blown char) also present. Groundmass solid bitumen locally is cracked to a granular high-reflectance micrinite residue. Larger bitumen accumulations show brightness variations presumed related to metal content (Brett Valentine, USGS, written communication, 2015). Some less-common larger, darker, granular solid

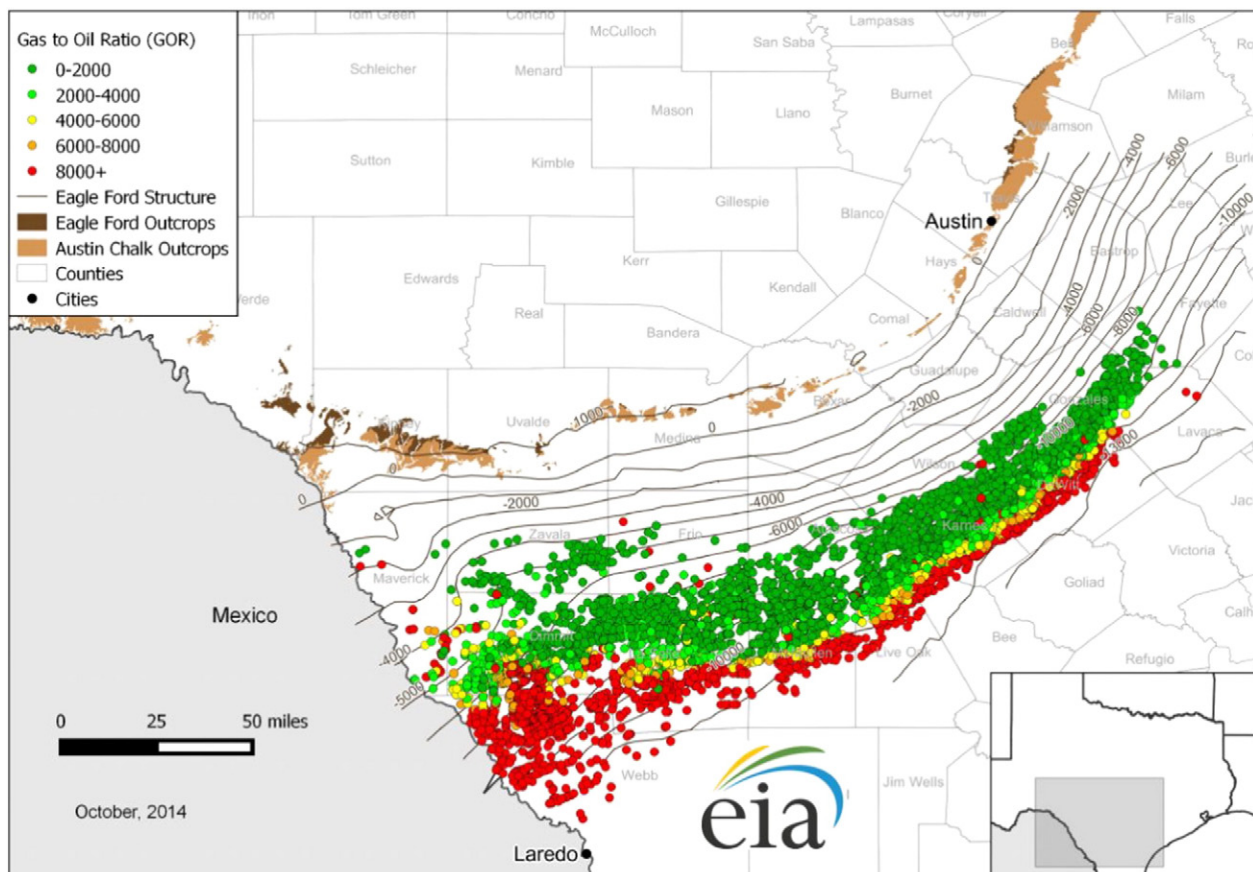


Fig. 16. Map of initial gas-to-oil ratio (GOR, in cubic feet per barrel) in Eagle Ford wells. (Source: From Energy Information Administration (2014)).

bitumen accumulations slough and etch in fluorescent light. Groundmass solid bitumen has mean BR_o of 0.90% (representing in situ thermal maturity) and the granular low reflectance solid bitumen has BR_o of 0.45–0.65%. As described above, solid bitumen constitutes the majority of the organic matter in this thermally mature shale sample, indicating that a geochemical ‘kerogen’ type obtained from pyrolysis is rather a measure of the relative H richness of the solid bitumen present. Based on transmitted light thin section and SEM investigation, Fishman et al. (2015) interpreted organic matter in this core as derived from a planktonic kerogen deposited as ‘marine snow’ sensu Macquaker et al. (2010); however, as described here, incident light organic petrographic observation indicates the organic matter is solid bitumen.

5.1.2. Eagle Ford Formation

Development of the Upper Cretaceous Eagle Ford Formation in south Texas has included >15,000 horizontal wells put on production between January 2008 and January 2016 (IHS Energy Group, 2016). Following the decline of oil prices from mid-2014, oil production peaked in early 2015 at about 1.65 million bbls/day and has since retreated to about 1.2 million bbls/day as of January 2016 (Energy Information Administration, 2016). The Eagle Ford consists of interbedded marl and limestone, deposited in distal waters on a sediment-starved marine carbonate platform (Denne et al., 2014; Lowery et al., 2014; Eldrett et al., 2015). Strata dip towards the Gulf of Mexico and well depths range from about 4000–14,000 ft (1200–4200 m) below surface with thermal maturity and produced hydrocarbon product generally corresponding to present-day burial depths (Energy Information Administration, 2014; Fig. 16), except in the western Maverick Basin where Laramide tectonics have produced basin inversion structures (Wayne Camp, Anadarko, written communication, 2016).

Despite the importance of unconventional hydrocarbon production from the Eagle Ford, there are few public studies which have used a traditional organic petrology approach. Robison (1997) described kerogen concentrates from organic-rich (1–8 wt.% TOC) mudstone samples from outcrops near Waco and Austin, Texas. High HI values from some lower Eagle Ford samples (>500 mg HC/g TOC) and the presence of abundant amorphous fluorescent kerogen (60–75% of total kerogen) were interpreted to indicate good source potential from oil-prone Type II marine kerogen. Thermal maturity was not explicitly addressed; however, T_{max} values <430 °C and PI values <0.1 suggest his samples were immature for hydrocarbon generation. Similar TOC contents were observed in immature Eagle Ford mudstone outcrop samples in a chemostratigraphic study by Boling and Dworkin (2015), who proposed that high organic productivity during lower Eagle Ford deposition created anoxia in bottom waters. As part of a larger study Hackley et al. (2015) described the organic petrology of early mature (~0.50% R_o) Boquillas Formation marl from west Texas (Eagle Ford equivalent) with abundant vitrinite, inertinite, and solid bitumen. Solid bitumen varied in presentation, including low-reflecting fluorescent solid

bitumens in-filling primary porosity in planktic foraminifera as well as higher reflectance solid bitumens present in the mineral matrix. Amorphous organic matter with moderate fluorescence was present in addition to discrete algal bodies. Fig. 17A illustrates gas condensate window thermal maturity (~1.2% BR_o) organic-rich (~6 wt.% TOC) Eagle Ford shale core sample containing abundant foraminifera, mostly filled with secondary carbonate and non-fluorescent solid bitumen. Streaks of solid bitumen are present, and solid bitumen also is finely disseminated in the groundmass as a fine-grained network. Vitrinite and small fragments of inertinite are present locally. In Fig. 17B a dry gas window (~1.8% BR_o) organic-rich (5.1 wt.% TOC) Eagle Ford sample shows many of the same features.

Edman and Pitman (2010) reported difficulty obtaining vitrinite reflectance measurements on oil window mature (0.6–1.2% R_o) Eagle Ford samples from First Shot Field (7200–9200 ft.; 2200–2800 m) because vitrinite was rare. These workers noted S contents generally were >1 wt.% in produced Eagle Ford oils, concluding oils were sourced from a Type IIS marine kerogen. Source rock extract analyses were included in their study; however, S concentrations of extracts were not determined or not reported. Based on similarities between Eagle Ford oils and extracts for Pr/Ph, C_{29}/C_{30} hopane and other biomarker ratios, Edman and Pitman (2010) concluded Eagle Ford oils were sourced from both marl and shale layers within the Eagle Ford which mixed during short distance migration. Despite the fact that published organic petrology studies are lacking in the Eagle Ford, microscopy has been performed for hydrocarbon exploration and the information included as supporting information, e.g., R_o values, in industry reports (Cusack et al., 2010).

Many workers have applied SEM approaches in efforts to understand organic porosity in the Eagle Ford. Walls and Sinclair (2011) used ‘digital rock physics’ models generated from 3D FIB-SEM volumes of early oil and mixed oil/condensate/gas thermal maturity core samples. They concluded organic-rich samples with high porosity have higher permeability than organic-poor samples with similar porosity, demonstrating an interconnected porosity in the solid bitumen network. They considered this result preliminary and it was not repeated in later papers by the authors and colleagues which examined additional samples at higher maturity (Driskill et al., 2013a,b). Instead, Driskill et al. (2013b) observed organic matter pore type, size, and permeability to vary with thermal maturity, finding ‘pendular’ or bubble pores in the oil window whereas spongy organic matter with bubble and foam pores developed in the gas/condensate window (Fig. 18). Organic pores in the dry gas window were smaller in average diameter with lower permeability than from the oil window. All organic matter pores were interpreted to result from conversion of organic matter to hydrocarbons.

Jennings and Antia (2013) also observed a relationship between organic porosity and thermal maturity, finding organic pores were not developed in Eagle Ford shales with <0.7% R_o , developing at 0.7–1.0% R_o ,

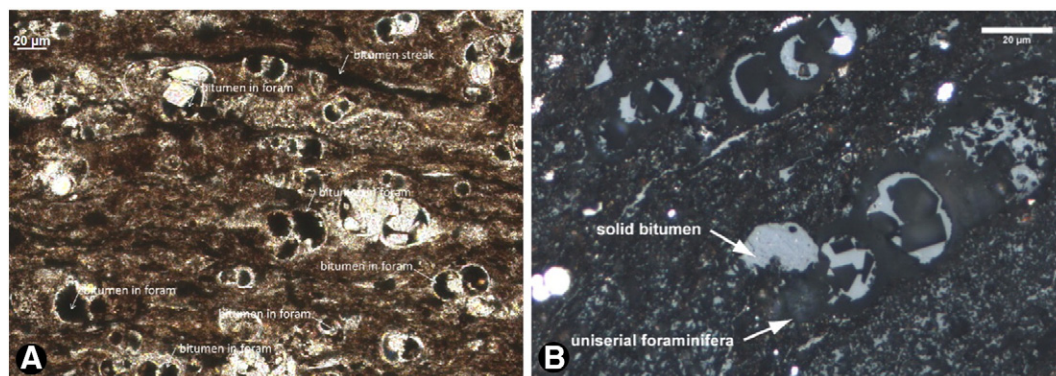


Fig. 17. Foraminifera filled with solid bitumen in A. Wet gas-condensate (~1.2% BR_o) and B. dry gas thermal maturity (~1.8% BR_o) Eagle Ford Formation samples. A. Transmitted, plane-polarized light, oil immersion. B. Incident white light, oil immersion.

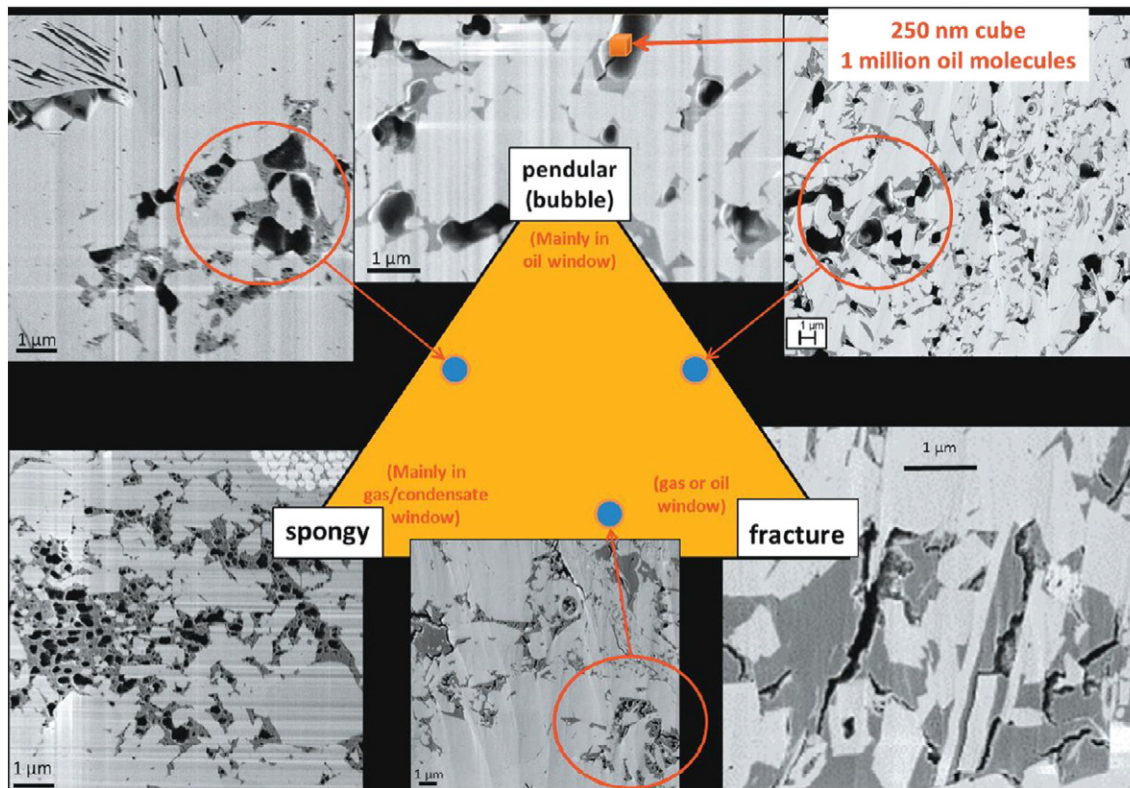


Fig. 18. SEM images showing 3 organic porosity types common in Eagle Ford Formation samples. Pendular organic porosity was most common in oil window thermal maturity whereas spongy porosity is more common in the condensate and gas window. Fracture organic porosity is not common in the Eagle Ford. From Driskill et al. (2013b). (Source: Reprinted by permission of the American Association of Petroleum Geologists, whose permission is required for further use).

best developed in the range 1.4–1.6% R_o and less abundant at values $>1.7\%$ R_o . They indicated that their results showed relationships between pore abundance and type, pore connectivity, and effective permeability. However, these relationships were not quantified in their paper and they also stated “common vertical and lateral variability in the presence and abundance of organic porosity, even in similar microfacies, suggests that the parameters controlling organic nanopore development are not fully understood and deserve additional detailed studies.”

Camp (2014) examined laminated gray to dark gray organic-rich (>2 wt.% TOC) Eagle Ford mudstone from south Texas via FE-SEM using Ar ion-milled samples to identify mineral and solid bitumen cements. Camp (2014) suggested that observations of cements within foraminifera chambers may provide a good method to assess regional variations in diagenesis because these areas were less influenced by variations in matrix grain composition and may therefore serve as stable crucibles from which to make comparative observations. With the possible exception of pyrite, Camp (2014) observed that mineral cements pre-dated organic matter cements. Camp (2015) further addressed the diagenetic evolution of organic matter cements by comparing observations of Eagle Ford samples at different levels of thermal maturity. In his diagenetic model, organic matter cements were interpreted as a byproduct of residual oil retained in the source rock following hydrocarbon expulsion. He concluded that organic matter cements were the most pervasive type of cement observed in the Eagle Ford samples. The impact of organic matter cement on shale reservoir quality was observed to vary with thermal maturity forming bitumen plugs (potential seals) in low thermal maturity updip areas, and connected porous networks in downdip gas mature areas. Camp (2015) concluded that the commonly reported nanopores in organic matter reside within gas mature organic matter cements (solid bitumen), rather than within kerogen particles similar to observations of Bernard et al. (2012a) in the Mississippian Barnett shale (see below).

The organic matter in thermally mature Eagle Ford samples as observed by SEM is dominated by solid bitumen as observed by the presence of void-filling textures. Despite the inability of SEM to differentiate organic matter types other than via textural analysis, identification of this material as solid bitumen (partially soluble) in the Eagle Ford is confirmed by comparison of S1 values of pre- (higher S1) and post-extracted (lower S1) limestone samples (Fishman et al., 2014). These workers also noted organic-rich mudstones showed loss of a low temperature ‘shoulder’ on the S2 peak upon extraction, also interpreted to be due to solid bitumen extraction. Based on textural evidence of solid bitumen embayed against euhedral carbonate, Fishman et al. (2013, 2014) concluded oil wet solid bitumen was emplaced after water wet diagenetic growth of carbonate, consistent with the observations by Camp (2014, 2015).

Pommer and Milliken (2015) used SEM to document destruction of primary porosity with increasing thermal maturity through compaction, cementation and emplacement of solid bitumen. Mineral-associated pores became smaller and less abundant with thermal maturity advance and the best development of organic porosity in Eagle Ford solid bitumen occurred in the wet gas window where pores were about 13 nm in median diameter. Organic pores were present at lower maturities but only in minor volumes and these pores may be artifacts of sample preparation and vacuum pressure conditions or degassing/dehydration of solid bitumens after removal of the sample from the subsurface.

SEM approaches to organic matter characterization have also been used to research mechanical properties of Eagle Ford shale reservoirs. Although not explicitly identifying their samples as Eagle Ford, Emmanuel et al. (2016) examined organic-rich shales “from a carbonate-rich Cretaceous source rock in the southern United States” using SEM and atomic force microscopy techniques. Their work showed kerogen to be stiffer than solid bitumen at all levels of thermal maturity (0.4–1.2% R_o) and that kerogen becomes stiffer with maturation

whereas the stiffness of solid bitumen remained consistent across the oil window.

5.1.3. Niobrara Formation

The Upper Cretaceous Niobrara Formation of the Western Interior Seaway is composed of rhythmically interbedded chalk and marl and is widely distributed throughout the Rocky Mountain basins (Locklair and Sageman, 2008; Tessin et al., 2015). It has been developed as an unconventional tight oil play in the Denver-Julesburg Basin of Colorado and Wyoming (>3000 horizontal wells on production, IHS Energy Group, 2016) and as a gas producer in the Piceance Basin in western Colorado (Durham, 2013a). Petroleum geology was reviewed by Landon et al. (2001) in a regional study which evaluated Rock-Eval pyrolysis data from 43 cores of Niobrara equivalent strata, ranging from the San Juan Basin in New Mexico north to the Williston Basin in North Dakota. These analysts showed TOC contents ranged up to 8 wt.% in marl samples containing primarily a Type II kerogen. In the Denver-Julesburg Basin, marls typically contained 2–4 wt.% TOC with up to 7 wt.% TOC in low maturity samples (Luneau et al., 2011). Petroleum system assessments and related work by USGS provide a regional perspective on Niobrara thermal maturity and burial history (Law, 2002; Pawlewicz and Finn, 2002; Finn and Johnson, 2005).

Interest in the Niobrara as an unconventional tight oil play began in 2009 with the EOG Jake 2-01H well in the Denver-Julesburg Basin (Anderson et al., 2015) and later the WPX Energy “Beast” gas well in the Piceance Basin drilled in 2012 (Durham, 2013a). The Niobrara petroleum system was reviewed by Sonnenberg (2011) as part of the compilation ‘Revisiting and revitalizing the Niobrara in the Central Rockies’ edited by Estes-Jackson and Anderson (2011). However, apart from abstracts (e.g., Curtis et al., 2013; Laughrey et al., 2013) there has been little published on organic petrology and organic geochemistry of the Niobrara petroleum system and, to our knowledge, there are no

Niobrara studies which have focused on a traditional organic petrology approach.

Fig. 19A–B shows an immature (0.4–0.5% R_o ; 0.26% BR_o) organic-rich (6.84 wt.% TOC) Niobrara marl core sample from 591 ft. (180 m) in the Amoco No. 1 Rebecca K. Bounds well from Greeley County, western Kansas (see Dean et al., 1995). Sparse fluorescent telalginite is present in a strongly fluorescent bituminous groundmass; some of the bituminous groundmass is converting to a micrinite and solid bitumen residue. Similar to the Eagle Ford shale, foraminifera are abundant. Sparse vitrinite and inertinite are present. In Fig. 19C–D we show peak oil window (0.98–1.02% BR_o) organic-rich (2.45–3.59 wt.% TOC) Niobrara marl from outcrops at the Cemex quarry near Lyons, Colorado. Broken rock surfaces from fresh outcrops have a strong petroliferous odor. At this thermal maturity the bituminous groundmass has converted to a fine-grained network of non-fluorescent solid bitumen, some of which is granular in texture. Remnant inertinite also is present. The mineral groundmass has a mottled fluorescence and carbonate in-fillings of foraminifera have irregular fluorescence, suggesting the presence of live oil.

5.1.4. Tuscaloosa marine shale

Estimated to contain a 7 billion bbl resource (John et al., 1997), tight oil exploration in the Upper Cretaceous Tuscaloosa marine shale (TMS) of southwestern Mississippi looked promising in 2013–2014 with horizontal well initial production (IP) rates reported at 1000–1500 bbls/day of oil equivalent hydrocarbons (Durham, 2013b, 2014; Unconventional Oil & Gas Report, 2014a,b). Production of 38–45° API gravity oil occurs from the lower TMS section which shows higher log resistivity values (Allen et al., 2014; Goodrich, 2015). Over 70 horizontal wells were on production in mid-2015; however, drilling activity has since waned sharply due to the 2014–2015 drop in oil prices (Durham, 2015a; Unconventional Oil & Gas Report, 2015). In particular, this decline is due to high well costs relative to other shale plays because of deep

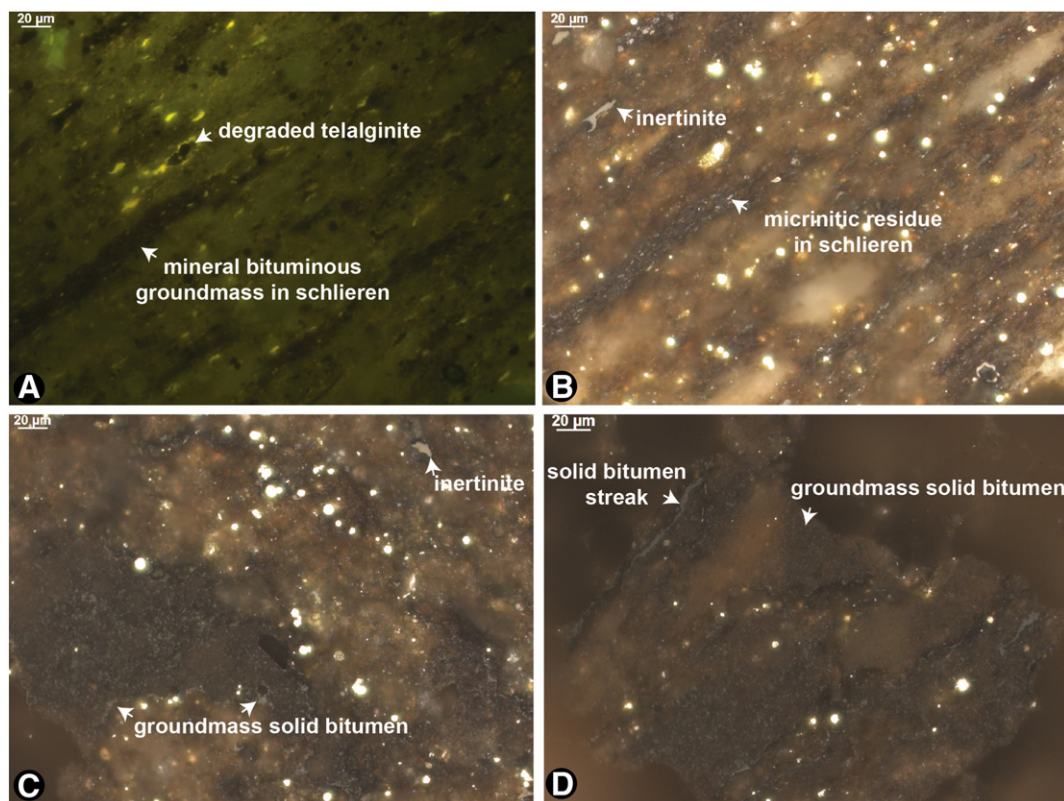


Fig. 19. Photomicrographs (oil immersion) of the Niobrara Formation. A–B. Immature (0.26% BR_o) organic-rich (6.84 wt.% TOC) Niobrara marl from 591 ft. (180 m) in the Amoco No. 1 Rebecca K. Bounds well, Greeley County, western Kansas. A. Fluorescence illumination. B. Same field as A in incident white light. C–D. Peak oil window (~1.02% BR_o) organic-rich (2.75% TOC) Niobrara marl (Niobrara B) from outcrops at the Cemex quarry near Lyons, Colorado, incident white light.

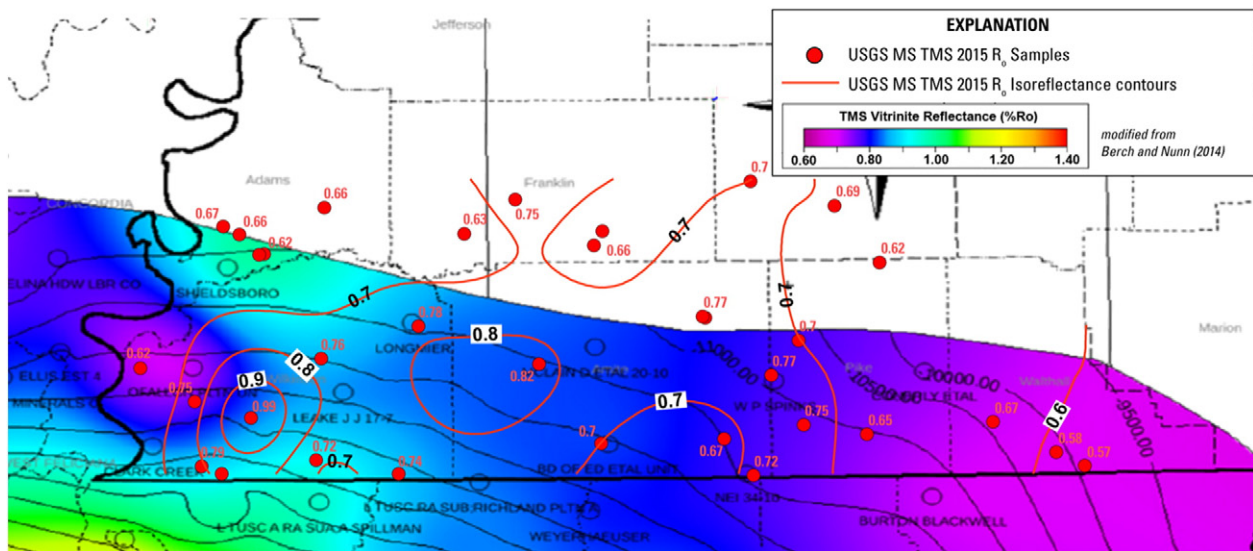


Fig. 20. Preliminary isoreflectance contours in the Tuscaloosa marine shale from modelling study of Berch and Nunn (2014) and unpublished USGS measured reflectance data (courtesy of Brett Valentine, USGS; see Valentine et al., 2015). TMS, Tuscaloosa marine shale.

drilling depths (generally 11,000–12,000 ft.; 3400–3700 m) and high clay content. Thermal maturity increases with present-day depth from early oil window updip to dry gas downdip (Berch and Nunn, 2014; Fig. 20); at present the unconventional play is only in the oil window.

An organic geochemistry study on core samples from the No. 1 Spinks well in Pike County, Mississippi by Miranda and Walters (1992) pre-dated the shale revolution. These researchers found TOC contents generally <1.0 wt.% and indicated “low concentrations of hydrogen-deficient organic matter” were present. Variations in hopane distribution were interpreted to record changes in bacterial consortia in sediments with little variation in overlying water column chemistry and biota. Heath et al. (2011) examined TMS samples through thin section and FIB-SEM to investigate pore networks and sealing character. These workers also reported low concentrations of Type II-III kerogen and TOC contents <1.0 wt.%. Low porosity in organic matter (<0.5%) was interpreted to be interconnected and a potential migration pathway for hydrocarbons. Berch and Nunn (2014) used sonic and resistivity logs to model TOC and R_o across the TMS play area, calibrating their model to a limited number of measured analyses from core and cuttings. Their study showed R_o increased with present-day burial depth in their study area (10,000–19,000 ft.; 3000–5800 m) with local variations related to differences in crustal thickness and thermal conductivity. They also related higher IP rates to locations of higher modelled TOC content while acknowledging that the predictions of their model may be impacted by variations in mineralogy, porosity and natural fractures. Lu et al. (2015) also studied the No. 1 Spinks core previously examined by Miranda and Walters (1992), concluding the TMS was self-sourced with a greater proportion of marine kerogen in the deeper high-resistivity zone as indicated by higher HI values and greater porosity in organic matter.

To date, there have been no studies published describing organic petrology of the TMS although preliminary work by the USGS has indicated the presence of a mixed Type II-III kerogen with dominance of Type III (Valentine et al., 2015) in early-peak oil window thermal maturity samples (0.6–1.0% R_o). Total organic carbon content generally is <1.0 wt.% and average HI values <100 mg HC/g TOC suggest poor source potential. Organic matter is dominated by terrestrial vitrinite and inertinite with minor marine alginite found locally.

In the Lower Tuscaloosa immediately below the TMS, thin shales (10–20 ft.; 3–6 m) with some organic-rich (TOC up to 9 wt.%) layers contain oil-prone kerogen (HI up to 450 mg HC/g TOC) at oil window thermal maturities (0.75–0.8% R_o). A shale sample from 11,068 ft.

(3374 m) in the Samedan No. 2C.W. Andrews well contains a brightly fluorescent organic-rich groundmass with lamellar algal(?) kerogen (Fig. 21A–F). Textures in the lamellar kerogen are suggestive of a cohesive microbial mat which folds and drapes over framboidal pyrite. Fluorescent solid bitumen is abundant and, similar to the TMS, vitrinite and inertinite are present although subordinate in amount to oil-prone kerogen. These thin shales with moderate-good source rock properties at mid-oil window thermal maturity may have sourced conventional oil accumulations in Lower and Upper Tuscaloosa sandstone reservoirs. However, samples were obtained from the tops and bottoms of pre-shale revolution legacy cores (1980s–1990s) which targeted conventional sandstone reservoirs. Therefore, the thickness and regional extent of thin organic-rich Lower Tuscaloosa shales is not known.

5.1.5. Other tight oil systems

Other tight oil systems in North America include shale and mudrock formations in the Western Canada Sedimentary Basin such as the Second White Specks, Exshaw, and Nordegg, the Cline, Wolfcampian and other shales in the Permian Basin of Texas, and marls in the Monterey Formation in the basins of southern California. In some of these cases, the lithologies are present across a range of thermal maturities and thus may also produce condensate and dry gas in some areas (see Duvernay discussed in Section 5.2 below). We cannot address all tight oil units individually; herein we briefly present studies with well-documented organic petrology information, e.g., Second White Specks (Furmann et al., 2014, 2015), or because the shales are important resources in the total production mix, e.g., Wolfcampian shales in the Permian Basin. Moreover, some of the North American tight oil systems are not self-sourced and are unconventional only in the sense that they have received the new applications of horizontal drilling and hydraulic fracturing during the last decades (e.g., Austin Chalk, Granite Wash, Mississippian Lime; Fig. 11); these units are not considered herein.

The Devonian-Mississippian Exshaw Formation of Alberta, also called the “Alberta Bakken” (Hartel et al., 2014) contains high TOC content but is thin at 6 m on average (Creaser et al., 2002) and positive exploration results have so far been sparse (Park, 2013). A study by Caplan and Bustin (1998) documented up to 17 wt.% TOC in low maturity Exshaw shales containing bituminite, dispersed alginite (*Tasmanites* and leiospheres) with lesser amounts of detrital fragmented liptinite (liptodetrinite), and terrestrial inertinite and vitrinite. High TOC contents corresponded to periods of high primary productivity and organic matter preservation under anoxic conditions.

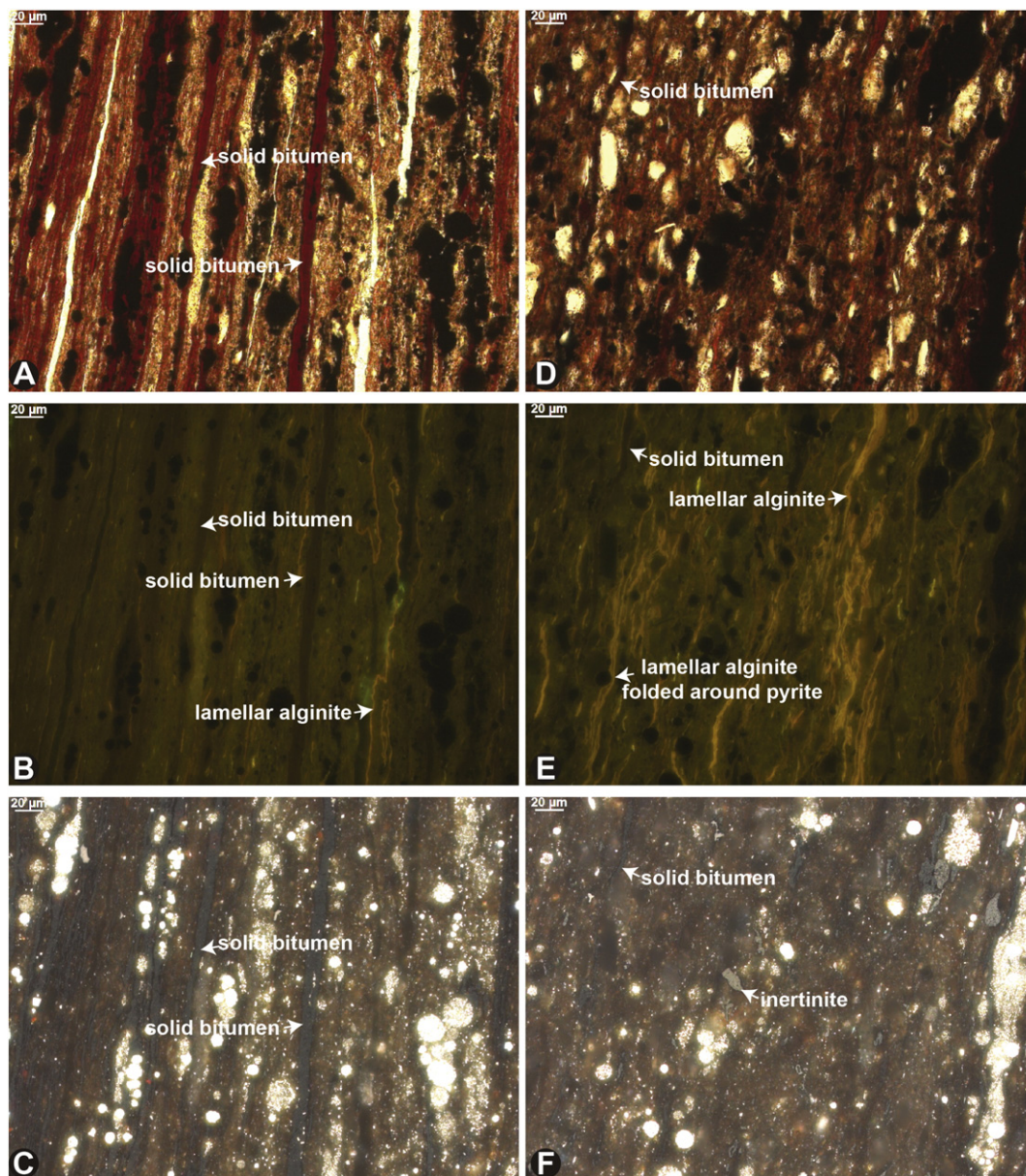


Fig. 21. Photomicrographs (all oil immersion) of organic matter in an organic-rich (~7 wt.% TOC) oil window maturity (~0.75–0.80% R_o) Lower Tuscaloosa shale sample from the Samedan No. 2 C.W. Andrews well at 11,068 ft (3374 m), Amite County, Mississippi. A. Transmitted plane-polarized light. B. Same field as A under blue light fluorescence. C. Same field as A–B in white incident light. D. Transmitted plane-polarized light. E. Same field as D under blue light fluorescence. F. Same field as D–E in white incident light.

Source rock properties of the Lower Jurassic Nordegg Member of the Fernie Formation were examined by Riediger et al. (1990) and Riediger and Bloch (1995) who documented abundant bituminite in low maturity samples with lesser amounts of Type III kerogen. Bituminite is the product of bacterial decomposition of organic matter in a low Fe environment resulting in sulfurization and production of a Type IIS kerogen. In comparison to the similar Duvernay Formation (see below), exploration for unconventional resources has seen little activity (Wüst et al., 2015).

Furmann et al. (2014, 2015) evaluated organic petrology of the Cenomanian-Turonian Second White Specks Formation in the Western Canada Sedimentary Basin, where limited vertical shale exploration wells have had mixed results to-date (Mackay, 2015). Furmann et al. (2014, 2015) reported difficulty finding terrestrial vitrinite and inertinite in the Second White Specks where alginite and AOM dominates the organic matter in samples up through the peak oil window (0.40–0.90% R_o). Solid bitumen was observed in abundances of up to >40 vol.% of the organic matter. Stasiuk and Goodarzi (1988) examined

immature (0.28% R_o) Second White Specks marl samples from southern Saskatchewan and described minor fluorescent *Tasmanites*, acritarchs and dinoflagellates occurring in a matrix of bituminite.

The Early Permian Wolfcampian mudrocks (including Spraberry Formation) of the Permian Basin in Texas are in the peak oil window with TOC contents of up to 6.0 wt.% (Baumgardner et al., 2014). Vitrinite reflectance data compiled by Tucker Hentz of the Texas Bureau of Economic Geology (BEG) from Wolfcampian and Leonardian mudrocks indicated thermal maturities in the early-mid oil window, ranging from 0.4–1.0% R_o with TOC contents of 2–6 wt.% (Tucker Hentz, BEG, written communication, 2016; see also Hamlin and Baumgardner, 2012). Earlier workers showed Spraberry Formation oils were sourced from Spraberry mudrocks containing a Type II marine kerogen in the early oil window (Scott and Hussain, 1988). Pawlewicz et al. (2005) also compiled measured R_o values from strata in the Permian Basin. To our knowledge, Landis et al. (1991) presented the only peer-reviewed study which included organic petrography applied to Wolfcampian shales, describing fluorescence properties of bedding-parallel solid bitumen

(exsudatinite) veins in Wolfcampian shales of peak oil and lower thermal maturity. Their study was part of a larger investigation of shale in the Permian Basin which described Wolfcampian strata as comprised of mature source rocks with oil and oil/gas prone organic matter rich in liptinite, mainly *Tasmanites* telalginite and detrital unstructured material (mineral bituminous groundmass or bituminite), and poor in vitrinite and inertinite (Landis, 1990). Landis (1990) did not use the term 'solid bitumen' in his study but due to the importance he ascribed to exsudatinite we assume fluorescent solid bitumen is present. Given the recent development of Wolfcampian shales as an unconventional tight oil play (Durham, 2015b) new organic petrographic studies are warranted. A digital rock modelling study by Walls and Morcote (2015) applied high resolution FIB-SEM imaging to Wolfcampian shale core samples to compute the properties of total porosity, connected porosity, percentage of solid organic matter, and organic matter-associated porosity. The modelled results were used to derive vertical and horizontal permeability and pore size distributions, showing large variabilities in porosity and permeability as well as allowing visualization of the interconnected nature of organic and inorganic porosity. The authors reached the intuitive conclusion that zones with higher organic porosity should reservoir greater proportions of hydrocarbons than zones with lower organic porosity but difficulties to utilizing this approach to target a landing zone include upscaling to reservoir scale through well log calibration to rock models.

The Miocene Monterey Formation of southern California is the source rock for sulfur-rich oils produced from conventional reservoirs (Orr, 1986). Unconventional exploration has thus far been largely unsuccessful due to the highly tectonized nature of the Monterey and broad variations in its lithology (Brown, 2012; Seeley, 2014). Organic matter ranges up to 23 wt.% TOC content dominated by Type II kerogen (Johnson and Grimm, 2001; John et al., 2002); calcareous nannofossils are abundant (Laurent et al., 2015). In Fig. 22 we show an organic-rich (~6 wt.% TOC) low maturity (~0.25% BR_o) Monterey marl sample containing abundant foraminifera with open and solid bitumen-filled porosity. Dispersed AOM is present in a fluorescent groundmass; rare scattered vitrinite and inertinite also is present. Granular solid bitumen with higher reflectance (~0.53% BR_o) also is present in sparse amounts and may represent a residual product of kerogen conversion.

5.2. Shale condensate and dry gas

Shale condensate and dry gas plays include the original North American play which launched the shale revolution; the Barnett Shale of north-central Texas. Also discussed herein in the context of organic petrology are the Paleozoic shale plays of the Appalachian Basin (Utica, Marcellus), the Woodford Shale in the midcontinent, the Haynesville-Bossier play in the Gulf Coast, and the Duvernay in the Western Canada Sedimentary Basin. Although application of

fluorescence microscopy is not relevant to characterization of shale in the condensate and dry gas windows, organic petrology is still a powerful tool for reservoir characterization, and thermal maturity as determined through reflectance analysis remains a primary component of characterization (Curtis, 2002; Wang and Gale, 2009). Gas adsorption studies have demonstrated a clear and unequivocal correlation between organic matter abundance and adsorption volumes, indicating high TOC, thermally mature marine shales with abundant solid bitumen are the better gas reservoirs (e.g., Zhang et al. 2012; Wang et al., 2016). SEM petrography demonstrates that nanoporosity in organic matter dominantly is present in solid bitumen and increases with thermal maturity due to exsolution of gas phase hydrocarbons (Bernard et al., 2012a; Bernard and Horsfield, 2014), whereas terrestrial organic matter contains little pore volume (e.g., Klaver et al., 2015). In the remaining sections of this paper, we review organic petrology applications in the North American shale condensate and dry gas shale plays.

5.2.1. Barnett Shale

The Mississippian Barnett Shale is the main hydrocarbon source rock in the Fort Worth Basin (Hill et al., 2007) and first produced natural gas through vertical wells beginning in 1981 by Mitchell Energy (Curtis, 2002). About 5700 horizontal wells were put on production between January 2010 and January 2016 (IHS Energy Group, 2016). Bowker (2007) noted a correspondence between TOC content (avg. ~4.5 wt.%) and adsorbed gas-in-place in the Barnett, providing a general rule of thumb that a minimum of about 2.5–3 wt.% TOC is necessary for a viable shale gas reservoir. Thermal maturity ranges from immature in the southwestern part of the basin to overmature in the northeast (Fig. 23) (Pollastro et al., 2007; Romero-Sarmiento et al., 2013).

The Barnett play launched the shale revolution in North America (Zuckerman, 2013; Gold, 2015) and a number of studies have been completed regarding its petroleum system properties and organic geochemistry. Loucks and Ruppel (2007) interpreted Barnett lithofacies to represent deep water anoxic sedimentation which preserved plankton transported from shallower waters. Jarvie et al. (2007) described immature to early oil window Barnett samples from the southern part of the basin as containing a Type II marine oil-prone kerogen based on Rock-Eval (HI 390–475 mg HC/g TOC), composed of "95–100% amorphous (structureless) organic matter with occasional algal *Tasmanites*, confirming the chemical kerogen type" and also noted the presence of minor terrestrial organics. Hickey and Henk (2007) described high TOC (avg. 5 wt.%) "organic shale" from the core shale gas area in Newark East field, noting "[a]lgal-cyst (*Tasmanites*)-like structures" replaced by microcrystalline silica. At this thermal maturity (~1.3% R_o, Montgomery et al., 2005) Type II oil-prone kerogens have converted to hydrocarbons and it is presumed that the organic matter responsible for the TOC values noted by Hickey and Henk (2007) is dominantly solid bitumen. Chalmers et al. (2012) imaged organic porosity in a dry gas

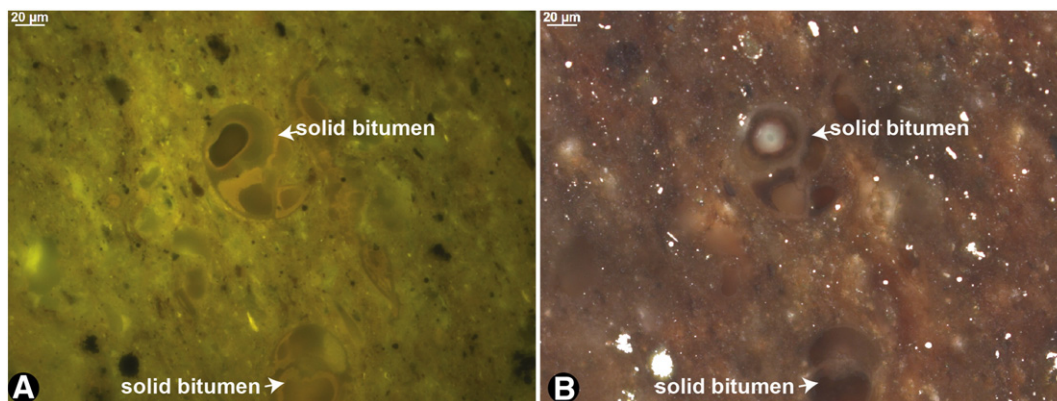


Fig. 22. Photomicrographs of organic matter in organic-rich (~6 wt.% TOC) immature (~0.25% BR_o) Monterey marl outcrop sample, Santa Barbara County, California. A. Fluorescence, oil immersion. B. Same field as A in incident white light, oil immersion.

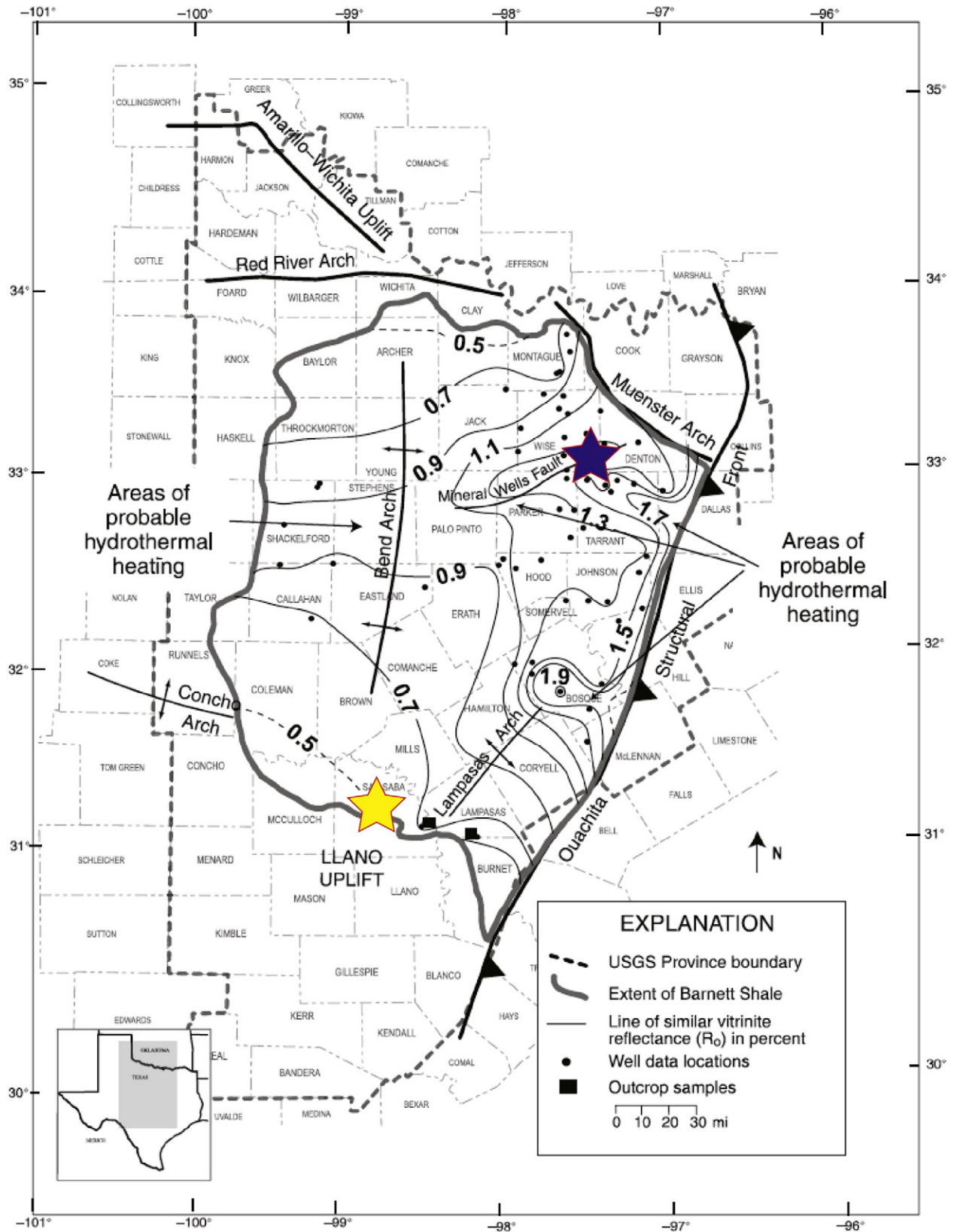


Fig. 23. Barnett Shale thermal maturity from vitrinite reflectance data. Purple and yellow stars show location of high and low maturity samples, respectively, discussed in the text and imaged in Fig. 24. (Source: From Pollastro et al. (2007)).

window thermal maturity Barnett Shale sample, describing the pore network as associated with “kerogen”; however, correlative optical microscopy was not reported. At this thermal maturity it is likely that the

only “kerogen” remaining is Type III terrestrial material. In a now landmark study, Loucks et al. (2009) documented nanopore systems in the Barnett Shale in which porosity occurred primarily as intraparticle

nanopores (median ~ 100 nm) in organic matter. Their study noted the absence of organic pores at low maturity (<0.7% R_o) and presence of organic pores at high maturity (>0.8% R_o), proposing that decomposition of organic matter during thermal maturation created hydrocarbons which filled the ‘bubbles’ created by kerogen conversion. Loucks et al. (2009) did not identify the organic matter observed by SEM in their study; petrographic examination (described below) shows the presence of amorphous kerogen with some solid bitumen in low maturity Barnett samples and absence of kerogen at higher maturity (except refractory Type III terrestrial organic matter) where it is replaced by abundant solid bitumen.

Bernard et al. (2012a) used synchrotron-based scanning transmission X-ray microscopy (STXM) to document chemical evolution of Barnett Shale organic matter from low to high maturity. At low maturity organic matter contained “a significant aliphatic component and an important concentration of oxygen and sulfur-containing functional groups” grading with increasing maturity to “an overmature kerogen dominated by poorly condensed aromatic structures.” Further, Bernard et al. (2012a) observed “the presence of pre-oil solid bitumen in samples of oil window maturity, very likely genetically derived from thermally degraded kerogen” and “formation of nanoporous pyrobitumen” for “samples of gas window maturity, likely resulting from the formation of gaseous hydrocarbons by secondary cracking of bitumen compounds.”

Work by Romero-Sarmiento et al. (2013) calculated basinal evolution of TOC, organic porosity and gas retention capacity in the Barnett through a modelling approach. Although relying on broad assumptions, their model generally was consistent with available rock data (measured TOC, thermal maturity, gas content and organic porosity) and showed organic porosity varied from 0% in immature areas to 4% of total rock volume in organic-rich mature areas. Modelled methane

retained in the Lower Barnett ranged 20–60 scf/t (1–3 kg/m³) concentrated mainly in the mature areas of the basin. A second study by this group (Romero-Sarmiento et al., 2014) applied organic petrography, Raman micro-spectrometry and high resolution transmission electron microscopy (HRTEM) to a thermal maturity sequence of 10 Barnett Shale samples ranging from immature to dry gas window thermal maturity from the core producing area. They described terrestrial vitrinite and inertinite in an oil window mature sample (~0.94% R_o) and “meta-alginate”, an interpreted relict algal body which showed remnant fluorescence. At 1.4% R_o alginate was absent and solid bitumen was abundant. Deconvoluted Raman spectra suggested a broad band centered at about 1480 cm⁻¹ may correspond to oil trapped within organic porosity; however, this interpretation was preliminary and required “further investigation.” From HRTEM observations, they suggested carbon structure was disordered although concentric nanostructures were detected in overmature samples.

Recent work by Han et al. (2015) on a Barnett core from the oil window maturity area documented chromatographic fractionation of hydrocarbons during short distance (<175 ft.; 50 m) vertical migration, observing preferential retention of asphaltenes > resins > aromatic hydrocarbons > aliphatic hydrocarbons in a lower source layer and accumulation of aliphatic hydrocarbons in an overlying reservoir layer. In the reservoir layer, saturate-rich oil was preferentially sorbed on labile organic matter and contained in the primary porosity of biogenic quartz (sponge spicules), whereas dispersed oil found in the underlying source layer was depleted in saturate compounds. Although their work included organic petrography, it was not a primary focus of their paper.

An immature (0.35% R_o) Barnett Shale sample from 1256 ft. (383 m) in the Houston Oil & Minerals Walker D-1-1 well (API 424113010000) in San Saba County at the southern margin of the Fort Worth Basin is shown in Fig. 24A–B. This sample contains abundant inhomogeneous

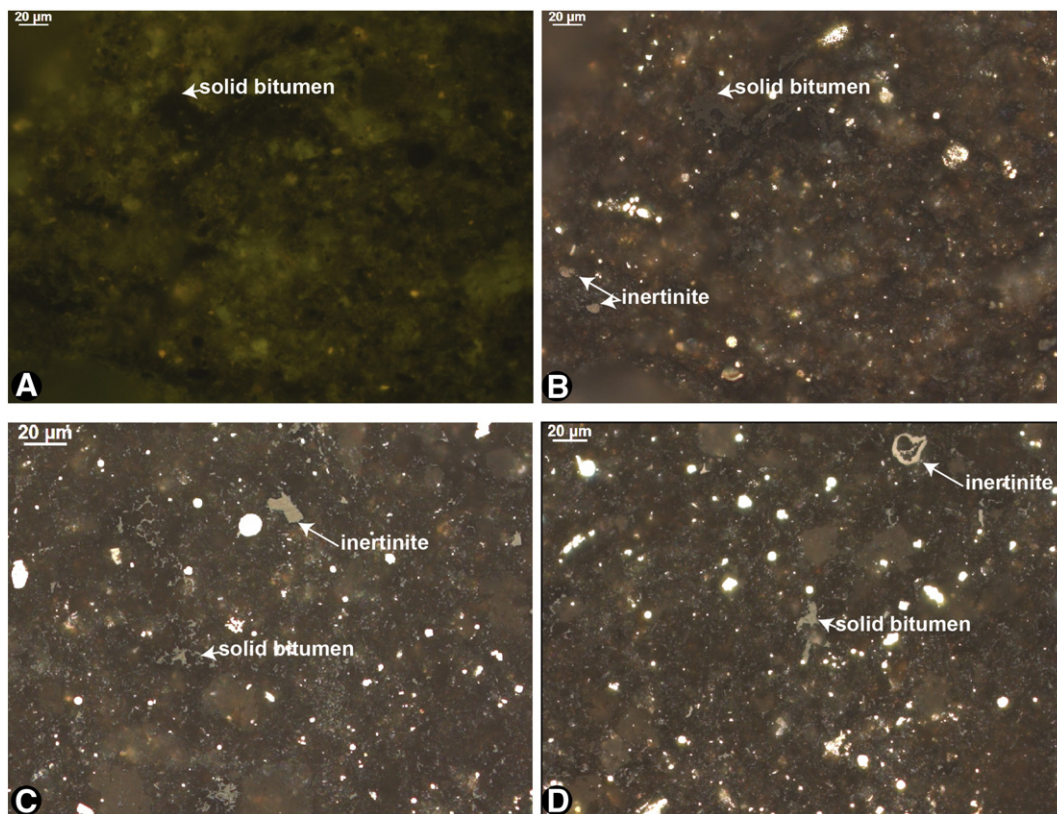


Fig. 24. Photomicrographs (in oil immersion) of organic matter in the Barnett Shale. A. Fluorescence image showing solid bitumen in an organic-rich (7.6 wt.% TOC), low maturity (0.35% R_o) Barnett Shale sample from 1256 ft (383 m) in the Houston Oil & Minerals Walker D-1-1 well in San Saba County, Texas. B. Same field as A under incident white light. C. Solid bitumen in organic-rich (~3.0 wt.% TOC) Barnett Shale sample of dry gas thermal maturity (~1.5% R_o) from 7223 ft (2202 m) in the Blakeley No. 1 well in Wise County, Texas. D. Solid bitumen from 7223 ft (2202 m) in the Blakeley No. 1 well.

solid bitumen with 0.28–0.44% BR₀ occurring in a groundmass texture. Most solid bitumen is non-fluorescent. A separate more homogeneous population has higher BR₀ of 0.55–0.65%. Some terrestrial inertinite (>0.8% R₀) is present, occurring in a pyrite-rich fluorescent groundmass presumed to contain some fraction of bituminite. An organic-rich (~3.0 wt.% TOC) Barnett Shale sample of dry gas thermal maturity (~1.5% BR₀) from the Blakely No. 1 well (API 424973304100) in Wise County near the core area of the Barnett Shale play contains abundant dispersed inertinite fragments and fine-grained solid bitumen in mineral interstices (Fig. 24C–D). Some solid bitumen is found in larger accumulations but most is intimately dispersed in the mineral matrix (cf Romero-Sarmiento et al., 2014).

5.2.2. Duvernay Formation

The Upper Devonian Duvernay Formation in the Western Canadian Sedimentary Basin of Alberta, Canada (Fig. 25), has emerged as a mixed gas/liquids play with thermal maturity ranging from the oil to dry gas window (Rivard et al., 2014). The Duvernay is divided into three members: a basal shaley Duvernay A, a middle carbonate-rich Duvernay B and an upper shaley Duvernay C, which is further

subdivided into C1 through C5 (Hume et al., 2014). Hence, media reports have compared it to the Eagle Ford of south Texas (Rodgers, 2014) in both the calcareous nature of the strata and the broad range in thermal maturity present across the play, increasing from northeast to southwest with burial depth. Previous research has identified the Duvernay as the source rock for conventional oil reservoirs within the adjacent stacked reef complexes of the Leduc Formation (Creaney and Allan, 1990; Allan and Creaney, 1991; Switzer et al., 1994). Interest in unconventional exploration in the Duvernay began around 2005–2008 with initial drilling in gas-rich areas. However, poor well performance caused interest to shift to the condensate window and a marked uptick in activity began around 2010–2011 (Dittrick, 2012, 2013; Raphael Wüst, Trican, written communication, 2016).

From regional studies of organic facies, Stasiuk and Fowler (2004) outlined the deposition of the most organic-rich Duvernay laminated shales in intermediate water depths (60–100 m), whereas Duvernay shales with lower amounts of organic matter were deposited in shallower waters (<40 m). Deposition of organic matter in shallower water was characterized by chitinous zooclasts, terrestrial phytoclasts and increased bioturbation. Preservation of organic matter was

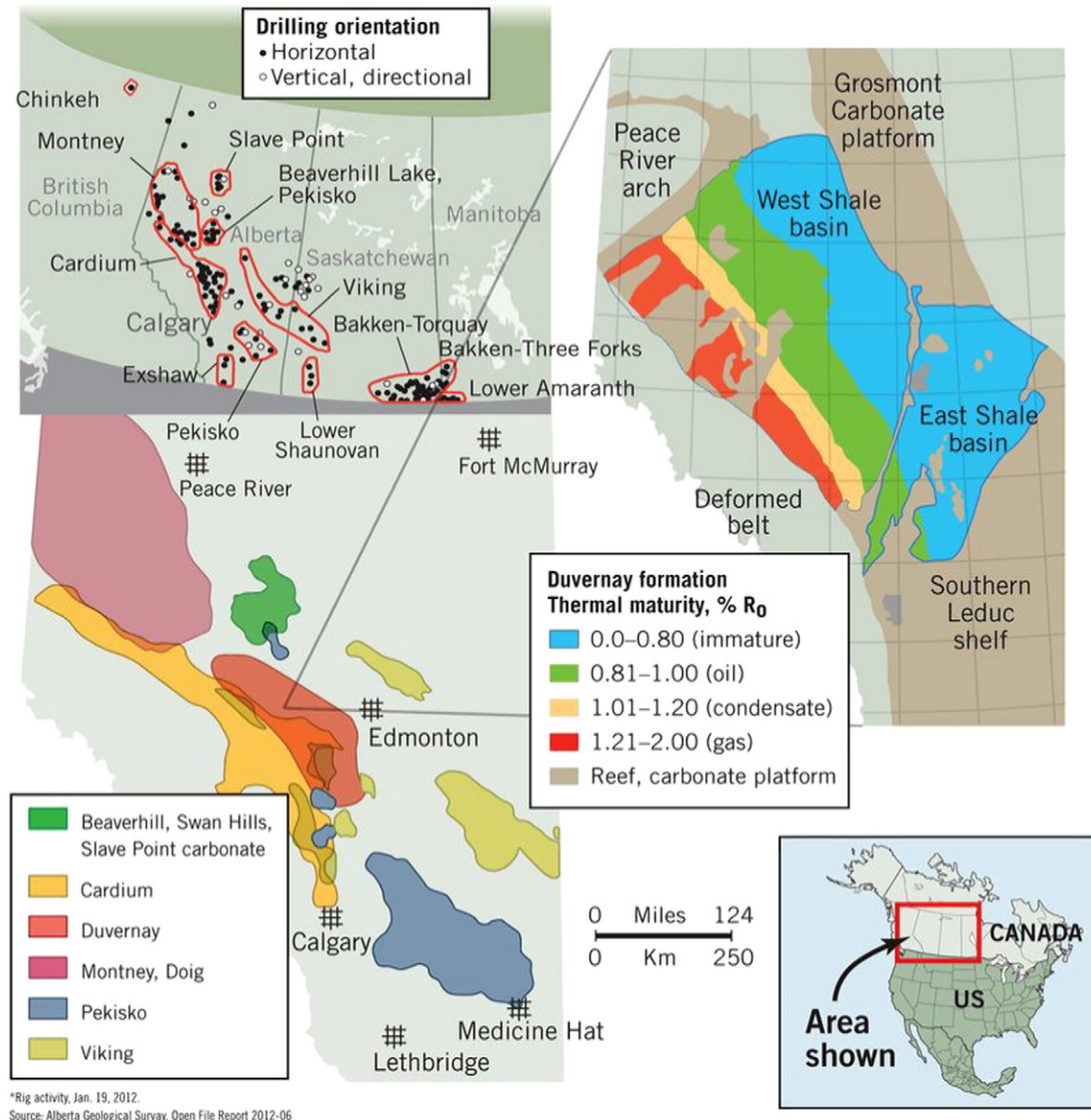


Fig. 25. Thermal maturity and drilling direction in the Duvernay play. (Source: From Rodgers (2014)).

facilitated by bottom water anoxia and low oxygenated water masses rather than productivity-driven as algal bloom layers have not been identified across both the eastern and western Duvernay depositional basins (Chow et al., 1995; Stasiuk, 1999a). Studies by Dunn et al. (2014) found a positive relationship between organic carbon and silica content, suggesting an in situ biogenic origin for silica. Their study also noted a correspondence between organic carbon and porosity, which was expanded by Chen and Jiang (2016) who determined that, similar to other shale gas plays, organic porosity development was related to thermal maturity advance and was most abundant (>6%) in overmature samples.

Duvernay TOC content is up to >20 wt.% in low maturity areas but a more typical range is 2–10 wt.% (Wüst et al., 2013a; Stankiewicz et al., 2015). Based on petrographic analyses, Wüst et al. (2013a) first suggested that >95% of the TOC content resided in solid bitumen in oil window to wet gas window mature Duvernay samples. Later work by Van de Wetering et al. (2015, 2016) confirmed that original kerogen macerals were not present in Duvernay samples from the oil and condensate windows (0.8–1.2% R_o), with the exception of minor inertinite, noting instead the presence of solid bitumen. Finally, Stankiewicz et al. (2015) identified solid bitumen as the dominant component of Duvernay shale samples in the oil window (0.6–1.1% BR_o) although a significant proportion of amorphous organic matter also was identified in their study.

Oil window maturity (0.56–0.70% BR_o) Duvernay samples contain a fluorescent mineral bituminous groundmass (defined by Teichmüller and Ottenjann, 1977). The mineral bituminous groundmass consists of organic matter intimately admixed with inorganic phases, where the organic matter occurs as small masses and wisps between and around mineral grains (Fig. 26A–B). The mineral bituminous groundmass presumably consists of very finely comminuted filamentous algae fragments along with bacterial biomass. Solid bitumen occurs in bimodal

reflectance populations with the higher reflectance population occurring as mostly homogeneous larger accumulations with discrete boundaries and the lower reflectance population occurring as more ragged, inhomogeneous accumulations with wispy and indistinct margins (Wüst et al., 2013a). Some solid bitumen displays weak fluorescence and rarely occurs with a fine mosaic or granular texture of multiple reflectance domains; such textures have been interpreted to result from “coking” as a result of exposure to higher temperatures such as from localized hydrothermal activity (e.g., Landis and Castaño, 1995). Vitrinite is not present (although, see Beaton et al., 2010) and/or is not texturally distinguishable from solid bitumen whereas inertinite is present in low quantities. Marine telalginite is relatively common; however, in the Duvernay samples examined by the authors it is a thin-walled prasinophyte and the unequivocal thick-walled tasmanitid alga such as are common in the central and eastern North America Upper Devonian shales (e.g., Woodford, New Albany, Huron) were rare or not present. In higher maturity Duvernay samples (1.2–1.5% BR_o), solid bitumen is the only organic matter present (Fig. 26C–D), similar to observations from the overlying Triassic Montney Formation, which produces from unconventional tight gas siltstone reservoirs (Sanei et al., 2015b; Wood et al., 2015, and see below).

5.2.3. Haynesville-Bossier formations

Horizontal development in the Upper Jurassic Haynesville-Bossier formations launched in 2008 and there were >3400 wells online in late 2015 (IHS Energy Group, 2016). The play is overpressured, contributing to steep decline curves from IP rates of up to 30 mmcf/day (Hammes et al., 2011). The Haynesville-Bossier is overmature across the play area in east Texas and west Louisiana; therefore, original kerogen type and properties are not known; however, most workers assume a marine Type II kerogen based on the mixed clastic/carbonate lithofacies (e.g., Ewing, 2001; Steinhoff et al., 2011; Hammes and

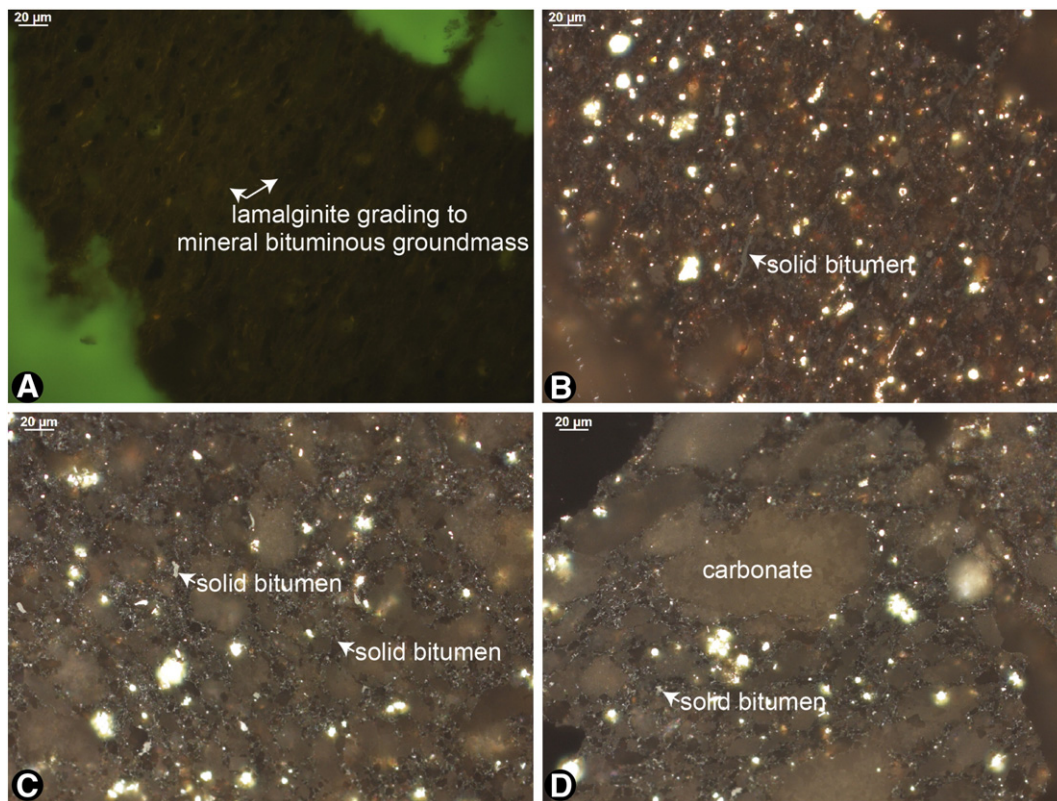


Fig. 26. Photomicrographs from Duvernay Formation shale samples (all under oil immersion). A. Blue light fluorescence image from an organic-rich (~7.5% TOC), immature (0.33% R_o) shale sample from 5882 ft (1793 m) in well location 1-23-49-25W4. B. Same field as A under incident white light. C. Solid bitumen in organic-rich (~2.5% TOC) late wet gas/early dry gas mature (~1.4% BR_o) Duvernay Formation shale under incident white light from 11,955 ft (3644 m) in well location 6-14-37-7W5. D. A second incident white light image from 11,955 ft (3644 m) in well location 6-14-37-7W5 showing solid bitumen occurring in interstices of carbonate-dominated mineral matrix.

Frébourg, 2012; Cicero and Steinhoff, 2013). A wide-ranging set of papers summarizing geology and reservoir engineering properties of the Haynesville-Bossier shale system were presented by Hammes and Gale (2013) and thermal maturation modelling was presented by Nunn (2012) and Amer et al. (2015); however, to our knowledge there are no studies published specific to organic petrology of the Haynesville.

Spain and McLin (2013) used Haynesville shale samples to show tandem secondary electron (SE) images compared to Ar ion-milled back scattered electron (BSE) images of the same sample surface. Samples were halved and imaged by the two methods; images were compared at the same scales. This technique allowed accurate documentation of organic porosity from the BSE images while simultaneously allowing identification and differentiation of mineral cements through Z contrast from the SE images.

A recent study by Klaver et al. (2015) examined the Haynesville-Bossier through broad-beam ion-milling and electron microscopy (BIB-SEM) of organic-rich (up to 5.6 wt.% TOC) overmature samples (1.8–2.5% R_o , measured on solid bitumen and converted to an equivalent R_o value). These workers reported that abundant solid bitumen and rare vitrinite constituted the organic matter content. A positive relationship was observed between development of organic matter porosity and thermal maturity advance. Pore sizes ranged from 4.4 μm to 36 nm in diameter, and followed a power law distribution which allowed extrapolation to smaller pore sizes probed by mercury injection techniques which found higher overall porosity than the BIB-SEM approach. Organic porosity was not developed in the scarce Type III terrestrial organic matter. Organic matter hosted pores were a minor component of porosity in Haynesville samples examined via SEM by Loucks et al. (2012) who noted most porosity was contained in interparticle and intraparticle locations.

In Fig. 27A–B we show solid bitumen in organic-rich (~2.7% TOC) Haynesville shale core from the BP A-8H T.W. George well (API 4220334557) in east Texas from depths of 11,366–11,366.2 ft. (3464 m). A fine granular solid bitumen matrix with high BR_o (~1.7%) pervades the mineral groundmass and is frequently present as a thin rim against euhedral authigenic carbonate. Minor lower reflectance (~0.8%) solid bitumen is present filling fractures on rock fragment margins and present in minor vugs. Scattered inertinite also is present. Our petrographic observations support and confirm the organic petrography results reported by Klaver et al. (2015).

5.2.4. Marcellus Formation

Black shales in the Devonian Marcellus Formation have emerged as an important gas play in the northern Appalachian Basin, particularly in northeast and southwest Pennsylvania and western West Virginia (Engelder and Lash, 2008; Parshall, 2015) where thermal maturity is in the dry gas window (Repetski et al., 2008; East et al., 2012). The

Marcellus has the greatest spatial extent of any North American shale play and throughout its overall distribution, thermal maturity ranges overall from immature to overmature and TOC ranges up to 11 wt.% (Obermajer et al., 1996). Initial Marcellus production began in 2004 with horizontal development in 2006–2007 (Wrightstone, 2009; Pickett, 2015); through mid-2014 there were >6700 horizontal wells online (IHS Energy Group, 2016).

Organic petrology studies of Obermajer et al. (1996, 1997) in southern Ontario included investigation of chitinozoa reflectance since vitrinite was not present in the Marcellus samples they examined. In immature samples, fluorescent amorphous hydrogen-rich marine Type II kerogen dominated the organic assemblage with lesser quantities of discrete planktonic algae including indeterminate acritarchs, and *Leiosphaeridia* and *Tasmanites*.

As part of a broader study, Chalmers et al. (2012) examined dry gas window maturity (~1.5% R_o) Marcellus shale cuttings samples by SEM and gas adsorption techniques, documenting intergranular porosity as well as organic porosity in low Z features interpreted to be clay-organic matter mixtures. Total porosity of about 3.7% was found to occur across a range of scales with a median pore diameter of about 3.9 nm. Of the other gas shales examined in this work (Haynesville, Doig, Woodford, Barnett) the Marcellus was found to have the highest micropore (<2 nm) volume (0.8 mL/100 g). Organic petrology was not the focus of the Chalmers et al. (2012) study and although they employed white light microscopy to measure reflectance, they referred only to “kerogen” and “organic matter” in descriptions of the organic constituents of their samples.

To understand water accessibility to mineral and organic surfaces during hydrofracturing, Gu et al. (2015) used FIB-SEM and neutron scattering techniques to study nanopores in dry gas window maturity (~2.2% R_o) Marcellus shale core samples from central Pennsylvania. Their investigation showed nanoscale pores in organic-poor, clay-rich samples were sheet-like in shape and occurred within clay aggregates whereas organic-rich samples contained bubble-like porosity which occurred in organic matter.

In an SEM study, Milliken et al. (2013) examined Marcellus shale samples from two widely spaced cores in western (~1.0% R_o) and eastern Pennsylvania (~2.1% R_o). Their study noted that TOC content exerted more control on organic matter hosted porosity than did thermal maturity, which showed no obvious relationships to organic matter pore type or abundance. They did, however, find that samples containing <5.5 wt.% TOC showed a positive correlation between porosity and TOC and samples containing >5.5 wt.% TOC showed no additional porosity increase. They also found median organic-hosted pore size decreased with increasing TOC content and that a larger fraction of the total organic matter-hosted pores were not visible with SEM (compared to porosity determined via bulk rock measurements) in samples with higher TOC content. Milliken et al. (2013) provided a robust discussion

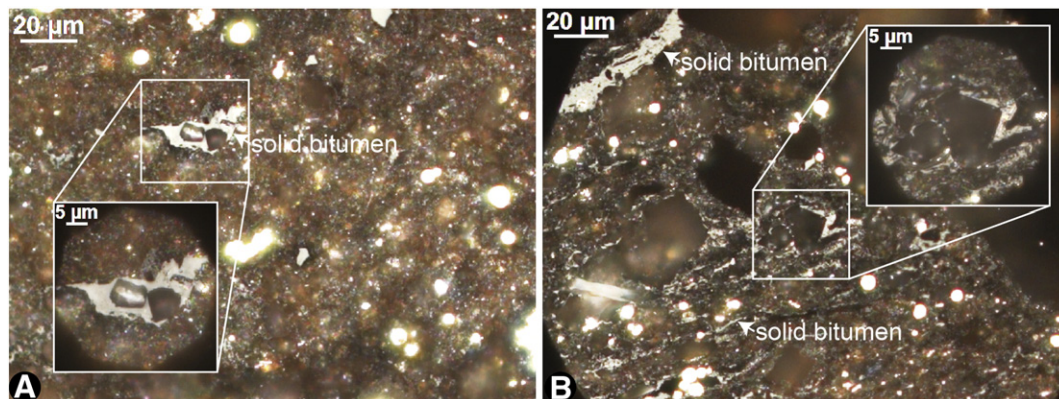


Fig. 27. Incident white light photomicrographs (under oil immersion) from Haynesville Formation shale showing solid bitumen embayed against euhedral carbonate. A. and B. solid bitumen in organic-rich (~2.7 wt.% TOC), dry gas mature (~1.7% R_o) shale from 11,366–11,366.2 ft (3464 m) in the BP A-8H T.W. George (API 4220334557) well in east Texas.

to explain these observations, examining questions related to the interconnected nature of the organic matrix and its control on gas expulsion and pore collapse as well as the influence of organic matter type on porosity development. Ultimately their study concluded that more work is needed to understand development of organic porosity.

Ryder et al. (2013) examined thermal maturity of Devonian shales (including the Marcellus) in the northern Appalachian Basin through evaluation of a broad range of geochemical and petrographic parameters. The objective of their study was to evaluate the possibility of vitrinite reflectance suppression as an explanation for why Devonian shale source rock R_o values are lower than overlying Pennsylvanian coal $R_o(\text{max})$ values (Ruppert et al., 2010) in some areas, e.g., Illinois Basin (Barrows and Cluff, 1984; Nuccio and Hatch, 1996), and east-central Ohio (Rowan et al., 2004), which had led some previous researchers (e.g., Cole et al., 1987) to invoke explanations of long-distance oil migration from source kitchens to the southeast. The

Ryder et al. (2013) study found application of a correction factor to shale R_o values (Lo, 1993) gave inconsistent results. They suggested that low R_o values in low maturity Devonian shale instead resulted from inclusion of solid bitumen reflectance measurements in vitrinite reflectance histograms. This result was later confirmed and expanded by Hackley et al. (2013) in a biomarker thermal maturity study.

An SEM study by Schieber (2013) illustrated some of the difficulties encountered in identification of organic matter using only this technique. By analogy to low maturity New Albany Shale samples (0.57% R_o), Schieber (2013) described organic matter pores as occurring in amorphous bituminite/amorphinite kerogen (amorphinite is synonymous with bituminite or AOM, e.g., Hackley et al., 2016) in Marcellus shale samples at maturity $>2.0\%$ R_o . At this maturity, the amorphous organic matter can only be solid bitumen; all oil-prone kerogens are converted to hydrocarbons. His Fig. 12 (Fig. 28) showed a series of SEM images of 'kerogen', including some structured organic matter (som)

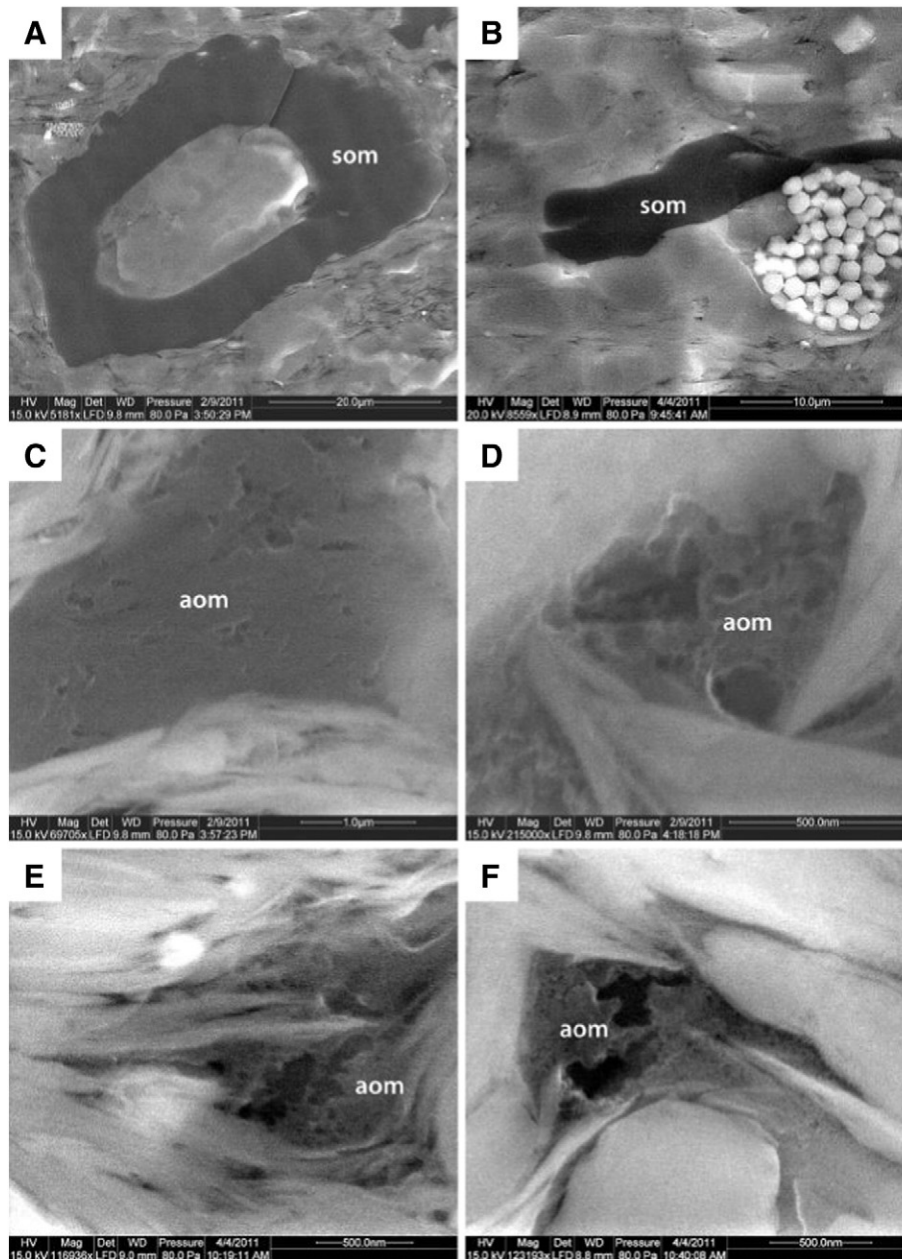


Fig. 28. Secondary electron images of gas-mature ($>2.0\%$ R_o) Marcellus Formation organic matter. A and B Structured organic matter (som). C–F. Amorphous organic matter (aom). From Schieber (2013).

(Source: Reprinted by permission of the American Association of Petroleum Geologists, whose permission is required for further use).

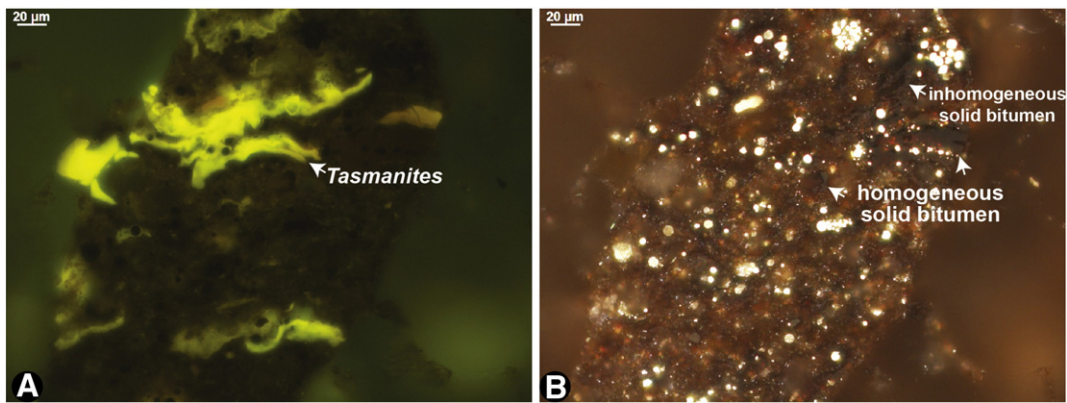


Fig. 29. Photomicrographs of organic matter in organic-rich (~14.2 wt.% TOC) immature (0.25% BR_o, 0.47% R_o) New Albany Shale collected from outcrop, Illinois Basin, Indiana. A. Blue light fluorescence showing *Tasmanites*. B. Same field as A showing homogeneous and inhomogeneous solid bitumen with low gray reflecting surfaces present at 'immature' conditions.

tentatively identified as *Tasmanites* (which may be terrestrial vitrinite or inertinite); the remainder of the 'kerogen' images (labeled aom, amorphous organic matter) showed solid bitumen. While Schieber (2013) acknowledged that his identifications were tentative and that amorphous bituminite/amorphinite may crack to solid bitumen, the som cannot be *Tasmanites*—it is not present at this thermal maturity. Further, Schieber (2013) did not recognize the potential for early hydrocarbon generation in his low maturity New Albany Shale samples. It is quite possible that some of the amorphous bituminite/amorphinite he identified in low maturity New Albany Shale is solid bitumen. In Fig. 29A–B we show a New Albany Shale sample from the Illinois Basin, Indiana, with BR_o of 0.25%, demonstrating that solid bitumen can be present at thermal maturities much lower than the conventional entrance to the oil window.

In Fig. 30A we show early mature (~0.5% BR_o) organic-rich (~8 wt.% TOC) Marcellus shale from the Eastern Gas Shales Project (EGSP) OH-4 well (Streib, 1981) in Ashtabula County, northwestern Ohio. *Tasmanites* are abundant in a fluorescent groundmass of bituminite and mineral matter (mineral bituminous groundmass). In Fig. 30B a dry gas thermal maturity (~1.6% R_o) organic-rich (~5 wt.% TOC) Marcellus sample from EGSP WV-6 well in Monongalia County, West Virginia, shows presence of a solid bitumen organic matrix with sparse inertinite, typical of the thermally mature shale plays discussed herein. Vitrinite is absent or unrecognizable and the oil-prone kerogens have been converted to hydrocarbons.

5.2.5. Utica Shale

Interest in unconventional potential in the Ordovician Utica Shale of the Appalachian Basin and southern Quebec dates to about 2006 when operators first began to assess shale gas target zones (Marcil et al., 2009). Production from the condensate window began around 2011 and actually targets interbedded limestone and shale in the underlying Point Pleasant Formation rather than in the clay-rich (up to 70%) Utica itself (Patchen and Carter, 2015). Most successful unconventional development has been in the gas condensate window in eastern Ohio (Dunnahoe, 2013) with >1100 horizontal wells on production in July 2015 (IHS Energy Group, 2016).

Prior to the shale revolution, regional sedimentology of the Utica was documented by Lehmann et al. (1995), and studies by Ryder et al. (1998) had suggested Utica black shales were the source of oils in conventional Cambrian and Ordovician sandstone and carbonate reservoirs in Ohio and adjoining areas. This conclusion was based on geochemical similarities (alkane envelopes, tricyclic terpanes, C isotopes) between oils and Utica source rock bitumen extracts. Utica thermal maturity ranges from immature in western Ohio to overmature east and south-east towards the Appalachian hinterland in central Pennsylvania (Repetski et al., 2008); the same southeasterly increase in thermal maturity is observed in Quebec (summarized in Lavoie et al., 2014). Hydrocarbon resource assessment by USGS suggested mean undiscovered resources of 940 mmbbl oil and 37 trillion cubic feet (Tcf) of gas (Kirschbaum et al., 2012); subsequent assessment by an industry-

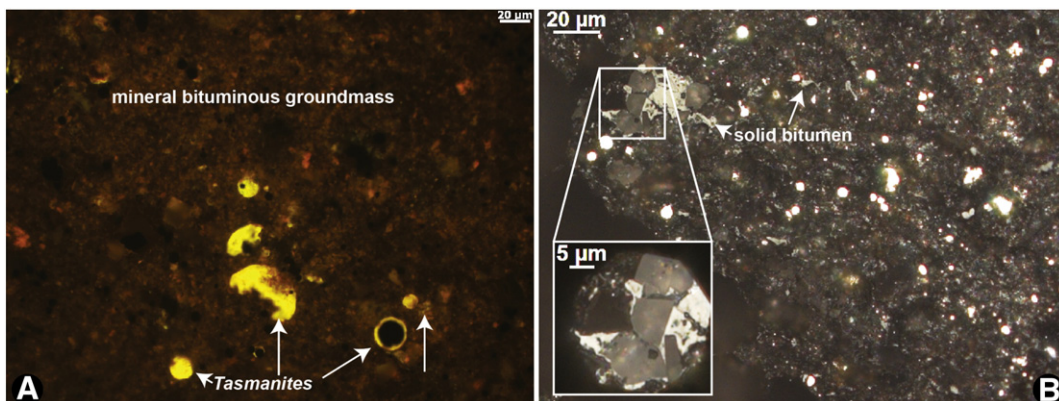


Fig. 30. Photomicrographs of organic matter in Marcellus Formation shale under oil immersion. A. Blue light fluorescence image showing *Tasmanites* in matrix of fluorescent mineral bituminous groundmass in organic-rich (~8 wt.% TOC), early mature (~0.5% R_o) Marcellus Formation shale at 1342–1343 ft (409 m) in the OH-4 Core 2839 well (Bessemer & Lake Erie Railroad Co., API 3400721087) from Ashtabula County, Ohio. B. Incident white light image showing solid bitumen showing embayment by euhedral carbonate in organic-rich (~5 wt.% TOC), dry gas mature (~1.6% R_o) Marcellus Formation shale from 7440.7 ft (2268 m) in the Eastern Gas Shales Project WV-6 well [Morgantown Energy Research Center (MERC) No. 1, API 4706120370] from Monongalia County, West Virginia.

funded consortium of State geological surveys predicted mean undiscovered oil resources of 1960 mmbbl oil and 782 Tcf gas (Patchen and Carter, 2015).

Organic petrography studies conducted as part of a larger study of the Utica petroleum system (Patchen and Carter, 2015) described the dominant organic matter as amorphinite (equivalent to bituminite or AOM) at low thermal maturity with some solid bitumen present. Higher amorphinite abundances were found associated with shale facies where the amorphinite was interpreted as derived from an algal source. Based on thin section petrography and SEM examination of ion-milled and broken rock surfaces, Patchen and Carter (2015) suggested Utica and Point Pleasant rocks contained little to no matrix porosity and instead that porosity was developed only in organic matter.

Haeri-Ardakani et al. (2015a,b) studied organic petrology of the Utica in southern Quebec, noting thermal maturity (late oil window to dry gas window) was related to present-day burial depth and organic matter was dominated by solid bitumen (migrabitumen) with lower proportions of zooclasts (chitinozoans and graptolites). Their study correlated hydrocarbon potential (S₂, mg HC/g rock) to abundance of solid bitumen, suggesting that solid bitumen formed from migration and dissemination of hydrocarbons into the clay-rich rock matrix. They also hypothesized that porous siltstone facies were reservoirs for migrated solid bitumen which originated locally from organic-rich facies within the section. Bowman and Mukhopadhyay (2014) suggested graptolite reflectance could help with determination of thermal maturity in the Ordovician but did not provide documentation specific to the organic petrology of the Utica/Point Pleasant. In the Haeri-Ardakani et al. (2015a,b) studies, solid bitumen and chitinozoan reflectance were cited as robust thermal maturity parameters, and converted to vitrinite reflectance equivalent values through the Bertrand (1990) and Bertrand and Malo (2001) conversion schemes. Chitinozoan reflectance in the Utica/Point Pleasant also successfully predicts thermal maturity through the vitrinite reflectance equivalent expression of Tricker et al. (1992) (Thomas Gentzis, Core Laboratories, written communication, 2016).

In Fig. 31 we show an immature (~0.25% BR_o) organic-rich (4.75% TOC) Utica mudstone sample from the Chevron Prudential 1-A (API 3410120196) well in Marion County, north-central Ohio. This sample from 1435.8 ft (437.6 m) contains abundant fluorescent AOM dispersed in a carbonate-dominated mineral matrix (carbonates also can exhibit fluorescence; it is important to distinguish organic fluorescence from fluorescence in the inorganic mineral groundmass). Two generations of solid bitumen are present: 1. an abundant low reflectance (~0.25% BR_o), weakly fluorescent population with an irregular granular surface widely disseminated in the mineral matrix, and 2. a less abundant, more homogeneous higher reflectance (~0.6% BR_o) population which has accumulated into small pods and nodules. The low reflectance solid bitumen may be a pre-oil exudate from the AOM, present in a

continuum from “disorganized,” complex kerogen molecules to more “organized” solid bitumen with a gray-reflecting surface. Rare fluorescent telalginite also is present.

5.2.6. Woodford Shale

The modern shale gas resource play in the Late Devonian-Early Mississippian Woodford Shale of Oklahoma began in 2004 with application of hydraulic fracturing technology and horizontal drilling modelled after the Barnett Shale (Cardott, 2012). There were 4063 Woodford Shale well completions in Oklahoma from 2004 to 2015 (Fig. 32A–B), with 4.0 Tcf of gas and 61.8 million bbls of liquid hydrocarbons produced from 3736 wells (Fig. 33A–B). Of 147 operators with Woodford Shale well completions from 2004 to 2015, most (132) drilled <5 wells.

The Woodford Shale gas play began in 2004 in the western part of the Arkoma Basin where the brittle, biogenic-silica-rich shale is >100 ft (30 m) thick. Thermal maturity of the Woodford in the Arkoma Basin (Fig. 32B) increases from 0.55% R_o at depths of about 2300 ft (700 m) in the west to overmature (>6.0% R_o) at depths >17,000 ft (>5200 m) in the east. The Arkoma Basin play is restricted to <3.0% R_o by low gas production rates and potential CO₂ dilution of the gas composition at higher thermal maturity. Woodford Shale oil- and condensate-rich plays in the Anadarko and Ardmore basins began in 2007. The Anadarko Basin play began in Canadian County where the Woodford Shale is >200 ft (>60 m) thick in the condensate window (<1.4% R_o; Cardott, 2012; Caldwell, 2014). Thermal maturity of the Woodford in the Anadarko Basin ranges from 0.49% R_o at depths of 3600 ft (1100 m) to 4.89% R_o at depths of 22,500 ft (6800 m; Cardott, 1989). Most condensate wells in the Woodford Shale are at <1.4% R_o in the Anadarko, Ardmore, and Arkoma Basins. The highest thermal maturity for a Woodford Shale condensate well is 1.67% R_o in the Arkoma Basin (Cardott, 2012).

In 2012, the Woodford play extended to the south as the South Central Oklahoma Oil Province (SCOOP) in the southeast part of the Anadarko Basin. Thermal maturity of the Woodford in the Ardmore Basin ranges from 0.49% R_o at outcrop to 2.45% R_o at depths of 18,500 ft (5600 m; Cardott, 2012). The Woodford Shale oil- and condensate-rich play in the northern part of the Ardmore Basin is at depths of 4600 ft (1400 m) to 15,000 ft (4600 m).

The organic matter contained in immature Woodford Shale is Type II kerogen with some rocks containing up to 25 wt.% TOC (Johnson and Cardott, 1992) and values of 5–15 wt.% TOC reported for marginally mature samples (Romero and Philp, 2012). Most organic matter in low maturity samples is bituminite (>80%) with minor telalginite, lamalginite, vitrinite, inertinite, and solid bitumen present (Lewan, 1987; Cardott and Chaplin, 1993). At higher maturities, solid bitumen dominates the organic assemblage (Cardott et al., 2015). Curtis et al. (2012b) recognized secondary nanoporosity development in solid bitumen beginning

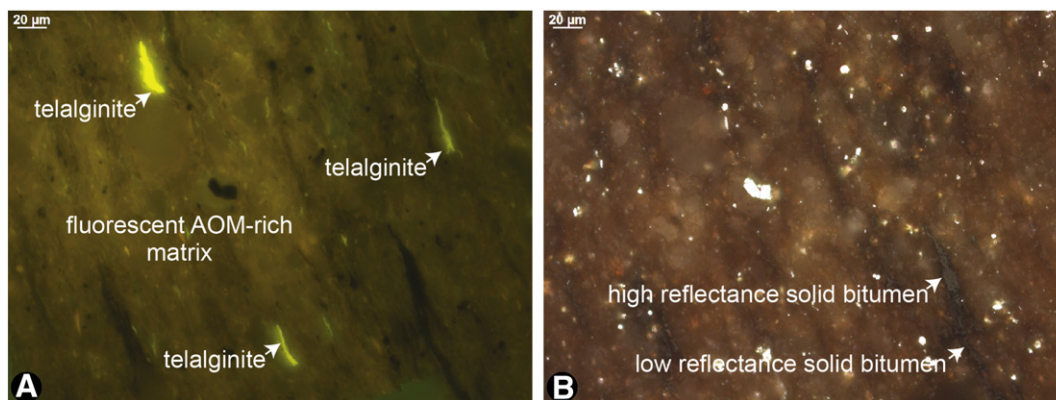


Fig. 31. Photomicrographs of organic-rich (4.75% TOC), immature (0.25% BR_o) lime-rich Utica mudstone from 1435.8 ft (437.6 m) in the Chevron Prudential 1-A (API 3410120196) well in Marion County, north-central Ohio. A. Blue light fluorescence image showing telalginite in AOM-rich matrix. B. Same field as A under incident white light showing high and low reflectance solid bitumen.

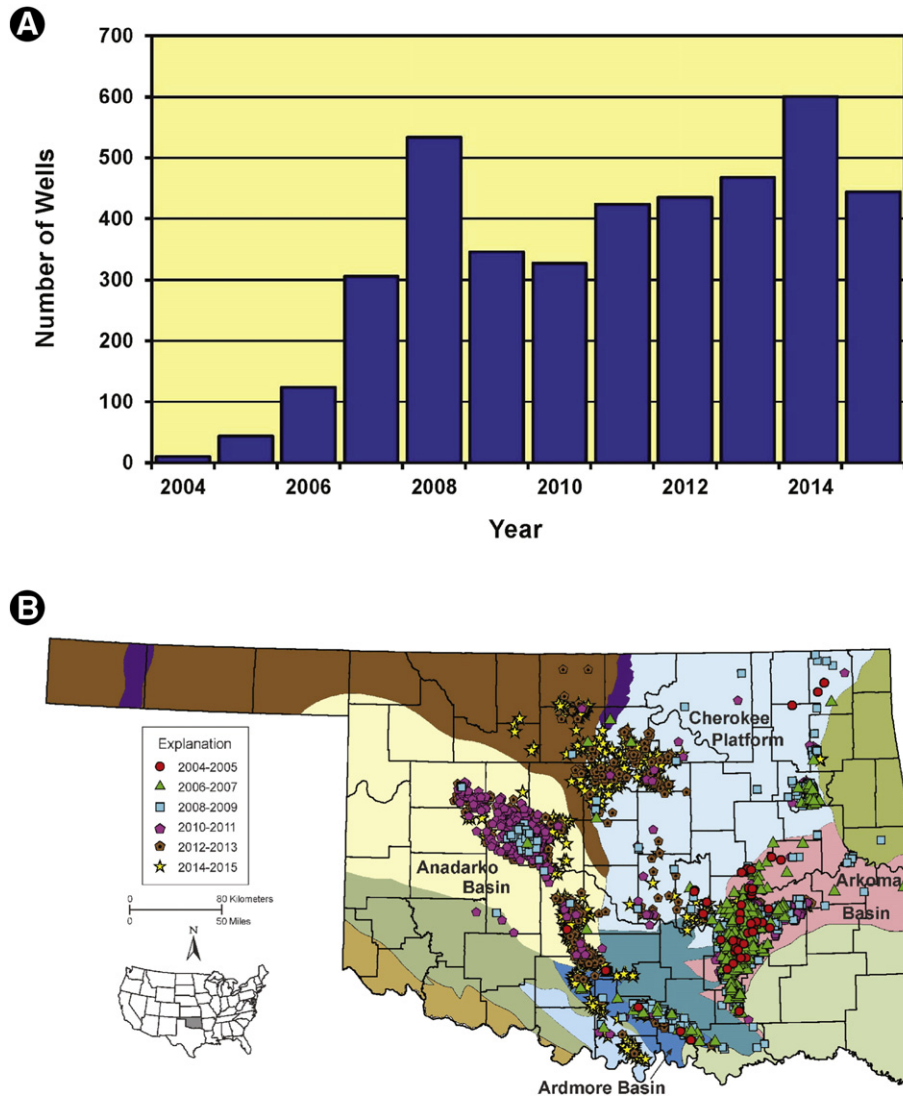


Fig. 32. A. Histogram of Woodford Shale well completions in Oklahoma. B. Map showing Woodford Shale well completions by year (2004–2015).

at 0.90% R_o using a dual-beam FIB-SEM with backscattered electrons. Cardott et al. (2015) described a post-oil solid bitumen network in the Woodford Shale using incident white light microscopy and FIB-SEM. Nanopores within and the brittle nature of the bitumen network were postulated to provide hydrocarbon storage sites and microfracture development as a potential primary migration pathway. Hu et al. (2015) noted a positive relationship between porosity and thermal maturity in artificially-matured, solvent-extracted Woodford Shale samples which they attributed to formation of nanoporosity (2–50 nm) during thermal transformation of organic matter. Löhr et al. (2015) noted absence of organic porosity in oil window maturity (0.5–1.1% R_o) Woodford Shale samples. However, pores were present in oil window mature samples after solvent extraction, suggesting they are open to hydrocarbon/bitumen migration in the oil window.

Fig. 34A–B shows a low maturity (0.41% BR_o , 12.16 wt.% TOC) Woodford Shale sample collected from outcrops in Carter County, Oklahoma. Similar to other immature Devonian-Mississippian North American shales, organic matter is dominated by fluorescent bituminite, with minor amounts of solid bitumen and inertinite also present. *Tasmanites* and *Leiosphaeridia* telalginite round out the organic assemblage.

In Fig. 12C we show an organic-rich (11.5 wt.% TOC) Woodford Shale sample from the Permian (Delaware) Basin in Pecos County, Texas. This

sample is in the late condensate-wet gas window (~1.35% BR_o) and the organic assemblage is dominated by solid bitumen.

5.2.7. Other shale gas systems

Numerous other shale gas plays presently are developed in North America (Figs. 2, 11). Here we provide brief mention from some of the plays with organic petrology and/or SEM studies in the eastern basins [New Albany, and Ohio (Huron) shales], Gulf Coast (Pearsall, other Aptian shales), the Western Canada Sedimentary Basin (Horn River, Muskwa and Montney shales), and Mississippian shales in the midcontinent (Fayetteville Shale), and Black Warrior Basin (Floyd Shale).

The Devonian-Mississippian New Albany Shale of the Illinois Basin has seen limited unconventional development as a shale gas system (Strąpoć et al., 2010), with some oil production in low maturity areas (Nuttall et al., 2015). Thermal maturity ranges from immature at the basin margins to dry gas (~1.4% R_o) in southern Illinois while TOC ranges 1–13 wt.% (Mastalerz et al., 2013). Organic petrology of low maturity (~0.45% R_o) New Albany samples was described by Mastalerz et al. (2012) who reported TOC contents of ~13 wt.% and total S content of 6.2 wt.%. Vitrinite and inertinite accounted for ~2 vol.% of the organic matter whereas bituminite and alginite were 90 vol.% or greater. These workers used FTIR to show alginite-dominated density fractions were

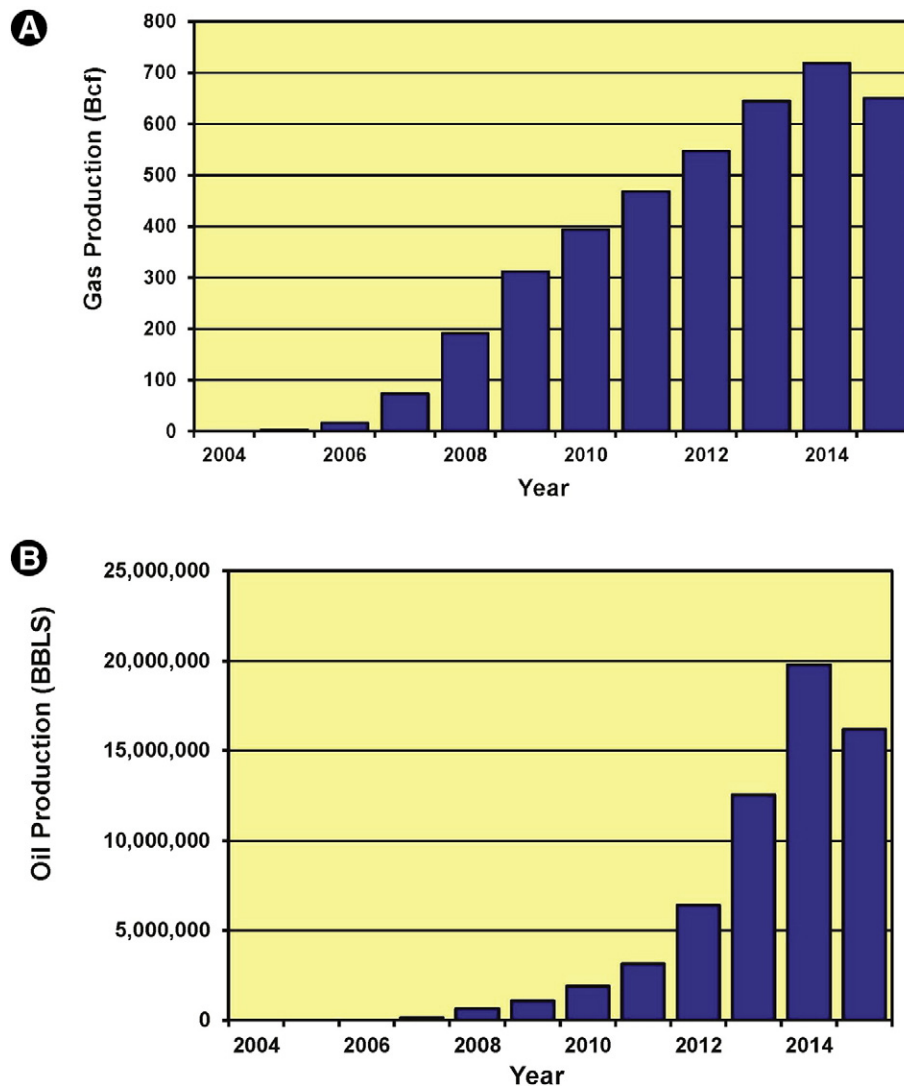


Fig. 33. A. Histogram of Woodford Shale gas production in Oklahoma. B. Histogram of Woodford Shale oil and condensate production in Oklahoma.

enriched in aliphatic H, carboxyl and carbonyl C, and contained less C in ether bonds (C–O–C) compared to bituminite-dominated fractions which were more aromatic. Wei et al. (2014) used solvent extraction to remove soluble bitumen from New Albany Shale samples finding this opens additional pore space for gas adsorption, dependent on thermal maturity, with pore volumes increasing more at higher maturities.

Organic petrology studies in the Upper Devonian Ohio Shale (Huron Member) includes work by Robl et al. (1987, 1992) and Taulbee et al. (1990) who determined lamellar alginite and bituminite were the most abundant organic matter types present in low maturity samples, followed by vitrinite and inertinite. These researchers observed correlations between concentrations of redox sensitive trace elements (Ni, V,

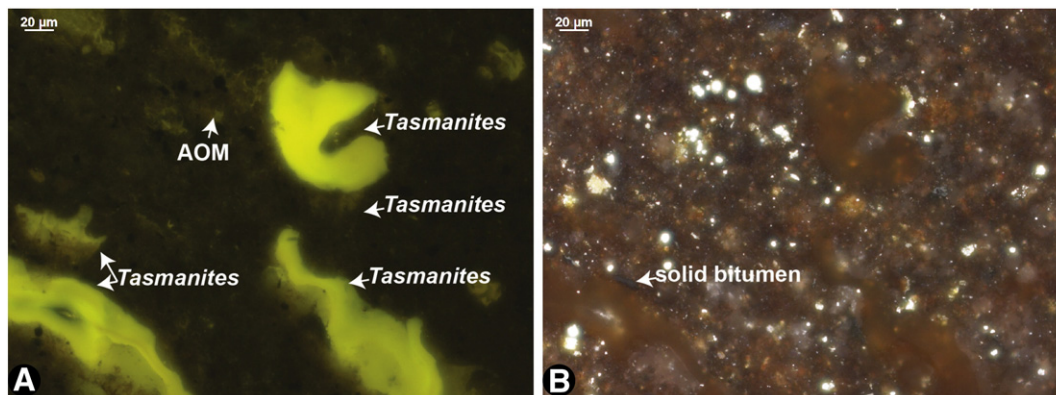


Fig. 34. Oil immersion photomicrographs of organic-rich (~12.2 wt.% TOC), immature (0.41% BR_o) Woodford Shale collected from outcrops in Carter County, Oklahoma. A. Blue light fluorescence image showing *Tasmanites* and amorphous organic matter. B. Same field as A under incident white light showing solid bitumen.

Cr, Cu) and organic matter as a result of these metals being less soluble under the strongly reducing conditions which preserve sedimentary organic matter (e.g., Tribouvillard et al., 2006). Taulbee et al. (1990) suggested lower bituminite concentrations in the Ohio Shale indicated less bacterial degradation than in equivalent New Albany shales and that in addition to contributions from algae, bituminite may also represent an end product of the bacterial re-working of vitrinite. This conclusion had been previously reported from observational studies (Masran and Pocock, 1981) but has not been further substantiated via experimental work.

Araujo et al. (2014) documented interlaboratory reproducibility in reflectance and spectral fluorescence measurements on a thermal maturity transect in the Huron Member of the Ohio Shale in the central Appalachian Basin. Their study concluded that new re-evaluations were required to examine and document correspondence between the reflectance and spectral fluorescence thermal maturity parameters in the Devonian shales.

Rimmer et al. (2004) used a 'terrestrial to marine maceral ratio' [(vitrinite + inertinite)/(alginite + bituminite)] to document an upsection increase in terrestrially derived material in Devonian-Mississippian black shales of the Appalachian Basin. This work was later expanded by Rimmer et al. (2015) to multiple Devonian-Mississippian shale cores from the Appalachian and Illinois Basins, to conclude that the frequency of fire occurrence increased up-section as a result of increased atmospheric O₂ and abundance of vascular plants as fuel.

In the Gulf Coast, the organic petrology of argillaceous lime wackestone and mudstones occurring in the Lower Cretaceous Pearsall Formation of south Texas was considered in the context of shale gas resources (Hackley, 2012). This study described dry gas window thermal maturity samples (1.2–2.2% R_o) of generally low organic content (avg. TOC <1.0 wt.%), concluding TOC content resided in solid bitumen which was interpreted to result from in situ cracking of oil generated from an original Type II kerogen. Further studies (Valentine et al., 2014; Hackley et al., 2014) examined thermal maturity and organic petrology of Aptian-age Pearsall Formation equivalent strata in the downdip Mississippi Salt Basin of southern Mississippi, concluding potential for shale gas resources was poor based on low organic content.

The Devonian Horn River and Muskwa formations of the Western Canadian Sedimentary Basin were evaluated for dry gas potential in a series of studies applying porosity measurement and SEM imaging techniques (Ross and Bustin, 2008, 2009; Dong and Harris, 2013; Dong et al., 2015). Relying on previous open-file reports by the Canadian Geological Survey (Potter et al., 2000, 2003), the organic assemblage of high maturity (1.6–1.7% R_o) Muskwa shale samples was described by Ross and Bustin (2009) as dominantly comprised of granular micrinite, interpreted as residual from conversion of bituminite kerogen to hydrocarbons. Studies by Dong and Harris (2013) and Dong et al. (2015) found a (poor) positive correlation between TOC content and porosity in high maturity (1.6–2.5% R_o) Horn River shale samples, which they interpreted to show that a large proportion of pores were developed in organic matter as documented by SEM investigation. Organic matter pores were interpreted to form during kerogen cracking to hydrocarbons and were observed to be smaller than inter- and intra-particle pores in the mineral matrix. However, from gas adsorption studies, Ross and Bustin (2008) suggested free gas (rather than gas adsorbed in or onto organic carbon or clays) was the dominant hydrocarbon component in these high temperature systems and that mineralogy exerted a major influence with carbonate-rich strata (lower TOC) showing lower gas capacities and silica-rich (higher TOC) strata showing higher gas capacity.

Horizontal development began in 2005 in the Triassic Montney Formation of western Alberta and eastern British Columbia (Dittrick, 2013). As mentioned above, gas production from the Montney occurs in tight siltstone reservoirs which have been charged by external source rocks. In general, the organic petrology of this high maturity play is dominated

by solid bitumen as documented in multiple studies (Wüst et al., 2013b; Sanei et al., 2015b; Wood et al., 2015). Utting et al. (2005) reported palynostratigraphic descriptions of oil window mature Montney samples, ascribing some oil-prone organic matter to reworking from older sources; however, it is difficult to compare data from the palynological approach (transmitted light, kerogen concentrates) to traditional organic petrology (incident light, whole rock samples). Ghanizadeh et al. (2015) reported bituminite co-occurring with solid bitumen in organic-lean wet gas maturity Montney Formation siltstones-sandstones but photographic evidence for presence of bituminite in their samples is weak.

Shale gas production in the shallow (~1500–6500 ft.; 460–1980 m) Mississippian Fayetteville Shale of the Arkoma Basin in north Arkansas has seen significant development in the last years with 3700+ horizontal wells starting production since 2010 (IHS Energy Group, 2016). Thermal maturity in the Fayetteville is overmature with reflectance values ranging from 1.5–5.0% (Ratchford et al., 2006; Li et al., 2010) and most shale gas development has occurred in the 2.0–3.2% R_o range (Houseknecht et al., 2014). Bai et al. (2013) presented a reservoir analysis of the Fayetteville by multiple techniques, including 'kerogen' evaluation through palynofacies analysis. However, due to high maturity, this approach did not provide much insight into the organic matter type, revealing mostly the presence of inert opaque material, which we interpret as solid bitumen. Their SEM imaging found a majority of organic pores were sub-micron sized (5–100 nm), consistent with many of the other SEM studies cited herein which reported organic porosity in gas mature shale organic matter.

Dembicki and Madren (2014) described the Mississippian Floyd Shale in the Black Warrior Basin as containing 2–7 wt.% TOC with >1.3% R_o, factors which they considered key in exploration for unconventional shale gas. They described the kerogen in less mature updip Floyd strata as oil-prone but did not present documentation. However, unconventional exploration has stalled in the Floyd due to absence of sealing lithologies and fluid sensitivity/proppant embedment issues encountered during drilling and completion.

6. Summary and conclusions

Herein, we have reviewed the current state-of-the-art for organic petrography applications to the North American shale oil and gas plays, including as many photographic examples as possible from the Bakken, Barnett, Duvernay, Eagle Ford, Haynesville, Marcellus, Niobrara, Utica, Woodford and other shales. Organic petrography is a powerful tool in these shale systems, allowing identification of the solid organic matter which contains most of the organic carbon measured by bulk geochemical analyses and thus enables understanding of the petrology of organic matter during diagenetic processes and catagenic kerogen conversion to hydrocarbons. Fluorescence microscopy is a powerful approach to organic petrology of shale reservoirs at early oil window thermal conditions but is not applicable at higher maturity due to loss of organic fluorescence. Solid bitumen constitutes the dominant organic matter present in oil-prone shale systems of peak oil maturity and beyond; oil-prone kerogens (algal material and amorphous organic matter) are converted to hydrocarbons (expelled or retained as solid bitumen) and not present in thermally mature shale systems whereas gas-prone refractory terrestrial kerogen macerals vitrinite and inertinite do persist to high maturity. This observation asserts that assigning a 'kerogen' type for peak oil and higher maturity rocks from Rock-Eval pyrolysis is misleading because what is measured by pyrolysis is dominated by solid bitumen, not kerogen. SEM studies of organic matter in shale reservoirs have resulted in major advances in our understanding of the interconnected porosity occurring in these nano-Darcy systems, demonstrating that organic porosity development occurs due to increase in thermal maturity and the generation of hydrocarbons. However, some studies have reported conflicting results and the SEM approach to shale organic matter characterization needs to be

augmented by correlative microscopy techniques which can shed light on individual organic matter types and distinguish kerogens from solid bitumen. This review further suggests new petrographic and in situ geochemical studies are warranted to document mobility and wettability of solid bitumens at subsurface reservoir conditions and to observe the potential for migration fractionation of this important shale reservoir component.

Acknowledgements

Technical reviews by Neely Bostick (USGS, Emeritus), Henrik Petersen (Maersk Oil) and Thomas Gentzis (Core Laboratories) improved this paper. Robert Burruss (USGS) provided helpful comments to clarify the information presented in Fig. 3. Brett Valentine (USGS) assisted with sample preparation and photomicrographs. Jim Hower (CAER) and Tucker Hentz (BEG) provided samples of Wolfcampian mudrocks and many other individuals contributed various samples as listed in Table 1. The following persons reviewed individual sections of the manuscript as regional experts: Bakken, Lavern Stasiuk (Shell Canada); Barnett, Dan Jarvie (Worldwide Geochemistry); Duvernay, Raphael Wüst (Trican Well Service); Eagle Ford, Wayne Camp (Anadarko) and Neil Fishman (Hess Corporation); Haynesville, Ursula Hammes (Texas Bureau of Economic Geology); Niobrara, Steve Sonnenberg (Colorado School of Mines). This research was funded by the USGS Energy Resources Program. Any use of trade, firm, or product names is for descriptive purposes only and does not imply endorsement by the U.S. Government.

References

- Abdullah, W., Buckley, J.S., Carnegie, A., Edwards, J., Herold, B., Fordham, E., Graue, A., Habashy, T., Seleznev, N., Signer, C., Hussain, H., Montaron, B., Ziauddin, M., 2007. Fundamentals of wettability. *Oilfield Rev.* 19, 44–61.
- Abraham, H., 1960. *Asphalts and Allied Substances (Sixth Edition, 5 Volumes)*. Van Nostrand Company, Inc., New York.
- Allan, J., Creaney, S., 1991. Oil families of the Western Canada Basin. *Bull. Can. Petrol. Geol.* 39, 107–122.
- Allen, J.E., Meylan, M.A., Heitmuller, F.T., 2014. Determining hydrocarbon distribution using resistivity, Tuscaloosa marine shale, southwestern Mississippi. *Gulf Coast Assoc. Geol. Soc. Trans.* 64, 41–57.
- Amer, A., di Primio, R., Ondrak, R., Unnithan, V., 2015. 4-D petroleum systems modelling of the Haynesville shale play: understanding gas in place. *Unconventional Resources Technology Conference Paper URTeC 2155539 (15 p)*.
- American Society for Testing and Materials (ASTM), 2015a. Standard Test Method for Microscopical Determination of the Reflectance of Vitrinite Dispersed in Sedimentary Rocks. Annual book of ASTM Standards: Petroleum Products, Lubricants, and Fossil Fuels; Gaseous Fuels; Coal and Coke sec. 5, v. 5.06: ASTM International, West Conshohocken, PA (<http://www.astm.org/Standards/D7708.htm>, (Accessed February 14, 2016)).
- American Society for Testing and Materials (ASTM), 2015b. Standard Test Method for Microscopical Determination of the Reflectance of the Vitrinite Reflectance of Coal. Annual Book of ASTM Standards: Petroleum Products, Lubricants, and Fossil Fuels; Gaseous Fuels; Coal and Coke sec. 5, v. 5.06 ASTM International, West Conshohocken, PA (<http://www.astm.org/Standards/D2798.htm> (Accessed April 6, 2016)).
- Anderson, D.S., Folcik, J.L., Melby, J.H., 2015. A short history of the “Jake” Niobrara horizontal oil discovery, Weld County, Colorado. *Mount. Geol.* 52, 5–12.
- Araujo, C.V., Borrego, A.G., Cardott, B., das Chagas, R.B.A., Flores, D., Gonçalves, P., Hackley, P.C., Hower, J.C., Kern, M.L., Kus, J., Mastalerz, M., Mendonça Filho, J.G., Mendonça, J.O., Menezes, T.R., Newman, J., Suarez-Ruiz, I., Sobrinho da Silva, F., Viegas de Souza, I., 2014. Petrographic thermal indices of a Devonian shale maturation series, Appalachian Basin, USA. *Int. J. Coal Geol.* 130, 89–101.
- Bai, B., Elgmati, M., Zhang, H., Wei, M., 2013. Rock characterization of Fayetteville shale gas plays. *Fuel* 105, 645–652.
- Banerjee, A., Sinha, A.K., Jain, A.K., Thomas, N.J., Misra, K.N., Chandra, K., 1998. A mathematical representation of rock-eval hydrogen index vs T_{max} profiles. *Org. Geochem.* 28, 43–55.
- Barker, C., 1974. Pyrolysis techniques for source rock evaluation. *Am. Assoc. Pet. Geol. Bull.* 58, 2349–2361.
- Barker, C.E., 1996. A comparison of vitrinite reflectance measurements made on whole-rock and dispersed organic matter concentrate mounts. *Org. Geochem.* 24, 251–256.
- Barker, C.E., Lewan, M.D., Pawlewicz, M.J., 2007. The influence of extractable organic matter on vitrinite reflectance suppression: a survey of kerogen and coal types. *Int. J. Coal Geol.* 70, 67–78.
- Barker, C.E., Pawlewicz, M.J., 1993. An empirical determination of the minimum number of measurements needed to estimate the mean random vitrinite reflectance of disseminated organic matter. *Org. Geochem.* 20, 643–651.
- Barrows, M.H., Cluff, R.M., 1984. New Albany Shale Group (Devonian-Mississippian) source rocks and hydrocarbon generation in the Illinois Basin. In: Demaison, G., Murvir, R.J. (Eds.), *Petroleum Geochemistry and Basin Evolution Vol. 36*. American Association of Petroleum Geologists Memoir, pp. 111–138.
- Baruch, E.T., Kennedy, M.J., Löhr, S.C., Dewhurst, D.N., 2015. Feldspar dissolution-enhanced porosity in Paleoproterozoic shale reservoir facies from the Barney Creek Formation (McArthur Basin, Australia). *Am. Assoc. Pet. Geol. Bull.* 99, 1745–1770.
- Baskin, D.K., Peters, K.E., 1992. Early generation characteristics of a sulfur-rich Monterey kerogen. *Am. Assoc. Pet. Geol. Bull.* 76, 1–13.
- Baumgardner Jr., R.W., Hamlin, H.S., Rowe, H.D., 2014. High-resolution core studies of Wolfcamp/Leonard basinal facies, southern Midland Basin Texas. American Association of Petroleum Geologists Search and Discovery Article No. 106077 (http://www.searchanddiscovery.com/documents/2014/106077baumgardner/ndx_baumgardner.pdf (Accessed December 23, 2015)).
- Bazilian, M., Brandt, A.R., Billman, L., Heath, G., Logan, J., Mann, M., Melaina, M., Statwick, P., Arent, D., Benson, S.M., 2014. Ensuring benefits from North American shale gas development: towards a research agenda. *J. Unconv. Oil Gas Res.* 7, 71–74.
- Beaton, A.P., Pawlowicz, J.G., Anderson, S.D.A., Berhane, H., Rokosh, C.D., 2010. Organic Petrography of the Duvernay and Muskwa Formations in Alberta: Shale Gas Data Release. ERCB/AGS Open File Report 2010–06. 147 p. http://ags.aer.ca/document/OFR/OFR_2010_06.PDF (Accessed April 4, 2016).
- Behar, F., Vandenberghe, M., 1987. Chemical modelling of kerogens. *Org. Geochem.* 11, 15–24.
- Berch, H., Nunn, J., 2014. Predicting potential unconventional production in the Tuscaloosa marine shale play using thermal modeling and log overlay analysis. *Gulf Coast Assoc. Geol. Soc. J.* 3, 69–78.
- Bernard, S., Wirth, R., Schreiber, A., Schulz, H.-M., Horsfield, B., 2012a. Formation of nanoporous pyrobitumen residues during maturation of the Barnett Shale (Fort Worth Basin). *Int. J. Coal Geol.* 103, 3–11.
- Bernard, S., Horsfield, B., Schulz, H.-M., Schreiber, A., Wirth, R., Vu, T.T.A., Perssen, F., Köntzner, S., Volk, H., Sherwood, N., Fuentes, D., 2010. Multi-scale detection of organic and inorganic signatures provides insights into gas shale properties and evolution. *Chem. Erde* 70, 119–133.
- Bernard, S., Horsfield, B., Schulz, H.-M., Wirth, R., Schreiber, A., 2012b. Geochemical evolution of organic-rich shales with increasing maturity: a STXM and TEM study of the Posidonia Shale (Lower Toarcian, northern Germany). *Mar. Pet. Geol.* 31, 70–89.
- Bernard, S., Horsfield, B., 2014. Thermal maturation of gas shale systems. *Annu. Rev. Earth Planet. Sci.* 42, 635–651.
- Bertrand, P., Pittion, J.L., Bernaud, C., 1986. Fluorescence of organic matter in relation to its chemical composition. *Org. Geochem.* 10, 641–647.
- Bertrand, R., 1990. Correlations among the reflectances of vitrinite, chitinozoans, graptolites and scolecodonts. *Org. Geochem.* 15, 565–574.
- Bertrand, R., 1993. Standardization of solid bitumen reflectance to vitrinite in some Paleozoic sequences of Canada. *Energy Sources* 15, 269–288.
- Bertrand, R., Héroux, Y., 1987. Chitinozoan, graptolite, and scolecodont reflectance as an alternative to vitrinite and pyrobitumen reflectance in Ordovician and Silurian strata, Anticosti Island, Quebec, Canada. *Am. Assoc. Pet. Geol. Bull.* 71, 951–957.
- Bertrand, R., Malo, M., 2001. Source rock analysis, thermal maturation and hydrocarbon generation in the Siluro-Devonian rocks of the Gaspé Belt basin, Canada. *Bull. Can. Petrol. Geol.* 49, 238–261.
- Boak, J., 2012. Common wording vs. historical terminology. *AAPG Explor.* 33 (8), 43 (<http://www.aapg.org/publications/news/explorer/column/articleid/1993/common-wording-vs-historical-terminology> (Accessed March 16, 2016)).
- Boling, K.S., Dworkin, S.I., 2015. Origin of organic matter in the Eagle Ford Formation. *Interpretation* 3, SH27–SH39.
- Borrego, A.G., 2009. Precision of vitrinite reflectance measurements in dispersed organic matter: reappraisal of the information from past commission II activities working group of the ICCP. *ICCP News* 48, 50–58.
- Borrego, A.G., Araujo, C.V., Balke, A., Cardott, B., Cook, A.C., David, P.P., Flores, D., Hámor-Vidó, M., Hiltmann, W., Kalkreuth, W., Koch, J., Kommeren, K., Kus, J., Ligouis, B., Marques, M., Mendonça Filho, J.G., Misz, M., Oliveira, L., Pickel, W., Reimer, K., Rhanasinghe, P.P., Suárez-Ruiz, I., Vieth, A., 2006. Influence of particle and surface quality on the vitrinite reflectance of dispersed organic matter: comparative exercise using data from the qualifying system for reflectance analysis working group of ICCPP. *Int. J. Coal Geol.* 68, 151–170.
- Bostick, N.H., 1974. Phytoclasts as indicators of thermal metamorphism, Franciscan assemblage and Great Valley sequence (Upper Mesozoic), California. *Geol. Soc. Am. Spec. Pap.* 153, 1–17.
- Bostick, N.H., 1979. Microscopic measurement of the level of catagenesis of solid organic matter in sedimentary rocks to aid exploration for petroleum and to determine former burial temperatures: a review. In: Scholle, P.A., Schluger, P.R. (Eds.), *Aspects of Diagenesis*. SEPM Special Publication Vol. 26, pp. 17–43.
- Bostick, N.H., Foster, J.N., 1975. Comparison of vitrinite reflectance in coal seams and in kerogen of sandstones, shales, and limestones in the same part of a sedimentary section. In: Alpern, B. (Ed.), *Petrographie de la matière organique des sédiments, relations avec la paleotemperature et le potentiel pétrolier*, pp. 13–25 Paris, CNRS.
- Bousige, C., Ghimbeu, C.M., Vix-Guterl, C., Pomerant, A.E., Suleimenova, A., Vaughn, G., Garbarino, G., Feygenson, M., Wildgruber, C., Ulm, F.-J., Pellenq, R.J.-M., Coasne, B., 2016. Realistic molecular model of kerogen's nanostructure. *Nat. Mater.* 15, 576–582.
- Bowker, K.A., 2007. Barnett shale gas production Ft. Worth basin: issues and discussion. *Am. Assoc. Pet. Geol. Bull.* 91, 523–533.
- Bowman, T.D., Mukhopadhyay, P.K., 2014. North American Ordovician Unconventional Oil Potential. *Unconventional Resources Technology Conference Paper 1935162 (7 p)*.
- Breyer, J.A., 2012. Shale reservoirs: giant resources for the 21st century. *AAPG Mem.* 97 (519 p).

- Broadhead, R.F., Gillard, L., 2007. The Barnett shale in southeastern New Mexico: distribution, thickness, and source rock characterization. New Mexico Bureau of Geology and Mineral Resources Open-File Report No. 502 (56 p).
- Brown, D., 2012. The Monterey shale: big deal or big bust? AAPG Explor. 33 (11), 8–12.
- Buchardt, B., Lewan, M.D., 1990. Reflectance of vitrinite-like macerals as a thermal maturity index for Cambrian–Ordovician Alum Shale, southern Scandinavia. Am. Assoc. Pet. Geol. Bull. 74, 394–406.
- Buiskool Toxopeus, J.M.A., 1983. Selection criteria for the use of vitrinite reflectance as a maturity tool. In: Brooks, J. (Ed.), Petroleum Geochemistry and Exploration of Europe. Blackwell Scientific Publications, Oxford, pp. 295–307.
- Bustin, R.M., Cameron, A.R., Grieve, D.A., Kalkreuth, W.D., 1985. Coal Petrology, Its Principles, Methods, and Applications. Geological Association of Canada Short Course Notes, v. 3, Second revised edition. (230 p).
- Caldwell, C., 2014. Anadarko Woodford Shale: how to tie a shoe. American Association of Petroleum Geologists Search and Discovery Article No. 80408 (52 p) http://www.searchanddiscovery.com/pdf2/documents/2014/80408caldwell/ndx_caldwell.pdf.html (Accessed December 22, 2015).
- Camp, W.K., 2014. Diagenesis of Organic-Rich Shale: Views From Foraminifera *Penetralia*. American Association of Petroleum Geologists Search and Discovery Article No. Eagle Ford Formation, Maverick Basin, Texas, p. 51054 http://www.searchanddiscovery.com/documents/2014/51054camp/ndx_camp.pdf (accessed August 9, 2015).
- Camp, W.K., 2015. Diagenetic evolution of organic matter cements in unconventional shale reservoirs. American Association of Petroleum Geologists Search and Discovery Article No. 90216 <http://www.searchanddiscovery.com/abstracts/html/2015/90216ace/abstracts/2087920.html> (Accessed February 5, 2016).
- Camp, W.K., Diaz, E., Wawak, B., 2013. Electron microscopy of shale hydrocarbon reservoirs. AAPG Mem. 102 (260 p).
- Camp, W.K., Wawak, B., 2013. Enhancing SEM grayscale images through pseudocolor conversion: examples from Eagle Ford, Haynesville, and Marcellus Shales 2013a In: Camp, W.K., Diaz, E., Wawak, B. (Eds.), Electron Microscopy of Shale Hydrocarbon Reservoirs 102. American Association of Petroleum Geologists Memoir, pp. 15–26.
- Caplan, M.L., Bustin, R.M., 1998. Palaeoceanographic controls on geochemical characteristics of organic-rich Exshaw mudrocks: role of enhanced primary production. Org. Geochem. 30, 161–188.
- Cardott, B.J., 1989. Thermal maturation of the Woodford shale in the Anadarko basin. In: Johnson, K.S. (Ed.), Anadarko Basin Symposium, 1988 Vol. 90. Oklahoma Geological Survey Circular, pp. 32–46.
- Cardott, B.J., 1994. Thermal maturity of surface samples from the frontal and central belts, Ouachita Mountains, Oklahoma. In: Suneson, N.H., Hemish, L.A. (Eds.), Geology and Resources of the Eastern Ouachita Mountains Frontal Belt and Southeastern Arkoma Basin, Oklahoma Vol. 29. Oklahoma Geological Survey Guidebook, pp. 271–276.
- Cardott, B.J., 2008. Shales closing 'conventional gap'. AAPG Explor. 29 (11), 75–78 <https://www2.aapg.org/explorer/2008/11nov/11novExplorer08.pdf> (accessed December 10, 2015).
- Cardott, B.J., 2012. Thermal maturity of the Woodford Shale gas and oil plays, Oklahoma, USA. Int. J. Coal Geol. 103, 109–119.
- Cardott, B.J., Chaplin, J.R., 1993. Guidebook for Selected Stops in the Western Arbuckle Mountains, Southern Oklahoma. Oklahoma Geological Survey Special Publication, p. 93 (55 p).
- Cardott, B.J., Kidwai, M.A., 1991. Graptolite reflectance as a potential thermal-maturation indicator. In: Johnson, K.S. (Ed.), Late Cambrian–Ordovician Geology of the Southern Midcontinent, 1989 Symposium Vol. 92. Oklahoma Geological Survey Circular, pp. 203–209.
- Cardott, B.J., Landis, C.R., Curtis, M.E., 2015. Post-oil solid bitumen network in the Woodford Shale, USA—a potential primary migration pathway. Int. J. Coal Geol. 139, 106–113.
- Carr, A.D., 2000. Suppression and retardation of vitrinite reflectance, part 1: formation and significance for hydrocarbon generation. J. Pet. Geol. 23, 313–343.
- Carr, A.D., Williamson, J.E., 1990. The relationship between aromaticity, vitrinite reflectance and maceral composition of coals: implications for the use of vitrinite reflectance as a maturity parameter. Org. Geochem. 16, 313–323.
- Carvajal-Ortiz, H., Gentzis, T., 2015. Critical considerations when assessing hydrocarbon plays using Rock-Eval pyrolysis and organic petrology data: data quality revisited. Int. J. Coal Geol. 152, 113–122 Part A.
- Castañón, J.R., Sparks, D.M., 1974. Interpretation of vitrinite reflectance measurements in sedimentary rocks and determination of burial history using vitrinite reflectance and authigenic minerals. In: Dutcher, R.R., Hacquebard, P.A., Schopf, J.M., Simon, J.A. (Eds.), Carbonaceous Materials as Indicators of Metamorphism Vol. 153. Geological Society of America Special Paper, pp. 31–52.
- Chalmers, G., Bustin, R.M., Power, I., 2012. Characterization of gas shale pore systems by porosimetry, pycnometry, surface area and FE-SEM/TEM image analysis: examples from the Barnett, Woodford, Haynesville, Marcellus, and Doig formations. Am. Assoc. Pet. Geol. Bull. 96, 1099–1119.
- Chatellier, J.-Y., Jarvie, D.M., 2013. Critical assessment of shale resource plays. AAPG Mem. 103 (186 p).
- Chen, J., Xiao, X., 2014. Evolution of nanoporosity in organic-rich shales during thermal maturation. Fuel 129, 173–181.
- Chen, Z., Jiang, C., 2016. A revised method for organic porosity estimation in shale reservoirs using Rock-Eval data: example from the Duvernay Formation in the Western Canada Sedimentary Basin. Am. Assoc. Pet. Geol. Bull. 100, 405–422.
- Chow, N., Wendte, J., Stasiuk, L.D., 1995. Productivity versus preservation controls on two organic-rich carbonate facies in the Devonian of Alberta: sedimentological and organic petrological evidence. Bull. Can. Petrol. Geol. 43, 433–460.
- Cicero, A.D., Steinhoff, I., 2013. Sequence stratigraphy and depositional environments of the Haynesville and Bossier Shales, east Texas and north Louisiana. In: Hammes, U., Gale, J. (Eds.), Geology of the Haynesville Gas Shale in East Texas and West Louisiana, USA Vol. 105. American Association of Petroleum Geologists Memoir, pp. 25–46.
- Clarkson, C.R., Solano, N., Bustin, R.M., Bustin, A.M.M., Chalmers, G.R.L., He, L., Melnichenko, Y.B., Radliński, A.P., Blach, T.P., 2013. Pore structure characterization of North American shale gas reservoirs using USANS/SANS, gas adsorption, and mercury intrusion. Fuel 103, 606–616.
- Cole, G.A., Drozd, R.J., Sedivy, R.A., Halpern, H.L., 1987. Organic geochemistry and oil-source correlations, Paleozoic of Ohio. Am. Assoc. Pet. Geol. Bull. 71, 788–809.
- Cook, A.C., 2011a. The petrographic microscope. In: Vasconcelos, L., Flores, D., Marques, M. (Eds.), ICCP Training Course on Dispersed Organic Matter. Plenum, Porto, pp. 199–216.
- Cook, A.C., 2011b. ICCP accreditation. In: Vasconcelos, L., Flores, D., Marques, M. (Eds.), ICCP Training Course on Dispersed Organic Matter. Plenum, Porto, pp. 221–230.
- Cornford, C., Gardner, P., Burgess, C., 1998. Geochemical truths in large data sets. I: geochemical screening data. Org. Geochem. 29, 519–530.
- Corrêa da Silva, Z., 1989. The rank evaluation of south Brazilian Gondwana coals on the basis of different chemical and physical parameters. Int. J. Coal Geol. 13, 21–39.
- Creaney, S., Allan, J., 1990. Hydrocarbon generation and migration in the Western Canada sedimentary basin. In: Brooks, J. (Ed.), Classic Petroleum Provinces Vol. 50. Geological Society of London Special Publication, pp. 189–202.
- Creaser, R.A., Sannigrahi, P., Chacko, T., Selby, D., 2002. Further evaluation of the re-Os geochronometer in organic-rich sedimentary rocks: a test of hydrocarbon maturation effects in the Exshaw Formation, Western Canada Sedimentary Basin. Geochim. Cosmochim. Acta 66, 3441–3452.
- Curiale, J.A., 1986. Origin of solid bitumens, with emphasis on biological marker results. Org. Geochem. 10, 559–580.
- Curiale, J.A., Curtis, J.B., 2016. Organic geochemical applications to the exploration for source-rock reservoirs: a review. J. Unconv. Oil Gas Res. 13, 1–31.
- Curtis, J.B., 2002. Fractured shale-gas systems. Am. Assoc. Pet. Geol. Bull. 86, 1921–1938.
- Curtis, J.B., Zumberge, J.E., Brown, S.W., 2013. Evaluation of Niobrara and Mowry Formation petroleum systems in the Powder River, Denver and Central Basins of the Rocky Mountains, Colorado and Wyoming, USA. 55. Houston Geological Society (7), 31, 33, 35 <http://archives.datapages.com/data/HGS/vol55/vol55no7/31.htm> (Accessed January 26, 2016).
- Curtis, M.E., Sondergeld, C.H., Ambrose, R.J., Rai, C.S., 2012a. Microstructural investigation of gas shales in two and three dimensions using nanometer-scale resolution imaging. Am. Assoc. Pet. Geol. Bull. 96, 665–677.
- Curtis, M.E., Cardott, B.J., Sondergeld, C.H., Rai, C.S., 2012b. Development of organic porosity in the Woodford Shale with increasing thermal maturity. Int. J. Coal Geol. 103, 26–31.
- Cusack, C., Beeson, J., Stoneburner, D., Robertson, G., 2010. The discovery, reservoir attributes, and significance of the Hawkville field and Eagle Ford shale trend, Texas. Gulf Coast Assoc. Geol. Soc. Trans. 60, 165–179.
- Dahl, B., Bojesen-Koefoed, J., Holm, A., Justwan, H., Rasmussen, E., Thomsen, E., 2004. A new approach to interpreting Rock-Eval S2 and TOC data for kerogen quality assessment. Org. Geochem. 35, 1461–1477.
- Davis, A., 1978. The reflectance of coal. In: Karr Jr., C. (Ed.), Analytical Methods for Coal and Coal Products Vol. v. 1. Academic Press, New York, pp. 27–81.
- Davis, A., 1984. Coal petrology and petrographic analysis. In: Ward, C.R. (Ed.), Coal Geology and Coal Technology. Blackwell Scientific Publications, Palo Alto, pp. 74–112.
- De Silva, P.N.K., Simons, S.J.R., Stevens, P., Philip, L.M., 2015. A comparison of North American shale plays with emerging non-marine shale plays in Australia. Mar. Pet. Geol. 67, 16–29.
- Dean, W.E., Arthur, M.A., Sageman, B.B., Lewan, M.D., 1995. Core Descriptions and Preliminary Geochemical Data for the Amoco Production Company Rebecca K. Bounds #1 Well, Greeley County, Kansas. U.S. Geological Survey Open-File Report, pp. 95–209 243 p. <http://pubs.usgs.gov/of/1995/0209/report.pdf> (Accessed January 25, 2016).
- Dembicki Jr., H., 1984. An interlaboratory comparison of source rock data. Geochim. Cosmochim. Acta 48, 2641–2649.
- Dembicki Jr., H., 2009. Three common source rock evaluation errors made by geologists during prospect or play appraisals. Am. Assoc. Pet. Geol. Bull. 93, 341–356.
- Dembicki Jr., H., Madren, J.D., 2014. Lessons learned from the Floyd shale play. J. Unconv. Oil Gas Res. 7, 1–10.
- Denne, R.A., Hinote, R.E., Breyer, J.A., Kosanke, T.H., Lees, J.A., Engelhardt-Moore, N., Spaw, J.M., Tur, N., 2014. The Cenomanian–Turonian Eagle Ford Group of south Texas: insights on timing and paleoceanographic conditions from geochemistry and micropaleontologic analyses. Palaeogeogr. Palaeoclimatol. Palaeoecol. 413, 2–28.
- Dittrick, P., 2012. More companies investing in Duvernay liquids potential. Oil Gas J. 110 (11) <http://www.ogj.com/articles/print/vol-110/issue-11/general-interest/more-companies-investing-in-duvernay.html> (Accessed January 22, 2016).
- Dittrick, P., 2013. Montney, Duvernay will be key to Canada shale oil, gas growth. Oil Gas J. 111 (4) <http://www.ogj.com/articles/print/volume-111/issue-4/general-interest/montney-duvernay-will-be-key-to-canada.html> (Accessed January 22, 2016).
- Donaldson, E.C., Alam, W., 2008. Wettability. Gulf Publishing Company, Houston, Texas (360 p).
- Dong, T., Harris, N.B., 2013. Pore size distribution and morphology in the Horn River Shale, Middle and Upper Devonian, northeastern British Columbia, Canada. In: Camp, W., Diaz, E., Wawak, B. (Eds.), Electron Microscopy of Shale Hydrocarbon Reservoirs Vol. 102. AAPG Memoir, pp. 67–79.
- Dong, T., Harris, N.B., Ayranci, K., Twemlow, C.E., Nassichuk, B.R., 2015. Porosity characteristics of the Devonian Horn River shale, Canada: insights from lithofacies classification and shale composition. Int. J. Coal Geol. 141–142, 74–90.
- Dow, W.G., 1977. Kerogen studies and geological interpretations. J. Geochem. Explor. 7, 79–99.
- Dow, W.G., O'Connor, D.I., 1982. Kerogen maturity and type by reflected light microscopy applied to petroleum exploration. In: Staplin, F.L., et al. (Eds.), How to Assess Maturation and Paleotemperatures Vol. 7. SEPM Short Course, pp. 133–157.

- Driskill, B., Walls, J., Sinclair, S.W., DeVito, J., 2013a. Micro-scale Characterization of the Eagle Ford Formation Using SEM Methods and Digital Rock Modeling. Unconventional Resources Technology Conference paper URTEC 1582375 (7 p).
- Driskill, B., Walls, J., Sinclair, S.W., DeVito, J., 2013b. Applications of SEM imaging to reservoir characterization in the Eagle Ford Shale, south Texas, U.S.A. In: Camp, W., Diaz, E., Wawak, B. (Eds.), *Electron Microscopy of Shale Hydrocarbon Reservoirs* Vol. 102. AAPG Memoir, pp. 115–136.
- Dunn, L., Schmidt, G., Hammermaster, K., Brown, M., Bernard, R., Wen, E., Befus, R., Gardner, S., 2014. The Duvernay Formation (Devonian): sedimentology and reservoir characterization of a shale gas/liquids play in Alberta, Canada. American Association of Petroleum Geologists Search and Discovery Article No. 10590 8 p. http://www.searchanddiscovery.com/documents/2014/10590dunn/ndx_dunn.pdf (Accessed January 23, 2016).
- Dunnahoe, T., 2013. Ohio's Utica shale development has room to grow. *Oil Gas J.* 111 (10), 44–45 <http://www.ogj.com/articles/print/volume-111/issue-10/general-interest/ohio-s-utica-shale-development-has-room-to-grow.html> (Accessed January 26, 2016).
- Durand, B., 1980. Sedimentary organic matter and kerogen: definition and quantitative importance of kerogen. In: Durand, B. (Ed.), *Kerogen: Insoluble Organic Matter from Sedimentary Rocks*. Editions Technip, Paris, pp. 13–34.
- Durham, L.S., 2013a. Rocky operators cautiously move ahead. *AAPG Explor.* 34 (6), 6–8.
- Durham, L.S., 2013b. Geologists excited about TMS potential. *AAPG Explor.* 34 (7), 16–18.
- Durham, L.S., 2014. Little known TMS play sees drilling surge. *AAPG Explor.* 35 (8), 12–16.
- Durham, L.S., 2015a. Oil price slams beleaguered TMS play. *AAPG Explor.* 36 (2), 46.
- Durham, L.S., 2015b. Wolfcamp play in Permian's Delaware Basin: potentially 'more productive than Eagle Ford'. *AAPG Explor.* 36 (8), 32.
- East, J.A., Swezey, C.S., Repetski, J.E., Hayba, D.O., 2012. Thermal maturity map of Devonian shale in the Illinois, Michigan, and Appalachian basins of North America. *US Geol. Surv. Sci. Invest. Map 3214* <http://pubs.usgs.gov/sim/3214/> (Accessed December 19, 2015).
- Edman, J.D., Pitman, J.K., 2010. Geochemistry of Eagle Ford Group source rocks and oils from the First Shot field area, Texas. *Gulf Coast Assoc. Geol. Soc. Trans.* 60, 217–234.
- Eldrett, J.S., Ma, C., Bergman, S.C., Ozkan, A., Minisini, D., Lutz, B., Jackett, S.-J., Macaulay, C., Kelly, A.E., 2015. Origin of limestone–marlstone cycles: astronomic forcing of organic-rich sedimentary rocks from the Cenomanian to early Coniacian of the Cretaceous Western Interior Seaway, USA. *Earth Planet. Sci. Lett.* 423, 98–113.
- Elgmami, M., Zobaa, M., Zhang, H., Bai, B., Obboh-Ikuenobe, F., 2011. Palynofacies analysis and submicron pore modeling of shale gas plays. *Soc. Pet. Eng. Pap. SPE 144267* (10 p).
- Emmanuel, S., Eliyahu, M., Day-Stirrat, R.J., Hofmann, R., 2016. Impact of thermal maturation on nano-scale elastic properties of organic matter in shales. *Mar. Pet. Geol.* 70, 175–184.
- Energy Information Administration, 2011. Bakken Formation oil and gas drilling activity mirrors development in the Barnett. <http://www.eia.gov/todayinenergy/detail.cfm?id=3750> (accessed August 26, 2015).
- Energy Information Administration, 2013. EIA to release new Drilling Productivity Report. <https://www.eia.gov/todayinenergy/detail.cfm?id=13451> (Accessed January 22, 2016).
- Energy Information Administration, 2014. Updates to the EIA Eagle Ford play maps. <https://www.eia.gov/maps/pdf/eagleford122914.pdf> (Accessed January 24, 2016).
- Energy Information Administration, 2015a. Top 100 U.S. oil and gas fields. <http://www.eia.gov/naturalgas/crudeoilreserves/top100/pdf/top100.pdf> (accessed August 28, 2015).
- Energy Information Administration, 2015b. International energy data and analysis. <http://www.eia.gov/beta/international/> (accessed August 28, 2015).
- Energy Information Administration, 2016. Drilling productivity report. <https://www.eia.gov/petroleum/drilling/pdf/dpr-full.pdf> (Accessed January 24, 2016).
- Engelder, T., Lash, G.G., 2008. Marcellus Shale play's vast resource potential creating stir in Appalachia. *Am. Oil Gas Rep.* 77–78 May 2008. (81–82, 85–87).
- Epstein, A.G., Epstein, J.B., Harris, L.D., 1977. Conodont color alteration: an index to organic metamorphism. *U.S. Geological Survey Professional Paper* 995 (27 p).
- Ercegovic, M., Kostić, A., 2006. Organic facies and palynofacies: nomenclature, classification and applicability for petroleum source rock evaluation. *Int. J. Coal Geol.* 68, 70–78.
- Estes-Jackson, J.E., Anderson, D.S. (Eds.), 2011. *Revisiting and Revitalizing the Niobrara in the Central Rockies*. Rocky Mountain Association of Geologists, Denver, Colorado, CD-ROM.
- Ewing, T.E., 2001. Review of Late Jurassic Depositional Systems and Potential Hydrocarbon Plays, Northern Gulf of Mexico Basin: Gulf Coast Geological Association of Geological Societies Transactions 51, 85–96.
- Finn, T.M., Johnson, R.C., 2005. Niobrara total petroleum system in the southwestern Wyoming Province. In: Team, U.S.G.S.S.W.P.A. (Ed.), *Petroleum Systems and Geologic Assessment of Oil and Gas in the Southwestern Wyoming Province, Wyoming, Colorado, and Utah*. U.S. Geological Survey Digital Data Series DDS-69-D 27 p. https://pubs.usgs.gov/dds/dds-069/dds-069-d/REPORTS/69_D_CH_6.pdf (Accessed May 22, 2016).
- Fishman, N.S., Egenhoff, S.O., Boehlke, A.R., Lowers, H.A., 2015. Petrology and diagenetic history of the upper shale member of the Late Devonian–Early Mississippian Bakken Formation, Williston Basin, North Dakota. In: Larsen, D., Egenhoff, S.O., Fishman, N.S. (Eds.), *Paying Attention to Mudrocks: Priceless!* Vol. 515. Geological Society of America Special Paper, Denver, CO, pp. 125–151.
- Fishman, N.S., Guthrie, J.M., Honarpour, M., 2013. The stratigraphic distribution of hydrocarbon storage and its effect on producible hydrocarbons in the Eagle Ford Formation, south Texas. Unconventional Resources Technology Conference Paper URTEC 1579007 6 p. <http://archives.datapages.com/data/urtec/2013/urtec-1579007-fishman.pdf> (Accessed February 5, 2016).
- Fishman, N.S., Guthrie, J.M., Honarpour, M., 2014. Development of organic and inorganic porosity in the Cretaceous Eagle Ford Formation, south Texas. Search and Discovery Article No. 50928 http://www.searchanddiscovery.com/documents/2014/50928fishman/ndx_fishman.pdf (Accessed December 11, 2015).
- Fishman, N.S., Hackley, P.C., Lowers, H.A., Hill, R.J., Evenhoff, S.O., Eberl, D.D., Blum, A.E., 2012. The nature of porosity in organic-rich mudstones of the Upper Jurassic Kimmeridge Clay Formation, North Sea, offshore United Kingdom. *Int. J. Coal Geol.* 103, 32–50.
- Furmman, A., Mastalerz, M., Schimmelmann, A., Pedersen, P.K., Bish, D., 2014. Relationships between porosity, organic matter, and mineral matter in mature organic-rich marine mudstones of the Belle Fourche and Second White Specks formations in Alberta, Canada. *J. Mar. Pet. Geol.* 54, 64–81.
- Furmman, A., Mastalerz, M., Brassell, S.C., Pedersen, P.K., Zajac, N.A., Schimmelmann, A., 2015. Organic matter geochemistry and petrography of Late Cretaceous (Cenomanian–Turonian) organic-rich shales from the Belle Fourche and Second White Specks formations, west-central Alberta, Canada. *Org. Geochem.* 85, 102–120.
- Gaswirth, S.B., Marra, K.R., Cook, T.A., Charpentier, R.R., Gautier, D.L., Higley, D.K., Klett, T.R., Lewan, M.D., Lillis, P.G., Schenk, C.J., Tennyson, M.E., Whidden, K.J., 2013. Assessment of undiscovered oil resources in the Bakken and Three Forks Formations, Williston Basin Province, Montana, North Dakota, and South Dakota, 2013. U.S. Geological Survey Fact Sheet 2013–3013 4 p. <http://pubs.usgs.gov/fs/2013/3013/> (Accessed December 21, 2015).
- Ghanizadeh, A., Clarkson, C.R., Aquino, S., Ardakani, O.H., Sanei, H., 2015. Petrophysical and geomechanical characteristics of Canadian tight oil and liquid-rich gas reservoirs: I. Pore network and permeability characterization. *Fuel* 153, 664–681.
- Goergen, E.T., Curtis, M.E., Jernigen, J., Sondergeld, C., Rai, C., 2014. Integrated petrophysical properties and multi-scaled SEM. Unconventional Resources Technology Conference Paper 1922739, 25–27 August (Denver, Colorado, USA, 10 p).
- Gold, R., 2015. *The Boom: How Fracking Ignited the American Energy Revolution and Changed the World*. Simon and Schuster (384 p).
- Goodarzi, F., 1985a. Organic petrology of Hat Creek coal deposit no. 1, British Columbia. *Int. J. Coal Geol.* 5, 377–396.
- Goodarzi, F., 1985b. Reflected light microscopy of chitinozoan fragments. *Mar. Pet. Geol.* 2, 72–78.
- Goodarzi, F., Norford, B.S., 1989. Variation of graptolite reflectance with depth of burial. *Int. J. Coal Geol.* 11, 127–141.
- Goodarzi, F., Gentzis, T., Snowdon, L.R., Bustin, R.M., Feinstein, S., Labonte, M., 1993. Effect of mineral matrix and seam thickness on reflectance of vitrinite in high to low volatile bituminous coals: an enigma. *Mar. Pet. Geol.* 10, 162–171.
- Goodrich, 2015. Tuscaloosa Marine Shale Presentation: November 2015. Goodrich Petroleum Corporation <http://goodrichpetroleum.investorroom.com/download/MgmtTMS.pdf> (Accessed December 18, 2015).
- Gu, X., Cole, D.R., Rother, G., Mildner, D.F.R., Brantley, S.L., 2015. Pores in Marcellus Shale: a neutron scattering and FIB-SEM study. *Energy Fuel* 29, 1295–1308.
- Gurba, L.W., Ward, C.R., 1998. Vitrinite reflectance anomalies in high-volatile bituminous coals of the Gunnedah basin, New South Wales, Australia. *Int. J. Coal Geol.* 36, 111–140.
- Hackley, P.C., 2012. Geological and geomechanical characterization of the Lower Cretaceous Pearsall Formation, Maverick Basin, south Texas, USA: a potential shale gas resource? *Am. Assoc. Pet. Geol. Bull.* 96, 1449–1482.
- Hackley, P.C., Araujo, C.V., Borrego, A.G., Bouzinos, A., Cardott, B., Cook, A.C., Eble, C., Flores, D., Gentzis, T., Gonçalves, P.A., Mendonça Filho, J.G., Hámor-Vidó, M., Jelonek, I., Kommeren, K., Knowles, W., Kus, J., Mastalerz, M., Menezes, T.R., Newman, J., Oikonomopoulos, I.K., Pawlewicz, M., Pickel, W., Potter, J., Ranasinghe, P., Read, H., Reyes, J., Rodriguez, G.D.L.R., Fernandes de Souza, I.V.A., Suarez-Ruiz, I., Sýkorová, I., Valentine, B.J., 2015. Standardization of reflectance measurements in dispersed organic matter: results of an exercise to improve interlaboratory agreement. *Mar. Pet. Geol.* 59, 22–34.
- Hackley, P.C., Fishman, N., Wu, T., Baugher, G., 2016. Organic Petrology and Geochemistry of Mudrocks from the Lacustrine Lucaogou Formation, Santanghu Basin, Northwest China: Application to Lake Basin Evolution (International Journal of Coal Geology) <http://authors.elsevier.com/sd/article/S0166516216302257> <http://dx.doi.org/10.1016/j.coal.2016.05.011>.
- Hackley, P.C., Kus, J., 2015. Thermal maturity of Tasmanites microfossils from confocal laser scanning fluorescence microscopy. *Fuel* 143, 343–350.
- Hackley, P.C., Ryder, R.T., Trippi, M.H., Alimi, H., 2013. Thermal maturity of northern Appalachian Basin Devonian shales: insights from sterane and terpane biomarkers. *Fuel* 106, 455–462.
- Hackley, P.C., Valentine, B.J., Enomoto, C.B., Lohr, C.D., Scott, K.R., Dulong, F.T., Bove, A.M., 2014. Aptian 'shale gas' prospectivity in the downdip Mississippi Interior Salt Basin, Gulf Coast, USA. Unconventional Resources Technology Conference (URTEC) Paper 1922696 (9 p).
- Haeri-Ardakani, O., Sanei, H., Lavoie, D., Chen, Z., Mechti, N., 2015a. Thermal maturity and organic petrology of the Upper Ordovician Utica and Lorraine Shales, southern Quebec, Canada. American Association of Petroleum Geologists Search and Discovery Article No. 51078 http://www.searchanddiscovery.com/documents/2015/51078ardakani/ndx_ardakani (accessed August 16, 2015).
- Haeri-Ardakani, O., Sanei, H., Lavoie, D., Chen, Z., Jiang, C., 2015b. Geochemical and petrographic characterization of the Upper Ordovician Utica Shale, southern Quebec, Canada. *Int. J. Coal Geol.* 138, 83–94.
- Hamlin, H.S., Baumgardner Jr., R.W., 2012. Wolfberry (Wolfcampian–Leonardian) Deepwater Depositional Systems in the Midland Basin: Stratigraphy, lithofacies, Reservoirs, and Source Rocks The University of Texas at Austin, Bureau of Economic Geology Report of Investigations No. 277. (62 p).
- Hammes, U., Frébourg, G., 2012. Haynesville and Bossier mudrocks: a facies and sequence stratigraphic investigation, east Texas and Louisiana. *Mar. Pet. Geol.* 31, 8–26.

- Hammes, U., Gale, J., 2013. Geology of the Haynesville gas shale in east Texas and west Louisiana. AAPG Mem. 105 (236 p).
- Hammes, U., Hamlin, H.S., Ewing, T.E., 2011. Geologic analysis of the Upper Jurassic Haynesville Shale in east Texas and west Louisiana. Am. Assoc. Pet. Geol. Bull. 95, 1643–1666.
- Han, Y., Mahlstedt, N., Horsfield, B., 2015. The Barnett Shale: compositional fractionation associated with intraformational petroleum migration, retention, and expulsion. Am. Assoc. Pet. Geol. Bull. 99, 2173–2202.
- Hao, F., Chen, J., 1992. The cause and mechanism of vitrinite reflectance anomalies. J. Pet. Geol. 15, 419–434.
- Hao, F., Sun, Y.C., Li, S.T., Zhang, Q.M., 1995. Overpressure Retardation of Organic Matter Maturation and Hydrocarbon Generation: A Case Study from the Yinggehai and Qiongdongnan Basins, offshore South China Sea: American Association of Petroleum Geologists Bulletin 79, 551–562.
- Hao, F., Zou, H., Gong, Z., Yang, S., Zeng, Z., 2007. Hierarchies of overpressure retardation of organic matter maturation: case studies from petroleum basins in China. Am. Assoc. Pet. Geol. Bull. 91, 1467–1498.
- Hart, B.S., Steen, A.S., 2015. Programmed pyrolysis (Rock-Eval) data and shale paleoenvironmental analyses: a review. Interpretation 3, SH41–SH58.
- Hartel, T.H.D., Richards, B.C., Langenberg, C.W., 2014. Wabamun, Bakken equivalent Exshaw and Banff Formations in core, cuttings and outcrops from southern Alberta. American Association of Petroleum Geologists Search and Discovery Article No. 50952 30 p. http://www.searchanddiscovery.com/documents/2014/50952hartel/ndx_hartel.pdf (Accessed February 28, 2016).
- Hartkopf-Fröder, C., Königshof, P., Littke, R., Schwarzbauer, J., 2015. Optical thermal maturity parameters and organic geochemical alteration at low grade diagenesis to anchimetamorphism: A review. Int. J. Coal Geol. <http://dx.doi.org/10.1016/j.coal.2015.06.005>.
- He, S., Middleton, M., Kaiko, A., Jiang, C., Li, M., 2002. Two case studies of thermal maturity and thermal modeling within the overpressured Jurassic rocks of the Barrow sub-basin, northwest shelf of Australia. Mar. Pet. Geol. 19, 143–159.
- Heath, J.E., Dewers, T.A., McPherson, B.J.O.L., Petrusak, R., Chidsey Jr., T.C., Rinehart, A.J., Mozley, P.S., 2011. Pore networks in continental and marine mudstones: characteristics and controls on sealing behavior. Geosphere 7, 429–454.
- Hickey, J.J., Henk, B., 2007. Lithofacies summary of the Mississippian Barnett Shale, Mitchell 2 T.P. Sims well, Wise County, Texas. Am. Assoc. Pet. Geol. Bull. 91, 437–443.
- Hill, R.J., Jarvie, D.M., Zumberge, J., Henry, M., Pollastro, R.M., 2007. Oil and gas geochemistry and petroleum systems of the Fort Worth Basin. Am. Assoc. Pet. Geol. Bull. 91, 445–473.
- Hoffman, E., Jenkner, A., 1932. Die Inkohlung und ihre Erkennung im Mikrobildung. Glückauf 68, 81.
- Houseknecht, D.W., Rouse, W.A., Paxton, S.T., Mars, J.C., Fulk, B., 2014. Upper Devonian–Mississippian stratigraphic framework of the Arkoma Basin and distribution of potential source-rock facies in the Woodford–Chattanooga and Fayetteville–Caney shale-gas systems. Am. Assoc. Pet. Geol. Bull. 98, 1739–1759.
- Hu, H., Zhang, T., Wiggins-Camacho, J.D., Ellis, G.S., Lewan, M.D., Zhang, X., 2015. Experimental investigation of changes in methane adsorption of bitumen-free Woodford Shale with thermal maturation induced by hydrous pyrolysis. Mar. Pet. Geol. 59, 114–128.
- Huang, W.L., 1996. Experimental study of vitrinite maturation: effects of temperature, time, pressure, water, and hydrogen index. Org. Geochem. 24, 233–241.
- Hume, D.W., Davies, G.R., Wüst, R.A.J., 2014. Duvernay gas liquids and geomechanics project. Canadian Discovery Ltd. Report 160 p. proprietary report, see http://www.canadiandiscovery.com/assets/PDFs/Studies/Duvernay_Brochure.pdf (Accessed March 2, 2016).
- Hunt, J.M., 1996. Petroleum Geochemistry and Geology. second ed. W.H. Freeman and Company, New York (743 pp).
- Hutton, A.C., Cook, A.C., 1980. Influence of alginite on the reflectance of vitrinite. Fuel 59, 711–716.
- ICCP (International Committee for Coal and Organic Petrology), 1971o. Determination of rank by reflectance measurement of vitrinite. In: ICPP (Ed.), International Handbook of Coal Petrography, Supplement to Second Edition (16 p).
- ICCP (International Committee for Coal and Organic Petrology), 1998o. The new vitrinite classification (ICCP System 1994). Fuel 77, 349–358.
- IHS Energy Group, 2016. US Well and Production Data. IHS Energy Group, 15 Inverness Way East, D205, Englewood, CO 80112, USA [includes data current as of January 2016]. (Accessed January 24, 2016).
- Inan, S., Goodarzi, F., Mumm, A.S., Arouri, K., Qathami, S., Ardakani, O.H., Inan, T., Tuwailib, A.A., 2016. The Silurian Qusaiba Hot Shales of Saudi Arabia: an integrated assessment of thermal maturity. Int. J. Coal Geol. 159, 107–119.
- Jaeger, H., 2013. Optical kerogen analysis: a new workflow in unconventional shale play analysis. Unconventional Resources Technology Conference Paper URTEC 1581418 (9 p).
- Jacob, H., 1965. Neue Erkenntnisse auf dem Gebiet der Lumineszenzmikroskopie fossiler Brennstoffe. Fortschr. Geol. Rheinl. 12, 569–588.
- Jacob, H., 1989. Classification, structure, genesis and practical importance of natural solid oil bitumen (“migrabitumen”). Int. J. Coal Geol. 11, 65–79.
- Jarvie, D.M., Claxton, B.L., Henk, F., Breyer, J.T., 2001. Oil and shale gas from the Barnett Shale, Fort Worth basin, Texas. Am. Assoc. Pet. Geol. Annu. Meet. Program 10, A100.
- Jarvie, D.M., Coskey, R.J., Johnson, M.S., Leonard, J.E., 2011. The geology and geochemistry of the Parshall area, Mountrail County, North Dakota. In: Robinson, J.W., LeFever, J.A., Gaswirth, S.B. (Eds.), The Bakken–three Forks Petroleum System in the Williston Basin. Denver, Colorado, Rocky Mountain Association of Geologists, pp. 229–268.
- Jarvie, D.M., Hill, R.J., Pollastro, R.M., 2005. Assessment of the gas potential and yields from shales: The Barnett Shale model. In: Cardott, B.J. (Ed.), Unconventional Energy Resources in the Southern Midcontinent, 2004 Symposium Vol. 110. Oklahoma Geological Survey Circular, pp. 37–50.
- Jarvie, D.M., Hill, R.J., Ruble, T.E., Pollastro, R.M., 2007. Unconventional shale-gas systems: the Mississippian Barnett Shale of north-central Texas as one model for thermogenic shale gas assessment. Am. Assoc. Pet. Geol. Bull. 91, 475–499.
- Jennings, D.S., Antia, J., 2013. Petrographic characterization of the Eagle Ford Shale, south Texas: mineralogy, common constituents, and distribution of nanometer-scale pore types. In: Camp, W., Diaz, E., Wawak, B. (Eds.), Electron Microscopy of Shale Hydrocarbon Reservoirs Vol. 102. AAPG Memoir, pp. 101–113.
- Jiao, K., Yao, S., Liu, C., Gao, Y., Wu, H., Li, M., Tang, Z., 2014. The characterization and quantitative analysis of nanopores in unconventional gas reservoirs utilizing FESEM–FIB and image processing: an example from the lower Silurian Longmaxi Shale, upper Yangtze region, China. Int. J. Coal Geol. 128–129, 1–11.
- Jin, H., Sonnenberg, S.A., 2012. Source rock potential of the Bakken shales in the Williston Basin, North Dakota and Montana. American Association of Petroleum Geologists Search and Discovery Article No. 20156 http://www.searchanddiscovery.com/documents/2012/20156jin/ndx_jin.pdf (Accessed December 21, 2015).
- Jin, H., Sonnenberg, S.A., 2014. Characterization for source-rock potential of the Bakken shales in the Williston Basin, North Dakota and Montana. American Association of Petroleum Geologists Search and Discovery Article No. 80356 http://www.searchanddiscovery.com/documents/2014/80356jin/ndx_jin.pdf (accessed August 26, 2015).
- John, C.J., Jones, B.L., Moncrief, J.E., Bourgeois, R., Harder, B.J., 1997. An unproven unconventional seven billion barrel oil resource: the Tuscaloosa Marine shale. BRI Bull. 7 (22 p).
- John, C.M., Föllmi, K.B., de Kaenel, E., Adatte, T., Steinmann, P., Badertscher, C., 2002. Carbonaceous and phosphate-rich sediments of the Miocene Monterey Formation at El Capitan State Beach, California, USA. J. Sediment. Res. 72, 252–267.
- Johnson, K.M., Grimm, K.A., 2001. Opal and organic carbon in laminated diatomaceous sediments: Saanich Inlet, Santa Barbara Basin and the Miocene Monterey Formation. Mar. Geol. 174, 159–175.
- Johnson, K.S., Cardott, B.J., 1992. Geologic framework and hydrocarbon source rocks of Oklahoma. In: Johnson, K.S., Cardott, B.J. (Eds.), Source Rocks in the Southern Midcontinent, 1990 Symposium Vol. 93. Oklahoma Geological Survey Circular, pp. 21–37.
- Johnsson, M.J., Howell, D.G., Bird, K.J., 1993. Thermal maturity patterns in Alaska: implications for tectonic evolution and hydrocarbon potential. Am. Assoc. Pet. Geol. Bull. 77, 1874–1903.
- Jones, R.W., Edison, T.A., 1978. Microscopic observations of kerogen related to geochemical parameters with emphasis on thermal maturation. In: Oltz, D.F. (Ed.), Low Temperature Metamorphism of Kerogen and Clay Minerals. Los Angeles, SEPM Pacific Section, pp. 1–12.
- Jones, J., Murchison, D.G., Saleh, S., 1972. Variation of vitrinite reflectivity in relation to lithology. In: Gaertner, H.W., Wehner, H. (Eds.), Advances in Organic Geochemistry 1971. Pergamon Press, Oxford, pp. 601–612.
- Josh, M., Esteban, L., Delle Piane, C., Sarout, J., Dewhurst, D.N., Clennell, M.B., 2012. Laboratory characterization of shale properties. J. Pet. Sci. Eng. 88–89, 107–124.
- Juliao, T., Suárez-Ruiz, I., Marquez, R., Ruiz, B., 2015. The role of solid bitumen in the development of porosity in shale oil reservoir rocks of the Upper Cretaceous in Columbia. Int. J. Coal Geol. 147–148, 126–144.
- Kaegi, D.D., 1985. On the identification and origin of pseudovitrinite. Int. J. Coal Geol. 4, 309–319.
- Kalkreuth, W., 1982. Rank and petrographic composition of selected Jurassic–Lower Cretaceous coals of British Columbia, Canada. Bull. Can. Petrol. Geol. 30, 112–139.
- Kalkreuth, W., Macauley, G., 1987. Organic petrology and geochemical (Rock-Eval) studies on oil shales and coals from the Pictou and Antigonish areas, Nova Scotia, Canada. Bull. Can. Petrol. Geol. 35, 263–295.
- Khorasani, G.K., Michelsen, J.K., 1994. The effects of overpressure, lithology, chemistry and heating rate on vitrinite reflectance evolution, and its relationship with oil generation. APEA J. 34 (pt. 1), 418–434.
- Kirschbaum, M.A., Schenk, C.J., Cook, T.A., Ryder, R.T., Charpentier, R.R., Klett, T.R., Gaswirth, S.B., Tennyson, M.E., Whidden, K.J., 2012. Assessment of undiscovered oil and gas resources of the Ordovician Utica Shale of the Appalachian Basin Province, 2012. U.S. Geological Survey Fact Sheet 2012–3116 6 p <http://pubs.usgs.gov/fs/2012/3116/FS12-3116.pdf> (Accessed March 2, 2016).
- Klaver, J., Desbois, G., Urai, J.L., Littke, R., 2012. BIB-SEM study of the pore space morphology in early mature Posidonia Shale from the Hils area, Germany. Int. J. Coal Geol. 103, 12–25.
- Klaver, J., Desbois, G., Littke, R., Urai, J.L., 2015. BIB-SEM characterization of pore space morphology and distribution in postmature to overmature samples from the Haynesville and Bossier shales. Mar. Pet. Geol. 59, 451–466.
- Kondla, D., Sanei, H., Embry, A., Ardakani, O.H., Clarkson, C.R., 2015. Depositional environment and hydrocarbon potential of the Middle Triassic strata of the Sverdrup Basin, Canada. Int. J. Coal Geol. 147–148, 71–84.
- Kus, J., 2015. Application of confocal laser-scanning microscopy (CLSM) to autofluorescent organic and mineral matter in peat, coals and siliciclastic sedimentary rocks: a qualitative approach. Int. J. Coal Geol. 137, 1–18.
- Kus, J., Tolmacheva, T., Dolezych, M., Gaedicke, C., Franke, D., Blumenberg, M., Piepjohn, K., Pleitsch, T., 2015. Organic matter type, origin and thermal maturity of Paleozoic, Mesozoic and Cenozoic successions of the New Siberian Islands, eastern Russia. Int. J. Coal Geol. 152, 125–146.
- Lan, Q., Xu, M., Binazadeh, M., Dehghanpour, H., Wood, J.M., 2015b. A comparative investigation of shale wettability: the significance of pore connectivity. J. Nat. Gas Sci. Eng. 27, 1174–1188.
- Lan, Q., Yassin, M.R., Habibi, A., Dehghanpour, H., Wood, J., 2015a. Relative permeability of unconventional rocks with dual-wettability pore-network. Unconventional Resources Technology Conference, SPE-178549-MS/URTEC 2153642 (14 p).
- Landis, C.R., 1990. Organic Maturation, Primary Migration, and Clay Mineralogy of Selected Permian Basin Shales unpublished PhD thesis Texas Tech University, Lubbock, Texas (227 p).

- Landis, C.R., Castañón, J.R., 1995. Maturation and bulk chemical properties of a suite of solid hydrocarbons. *Org. Geochem.* 22, 137–149.
- Landis, C.R., Gangopadhyay, S., Borst, W.L., 1991. Photochemistry of an unusual exsudatinite in Permian Basin shales. *Chem. Geol.* 93, 111–128.
- Landon, S.M., Longman, M.W., Luneau, B.A., 2001. Hydrocarbon source rock potential of the Upper Cretaceous Niobrara Formation, Western Interior Seaway of the Rocky Mountain region. *Mount. Geol.* 38, 1–18.
- Laughrey, C.D., 2014. Introductory geochemistry for shale gas, condensate-rich shales and tight oil reservoirs. URTEC Annual Meeting Short Course, Colorado Convention Center, Denver, Colorado (August 2014, 325 p).
- Laughrey, C.D., Billman, D.A., Canich, M.R., 2004. Petroleum geology and geochemistry of the Council Run gas field, north central Pennsylvania. *Am. Assoc. Pet. Geol. Bull.* 88, 213–239.
- Laughrey, C.D., Ruble, T.E., Purrzellera, P., Hooghan, K., Beuthin, J., Washburn, K., Dorsey, W., 2013. Dual mineral matrix and organic pore textures in thermally mature Niobrara Formation, Rocky Mountains region, USA: implications for tight-oil carbonate reservoir modeling. American Association of Petroleum Geologists Search and Discovery Article No. 90163, AAPG 2013 Annual Convention and Exhibition Pittsburgh, Pennsylvania, May 19–22, 2013 <http://www.searchanddiscovery.com/abstracts/html/2013/90163ace/abstracts/lau.htm> (Accessed January 26, 2016).
- Laurent, D., de Kaenel, E., Spangenberg, J.E., Föllmi, K.B., 2015. A sedimentological model of organic-matter preservation and phosphogenesis in the Miocene Monterey Formation at Haskell's Beach, Goleta (central California). *Sediment. Geol.* 326, 16–32.
- Lavoie, D., Rivard, C., Lefebvre, R., Séjourné, S., Thériault, R., Duchesne, M.J., Ahad, J.M.E., Wang, B., Benoit, N., Lamontagne, C., 2014. The Utica Shale and gas play in southern Quebec: geological and hydrogeological syntheses and methodological approaches to groundwater risk evaluation. *Int. J. Coal Geol.* 126, 77–91.
- Law, B.E., 2002. Basin-centered gas systems. *Am. Assoc. Pet. Geol. Bull.* 86, 1891–1919.
- LeFever, J.A., 1991. History of oil production from the Bakken Formation, North Dakota. In: Hanson, W.B. (Ed.), 1991 Guidebook to Geology and Horizontal Drilling of the Bakken Formation. Billings, Montana Geological Society, pp. 3–17.
- LeFever, J.A., LeFever, R.D., Nordeng, S.H., 2011. Revised nomenclature for the Bakken Formation (Mississippian–Devonian), North Dakota. In: Robinson, J.W., LeFever, J.A., Gaswirth, S.B. (Eds.), The Bakken–three Forks Petroleum System in the Williston Basin. Denver, CO, Rocky Mountain Association of Geologists, pp. 11–26.
- Legall, F.D., Barnes, C.R., Macqueen, R.W., 1981. Thermal maturation, burial history and hotspot development, Paleozoic strata of southern Ontario, Quebec, from conodont and acritarch colour alteration studies. *Bull. Can. Petrol. Geol.* 29, 492–539.
- Lehmann, D., Brett, C.E., Cole, R., Baird, G., 1995. Distal sedimentation in a peripheral foreland basin: Ordovician black shales and associated flysch of the western Taconic foreland, New York State and Ontario. *Geol. Soc. Am. Bull.* 107, 708–724.
- Levine, J.R., Davis, A., 1984. Optical anisotropy of coals as an indicator of tectonic deformation, Broad Top coal field, Pennsylvania. *Geol. Soc. Am. Bull.* 95, 100–108.
- Lewan, M.D., 1983. Effects of thermal maturation on stable organic carbon isotopes as determined by hydrous pyrolysis of Woodford Shale. *Geochim. Cosmochim. Acta* 47, 1471–1479.
- Lewan, M.D., 1985. Evaluation of petroleum generation by hydrous pyrolysis experimentation. *Philos. Trans. R. Soc. Lond.* 315, 123–134.
- Lewan, M.D., 1987. Petrographic study of primary petroleum migration in the Woodford Shale and related rock units. In: Doligez, B. (Ed.), Migration of Hydrocarbons in Sedimentary Basins. Editions Technip, Paris, pp. 113–130.
- Lewan, M.D., 1998. Sulfur-radical control on petroleum formation rates. *Nature* 391, 164–166.
- Lewan, M.D., Ruble, T.E., 2002. Comparison of petroleum generation kinetics by isothermal hydrous and non-isothermal open-system pyrolysis. *Org. Geochem.* 33, 1457–1475.
- Leythaeuser, D., MacKenzie, A., Schaeffer, R.G., Bjorøy, M., 1984. A novel approach for recognition and quantification of hydrocarbon migration effects in shale–sandstone sequences. *Am. Assoc. Pet. Geol. Bull.* 68, 196–219.
- Li, P., Ratchford, M.E., Jarvie, D.M., 2010. Geochemistry and thermal analysis of the Fayetteville Shale and Chattanooga Shale in the western Arkoma Basin of Arkansas. Arkansas Geological Survey, Information Circular 40 (205 p., CD-ROM).
- Lillis, P.G., 2013. Review of oil families and their petroleum systems of the Williston Basin. *Mount. Geol.* 50, 5–31.
- Lin, R., Davis, A., 1988. A fluorogeochemical model for coal macerals. *Org. Geochem.* 12, 363–374.
- Lo, H.B., 1993. Correction criteria for the suppression of vitrinite reflectance in hydrogen-rich kerogen: preliminary guidelines. *Org. Geochem.* 20, 653–657.
- Lo, H.B., Cardott, B.J., 1994. Detection of natural weathering of Upper McAlester coal and Woodford Shale, Oklahoma, U.S.A. *Org. Geochem.* 22, 73–83.
- Locklair, R.E., Sageman, B.B., 2008. Cyclostratigraphy of the Upper Cretaceous Niobrara Formation, Western Interior, USA: a Coniacian–Santonian orbital timescale. *Earth Planet. Sci. Lett.* 269, 540–553.
- Löhr, S.C., Baruch, E.T., Hall, P.A., Kennedy, M.J., 2015. Is organic pore development in gas shales influenced by the primary porosity and structure of thermally immature organic matter? *Org. Geochem.* 87, 119–132.
- Loucks, R.G., Reed, R.M., Ruppel, S.C., Hammes, U., 2010. Preliminary classification of matrix pores in mudrocks. *Gulf Coast Assoc. Geol. Soc. Trans.* 60, 435–441.
- Loucks, R.G., Reed, R.M., Ruppel, S.C., Hammes, U., 2012. Spectrum of pore types and networks in mudrocks and a descriptive classification for matrix-related mudrock pores. *Am. Assoc. Pet. Geol. Bull.* 96, 1071–1098.
- Loucks, R.G., Reed, R.M., Ruppel, S.C., Jarvie, D.M., 2009. Morphology, genesis, and distribution of nanometer-scale pores in siliceous mudstones of the Mississippian Barnett Shale. *J. Sediment. Res.* 79, 848–861.
- Loucks, R.G., Ruppel, S.C., 2007. Mississippian Barnett Shale: lithofacies and depositional setting of a deep-water shale-gas succession in the Fort Worth Basin, Texas. *Am. Assoc. Pet. Geol. Bull.* 91, 579–601.
- Lowery, C.M., Corbett, M.J., Leckie, R.M., Watkins, D., Miceli Romero, A., Pramu-dito, A., 2014. Foraminiferal and nannofossil paleoecology and paleoceanography of the Cenomanian–Turonian Eagle Ford Shale of southern Texas. *Palaeogeogr. Palaeoclimatol. Palaeoecol.* 413, 49–65.
- Lu, J., Ruppel, S.C., Rowe, H.D., 2015. Organic matter pores and oil generation in the Tuscaloosa marine shale. *Am. Assoc. Pet. Geol. Bull.* 99, 333–357.
- Luneau, B., Longman, M., Kaufman, P., Landon, S., 2011. Stratigraphy and petrophysical characteristics of the Niobrara Formation in the Denver Basin, Colorado and Wyoming. American Association of Petroleum Geologists Search and Discovery Article No. 50469 (21 p).
- Luo, Q., Zhong, N., Dai, N., Zhang, W., 2016. Graptolite-derived organic matter in the Wufeng–Longmaxi Formations (Upper Ordovician–Lower Silurian) of southeastern Chongqing, China: implications for gas shale evaluation. *Int. J. Coal Geol.* 153, 87–98.
- Ma, Y.Z., Holditch, S.A. (Eds.), 2015. Unconventional Oil and Gas Resources Handbook: Evaluation and Development. Gulf Professional Publishing, Waltham, MA (550 p).
- MacGowan, D.B., Surdam, R.C., 1990. Carboxylic acid anions in formation waters, San Joaquin Basin and Louisiana Gulf Coast, USA: implications for clastic diagenesis. *Appl. Geochem.* 5, 687–701.
- Mackay, P., 2015. Second White Specks Formation: new concepts for understanding fractured reservoirs. American Association of Petroleum Geologists Search & Discovery Article No. 110218 41 p. http://www.searchanddiscovery.com/documents/2015/110218mackay/ndx_mackay.pdf (Accessed March 21, 2016).
- Macquaker, J.H.S., Keller, M.A., Davies, S.J., 2010. Algal blooms and “marine snow”: mechanisms that enhance preservation of organic carbon in ancient fine-grained sediments. *J. Sediment. Res.* 80, 934–942.
- Mählmann, R.F., Frey, M., 2012. Standardisation, calibration and correlation of the Kübler-index and the vitrinite/bituminite reflectance: an inter-laboratory and field related study. *Swiss J. Geosci.* 105, 153–170.
- Mählmann, R.F., Le Bayon, R., 2016. Vitrinite and vitrinite like solid bitumen reflectance in thermal maturity studies: correlations from diagenesis to incipient metamorphism in different geodynamic settings. *Int. J. Coal Geol.* 157, 52–73.
- Mann, U., Neisel, J.D., Burchard, W.G., Heinen, V., Welte, D.H., 1994. Fluid-rock interfaces as revealed by cryo-scanning electron microscopy. *First Break* 12, 131–136.
- Marcil, J.-S., Lavoie, J., Dorris, P.K., Lavoie, V., 2009. Shale gas potential of the Quebec sedimentary basins. American Association of Petroleum Geologists Search and Discovery Article No. 80073 34 p. http://www.searchanddiscovery.com/documents/2009/80073marcil/ndx_marcil.pdf (Accessed March 2, 2016).
- Marshall, A.O., Nowaczewski, V., Marshall, C.P., 2013. Microchemical differentiation of conodont and scolecodont microfossils. *Palaios* 28, 433–437.
- Masran, T.C., Pocock, S.A.J., 1981. The classification of plant-derived particulate organic matter in sedimentary rocks. In: Brooks, J. (Ed.), Organic Maturation Studies and Fossil Fuel Exploration. Academic Press, London, New York, pp. 145–175.
- Mastalerz, M., Schimmelmann, A., Drobnik, A., Chen, Y., 2013. Porosity of Devonian and Mississippian New Albany Shale across a maturation gradient: insights from organic petrology, gas adsorption, and mercury intrusion. *Am. Assoc. Pet. Geol. Bull.* 97, 1621–1643.
- Mastalerz, M., Schimmelmann, A., Drobnik, A., Chen, Y., 2012. Influence of maceral composition on geochemical characteristics of immature shale kerogen: insights from density fraction analysis. *Int. J. Coal Geol.* 103, 60–69.
- Mastalerz, M., Wilks, K.R., Bustin, R.M., 1993. Variation in vitrinite chemistry as a function of associated liptinite content; a microprobe and FTIR investigation. *Org. Geochem.* 20, 555–562.
- McCarthy, K., Rojas, K., Niemann, M., Palmowski, D., Peters, K., Stankiewicz, A., 2011. Basic petroleum geochemistry for source rock evaluation. *Oilfield Rev.* 23 (2), 32–43.
- McCartney, J.T., Teichmüller, M., 1972. Classification of coals according to degree of coalification by reflectance of the vitrinite component. *Fuel* 51, 64–68.
- McNally, M.S., Brandt, A.R., 2015. The productivity and potential future recovery of the Bakken Formation of North Dakota. *J. Unconv. Oil Gas Res.* 11, 11–18.
- McTavish, R.A., 1978. Pressure retardation of vitrinite diagenesis, offshore northwest Europe. *Nature* 271, 648–650.
- McTavish, R.A., 1998. The role of overpressure in the retardation of organic matter maturation. *J. Pet. Geol.* 21, 153–186.
- Metcalfe, I., Riley, N.J., 2010. Conodont colour alteration pattern in the carboniferous of the Craven Basin and adjacent areas, northern England. *Proc. Yorks. Geol. Soc.* 58, 1–8.
- Miller, R., 2014. Shale reservoir evaluation: reservoir characterization and production properties. Core Laboratories Integrated Reservoir Solutions Short Course Notes (unpaginated).
- Milliken, K.L., Rudnicki, M., Awwiller, D.N., Zhang, T., 2013. Organic matter-hosted pore system, Marcellus Formation (Devonian), Pennsylvania. *Am. Assoc. Pet. Geol. Bull.* 97, 177–200.
- Miranda, R.M., Walters, C.C., 1992. Geochemical variations in sedimentary organic matter within a “homogeneous” shale core (Tuscaloosa Formation, Upper Cretaceous, Mississippi, USA). *Org. Geochem.* 8, 899–911.
- Modica, C.J., Lapiere, S.G., 2011. Estimation of kerogen porosity in source rocks as a function of thermal transformation: example from the Mowry shale in the Powder River Basin of Wyoming. *Am. Assoc. Pet. Geol. Bull.* 96, 87–108.
- Montgomery, S.L., Jarvie, D.M., Bowker, K.A., Pollastro, R.M., 2005. Mississippian Barnett Shale, Fort Worth basin, north-central Texas: gas shale play with multi-trillion cubic foot potential. *Am. Assoc. Pet. Geol. Bull.* 89, 155–175.
- Mukhopadhyay, P.K., 1994. Vitrinite reflectance as maturity parameter: petrographic and molecular characterization and its applications to basin modeling. In: Mukhopadhyay, P.K., Dow, W.G. (Eds.), Vitrinite Reflectance as a Maturity Parameter: Applications and Limitations Vol. 570. American Chemical Society Symposium Series, Washington, D.C., pp. 1–24.
- Mukhopadhyay, P.K., Dow, W.G., 1994. Vitrinite reflectance as a maturity parameter: applications and limitations. *Am. Chem. Soc. Symp. Series* 570 (294 pp).

- Naqishbandi, S.F., Jabbar, W.J., Al-Juboury, A.I., 2015. Hydrocarbon potential and porosity types of the Geli Khana Formation (Middle Triassic), northern Iraq. *Arab. J. Geosci.* 8, 739–758.
- Newman, J., 1997. New approaches to detection and correction of suppressed vitrinite reflectance. *Aus. Pet. Prod. Explor. Assoc. J.* 37, 524–535.
- Newman, J., Edman, J., Howe, J., LeFever, J., 2013. The Bakken at Parshall Field: inferences from new data regarding hydrocarbon generation and migration. *Unconventional Resources Technology Conference Paper 1578764* (10 p).
- Nordeng, S.H., LeFever, J.A., 2009. Organic geochemical patterns in the Bakken source system. North Dakota Geological Survey Geologic Investigations No. 79 <https://www.undeerc.org/bakken/pdfs/GI-79.pdf> (Accessed March 19, 2016).
- Nuccio, V.F., Hatch, J.R., 1996. Vitrinite reflectance suppression in the New Albany Shale, Illinois Basin: vitrinite reflectance and Rock-Eval data. U.S. Geological Survey Open-File Report 96–665 37 p. <http://pubs.usgs.gov/of/1996/0665/report.pdf> (Accessed March 1, 2016).
- Nunn, J.A., 2012. Burial and thermal history of the Haynesville Shale: implications for overpressure, gas generation, and natural hydrofracture. *Gulf Coast Assoc. Geol. Soc. J.* 1, 81–96.
- Nuttall, B.C., Parris, T.M., Beck, G., Willette, D.C., Mastalerz, M., Crockett, J., 2015. Oil production from low-maturity organic-rich shale: an example from the Devonian New Albany shale in the Illinois Basin, Breckinridge County, Kentucky. *American Association of Petroleum Geologists Search and Discovery Article No. 51196* http://www.searchanddiscovery.com/documents/2015/51196nuttall/ndx_nuttall.pdf (Accessed February 7, 2015).
- Obermajer, M., Fowler, M.G., Goodarzi, F., Snowdon, L.R., 1996. Assessing thermal maturity of Palaeozoic rocks from reflectance of chitinozoa as constrained by geochemical indicators: an example from southern Ontario, Canada. *Mar. Pet. Geol.* 13, 907–919.
- Obermajer, M., Fowler, M.G., Goodarzi, F., Snowdon, L.R., 1997. Organic petrography and organic geochemistry of Devonian black shales in southwestern Ontario, Canada. *Org. Geochem.* 26, 229–246.
- Orr, W.L., 1986. Kerogen/asphaltene/sulfur relationships in sulfur-rich Monterey oil. *Org. Geochem.* 10, 499–516.
- Ottenjann, K., Teichmüller, M., Wolf, M., 1975. Spectral fluorescence measurements of sporinites in reflected light and their applicability for coalification studies. In: *Alpern, B. (Ed.), Pétrographie de la Matière Organique Des Sediments. Relations avec la paleotemperature et le potentiel pétrolier.* CNRS, Paris, pp. 49–65.
- Over, J.D., 2007. Conodont biostratigraphy of the Chattanooga Shale, Middle and Upper Devonian, southern Appalachian Basin, eastern United States. *J. Paleontol.* 81, 1194–1217.
- Park, G., 2013. Hush over all the Exshaw. *Pet. News* 18 (13) <http://www.petroleumnews.com/pntruncate/799300015.shtml> (Accessed February 28, 2016).
- Parshall, J., 2015. Technology, efficiency, and midstream growth drive long-term future for Marcellus, Utica. *J. Pet. Technol.* 67 (11), 42–46.
- Partners, P.W.C., 2016. PacWest publishes updated shale/unconventional play maps. <https://www.ihs.com/btp/pacwest-consulting-partners.html> (Accessed May 25, 2016).
- Passy, Q.R., Bohacs, K.M., Esch, W.L., Klimentidis, R., Sinha, S., 2010. From oil-prone source rock to gas-producing shale reservoir: geologic and petrophysical characterization of unconventional shale-gas reservoirs. *Chinese Petroleum Society/Society of Petroleum Engineers International Oil and Gas Conference and Exhibition, Beijing, China, June 8–10, 2010, SPE Paper 131350* (29 p).
- Patchen, D.G., Carter, K.M., 2015. A geologic playbook for Utica Shale Appalachian Basin exploration. *Appalachian Oil and Natural Gas Consortium at West Virginia University* 188 p. http://nrce.wvu.edu/wp-content/uploads/FINAL_UTICA_REPORT_07012015.pdf (accessed August 28, 2015).
- Pavluš, J., Skupien, P., 2014. Lower Cretaceous black shales of the western Carpathians, Czech Republic: palynofacies indication of depositional environment and source potential for hydrocarbons. *Mar. Pet. Geol.* 57, 14–24.
- Pawlewicz, M., Barker, C.E., McDonald, S., 2005. Vitrinite reflectance data for the Permian Basin, west Texas and southeast New Mexico. U.S. Geological Survey Open-File Report 2005–1171 25 p. <http://pubs.usgs.gov/of/2005/1171/pdf/OFR-2005-1171.pdf> (Accessed December 23, 2015).
- Pawlewicz, M.J., Finn, T.M., 2002. Vitrinite reflectance data for the Greater Green River Basin, southwestern Wyoming, northwestern Colorado, and northeastern Utah. U.S. Geological Survey Open-File Report 02–339 15 p. <https://pubs.usgs.gov/of/2002/ofr-02-0339/ofr-02-0339.pdf> (Accessed May 22, 2016).
- Pernia, D., Bissada, K.K.A., Curiale, J., 2015. Kerogen based characterization of major gas shales: effects of kerogen fractionation. *Org. Geochem.* 78, 52–61.
- Peters, K.E., 1986. Guidelines for evaluating petroleum source rock using programmed pyrolysis. *Am. Assoc. Pet. Geol. Bull.* 70, 318–329.
- Peters, K.E., Cassa, M.R., 1994. Applied source rock geochemistry. In: *Magoon, L.B., Dow, W.G. (Eds.), The Petroleum System—from Source to Trap: American Association of Petroleum Geologists Memoir.* 60, pp. 93–120.
- Peters, K.E., Xia, X., Pomerantz, A.E., Mullins, O.C., 2016. Geochemistry applied to evaluation of unconventional resources. In: *Ma, Y.Z., Holditch, S.A. (Eds.), Unconventional Oil and Gas Resources Handbook: Evaluation and Development.* Gulf Professional Publishing, Waltham, MA, pp. 71–126.
- Petersen, H.H., Andersen, C., Carr, A.D., Thomsen, E., 2012. Vitrinite reflectance gradients of deep wells with thick chalk sections and high pressure: implications for source rock maturation, Danish-Norwegian Central Graben, North Sea. *Int. J. Coal Geol.* 100, 65–81.
- Petersen, H.L., Rosenberg, P., 1998. Reflectance retardation (suppression) and source rock properties related to hydrogen-enriched vitrinite in Middle Jurassic coals, Danish North Sea. *J. Pet. Geol.* 21, 247–263.
- Petersen, H.L., Schovsbo, N.H., Nielsen, A.T., 2013. Reflectance measurements of zooclasts and solid bitumen in Lower Paleozoic shales, southern Scandinavia: correlation to vitrinite reflectance. *Int. J. Coal Geol.* 114, 1–18.
- Petersen, H.L., Vosgerau, H., 1999. Composition and organic maturity of Middle Jurassic coals, North-East Greenland: evidence for liptinite-induced suppression of huminite reflectance. *Int. J. Coal Geol.* 41, 257–274.
- Pickett, A., 2015. Operators finding record wells and new frontiers in Marcellus/Utica. *Am. Oil Gas Rep.* 58 (7), 108–115.
- Pollastro, R.M., Jarvie, D.M., Hill, R.J., Adams, C.W., 2007. Geologic framework of the Mississippian Barnett Shale, Barnett-Paleozoic total petroleum system, Bend arch-Fort Worth Basin, Texas. *Am. Assoc. Pet. Geol. Bull.* 91, 405–436.
- Pommer, M., Milliken, K., 2015. Pore types and pore-size distributions across thermal maturity, Eagle Ford Formation, southern Texas. *Am. Assoc. Pet. Geol. Bull.* 99, 1713–1744.
- Potter, J., Goodarzi, F., Morrow, D.W., Richards, B.C., Snowdon, L.R., 2000. Organic Petrology, Thermal Maturity, and Rock-Eval/TOC Data for Upper Paleozoic Strata from Selected Wells Between 60° and 61°N and 122°W and 123°30' SW, District of Mackenzie: Geological Survey of Canada Open-File Report 3925 (15 p).
- Potter, J., Goodarzi, F., Morrow, D.W., Richards, B.C., Snowdon, L.R., 2003. Organic Petrology, Thermal Maturity and Rock-Eval/TOC Data for Upper Paleozoic to Upper Cretaceous Strata from Wells Near Liard River, Northeast British Columbia: Geological Survey of Canada Open-File Report. p. 1751 (20 p).
- Potter, J., Stasiuk, L.D., Cameron, A.R. (Eds.), 1998. *A Petrographic Atlas of Canadian Coal Macerals and Dispersed Organic Matter* (Canadian Society for Coal Science and Organic Petrology). (105 p).
- Pradier, B., Bertrand, P., Martinez, L., Laggoun-Defarge, F., 1991. Fluorescence of organic matter and thermal maturity assessment. *Org. Geochem.* 17, 511–524.
- Price, L.C., Barker, C.E., 1985. Suppression of vitrinite reflectance in amorphous rich kerogen – a major unrecognized problem. *J. Pet. Geol.* 8, 59–84.
- Quick, J.C., 1994. Isorank variation of vitrinite reflectance and fluorescence intensity. In: *Mukhopadhyay, P.K., Dow, W.G. (Eds.), Vitrinite Reflectance as a Maturity Parameter: Applications and Limitations Vol. 570.* American Chemical Society Symposium Series, pp. 64–75.
- Ratchford, M.E., Bridges, L.C., Jordan, D., Dow, W.G., Colbert, A., Jarvie, D.M., 2006. Organic geochemistry and thermal maturation analysis within the Fayetteville Shale study area-eastern Arkoma Basin and Mississippi Embayment regions, Arkansas. *Arkansas Geological Survey, Information Circular* 37, CD-ROM.
- Reed, R.M., Loucks, R.G., Ruppel, S.C., 2014. Comment on “Formation of nanoporous pyrobitumen residues during maturation of the Barnett Shale (Fort Worth Basin)” by Bernard et al. (2012). *Int. J. Coal Geol.* 127, 111–113.
- Reeder, S.L., Craddock, P.R., Rylander, E., Pirie, I., Lewis, R.E., Kausik, R., Kleinberg, R.L., Yang, J., Pomerantz, A.E., 2016. The reservoir producibility index: a metric to assess reservoir quality in tight-oil plays from logs. *Petrophysics* 57, 83–95.
- Reinsalu, E., Aarna, I., 2015. About technical terms of oil shale and shale oil. *Oil Shale* 32, 291–292.
- Rejebian, V.A., Harris, A.G., Huebner, J.S., 1987. Conodont color and textural alteration: an index to regional metamorphism, contact metamorphism, and hydrothermal alteration. *Geol. Soc. Am. Bull.* 99, 471–479.
- Repetski, J.E., Ryder, R.T., Weary, D.G., Harris, A.G., Trippi, M.T., 2008. Thermal maturity patterns (CAI and %R_o) in Upper Ordovician and Upper Devonian rocks of the Appalachian Basin: a major revision of USGS Map I917-E using new subsurface collections. U.S. Geological Survey Scientific Investigations Map SIM-3006 <http://pubs.usgs.gov/sim/3006/> (Accessed December 19, 2015).
- Rezaee, R., 2015. *Fundamentals of Gas Shale Reservoirs.* John Wiley & Sons, Hoboken, New Jersey, USA (456 p).
- Riediger, C.L., 1993. Solid bitumen reflectance and Rock-Eval Tmax as maturation indices: an example from the “Nordegg Member”, Western Canada Sedimentary Basin. *Int. J. Coal Geol.* 22, 295–315.
- Riediger, C.L., Fowler, M.G., Snowdon, L.R., Goodarzi, F., Brooks, P.W., 1990. Source rock analysis of the Lower Jurassic “Nordegg Member” and oil-source rock correlations, northwestern Alberta and northeastern British Columbia. *Bull. Can. Petrol. Geol.* 38A, 236–249.
- Riediger, C.L., Bloch, J.D., 1995. Depositional and diagenetic controls on source-rock characteristics of the Lower Jurassic “Nordegg Member”, western Canada. *J. Sediment. Res.* A65, 112–126.
- Rimmer, S.M., Hawkins, S.J., Scott, A.C., Cressler III, W.L., 2015. The rise of fire: Fossil charcoal in Late Devonian marine shales as an indicator of expanding terrestrial ecosystems, fire, and atmospheric change. *Am. J. Sci.* 315, 713–733.
- Rimmer, S.M., Thompson, J.A., Goodnight, S.A., Robl, T.L., 2004. Multiple controls on the preservation of organic matter in Devonian-Mississippian marine black shales: geochemical and petrographic evidence. *Palaeogeogr. Palaeoclimatol. Palaeoecol.* 215, 125–154.
- Rippen, D., Little, R., Bruns, B., Mahlstedt, N., 2013. Organic geochemistry and petrography of Lower Cretaceous Wealden black shales of the Lower Saxony Basin: the transition from lacustrine oil shales to gas shales. *Org. Geochem.* 63, 18–36.
- Rivard, C., Lavoie, D., Lefebvre, R., Séjourné, S., Lamontagne, C., Duchesne, M., 2014. An overview of Canadian shale gas production and environmental concerns. *Int. J. Coal Geol.* 126, 64–76.
- Robert, P., 1971. Etude pétrographique des matières organiques insolubles par la mesure de leur pouvoir réflecteur: contribution à l'exploration pétrolière et à la connaissance des bassins sédimentaires. *Rev. Inst. Franç. Pétrole* 26, 105–135.
- Robert, P., 1988. Organic Metamorphism and Geothermal History: Microscopic Study of Organic Matter and Thermal Evolution of Sedimentary Basins. *Elf-Aquitaine & Reidel Publishing Company, Dordrecht* (311 p).
- Robison, C.R., 1997. Hydrocarbon source rock variability within the Austin Chalk and Eagle Ford Shale (Upper Cretaceous), East Texas, U.S.A. *Int. J. Coal Geol.* 34, 287–305.
- Robl, T.L., Taulbee, D.N., Barron, L.S., Jones, W.C., 1987. Petrologic chemistry of a Devonian Type II kerogen. *Energy Fuel* 1, 507–513.
- Robl, T.L., Rimmer, S.M., Barron, L.S., 1992. Organic petrography of Mississippian and Devonian shales in east-central Kentucky. *Fuel* 71, 267–271.

- Rodgers, B., 2014. Declining costs enhance Duvernay shale economics. *Oil Gas J.* 112 (9), 70–76.
- Romero, A.M., Philp, R.P., 2012. Organic geochemistry of the Woodford Shale, southeastern Oklahoma: how variable can shales be? *Am. Assoc. Pet. Geol. Bull.* 96, 483–517.
- Romero-Sarmiento, M.-F., Ducros, M., Carpentier, B., Lorient, F., Cacas, M.-C., Pegaz-Fiorinet, S., Wolf, S., Rohais, S., Moretti, I., 2013. Quantitative evaluation of TOC, organic porosity and gas retention distribution in a gas shale play using petroleum system modeling: application to the Mississippian Barnett Shale. *Mar. Pet. Geol.* 45, 315–330.
- Romero-Sarmiento, M.-F., Rouzaud, J.-N., Bernard, S., Deldicque, D., Thomas, M., Littke, R., 2014. Evolution of Barnett Shale organic carbon structure and nanostructure with increasing maturation. *Org. Geochem.* 71, 7–16.
- Ross, D.J.K., Bustin, R.M., 2008. Characterizing the shale gas resource potential of Devonian-Mississippian strata in the Western Canada sedimentary basin: application of an integrated formation evaluation. *Am. Assoc. Pet. Geol. Bull.* 92, 87–125.
- Ross, D.J.K., Bustin, R.M., 2009. The importance of shale composition and pore structure upon gas storage potential of shale gas reservoirs. *J. Mar. Petrol. Geol.* 26, 916–927.
- Rowan, E.L., Ryder, R.T., Repetski, J.E., Trippi, M.H., Ruppert, L.F., 2004. Initial results of a 2D burial/thermal history model, central Appalachian basin, Ohio and West Virginia. U.S. Geological Survey Open-File Report 2004–1445 12 p. <http://pubs.usgs.gov/of/2004/1445/> (March 1, 2016).
- Ruppert, L.F., Hower, J.C., Ryder, R.T., Levine, J.R., Trippi, M.H., Grady, W.C., 2010. Geologic controls on thermal maturity patterns in Pennsylvanian coal-bearing rocks in the Appalachian basin. *Int. J. Coal Geol.* 81, 169–181.
- Ryder, R.T., Burruss, R.C., Hatch, J.R., 1998. Black shale source rocks and oil generation in the Cambrian and Ordovician of the central Appalachian Basin, USA. *Am. Assoc. Pet. Geol. Bull.* 82, 412–441.
- Ryder, R.T., Hackley, P.C., Trippi, M.H., Alimi, H., 2013. Evaluation of thermal maturity in the low maturity Devonian shales of the northern Appalachian Basin. *American Association of Petroleum Geologists Search and Discovery Article 10477* Parts 1 (67 p.) and 2 (177 p.) http://www.searchanddiscovery.com/documents/2013/10477ryder/ndx_ryder.pdf (accessed August 12, 2015).
- Sanei, H., Haeri-Ardakani, O., Wood, J.M., Curtis, M.E., 2015a. Effects of nanoporosity and surface imperfections on solid bitumen reflectance (BRo) measurements in unconventional reservoirs. *Int. J. Coal Geol.* 138, 95–102.
- Sanei, H., Wood, J.M., Haeri-Ardakani, O., Clarkson, C.R., Jiang, C., 2015b. Characterization of organic matter fractions in an unconventional tight gas siltstone reservoir. *Int. J. Coal Geol.* 150–151, 296–305.
- Schieber, J., 2013. SEM observations on ion-milled samples of Devonian black shales from Indiana and New York: the petrographic context of multiple pore types. In: Camp, W., Diaz, E., Wawak, B. (Eds.), *Electron Microscopy of Shale Hydrocarbon Reservoirs* Vol. 102. AAPG Memoir, pp. 153–171.
- Schito, A., Corrado, S., Aldega, L., Grigo, D., 2016. Overcoming pitfalls of vitrinite reflectance measurements in the assessment of thermal maturity: the case history of the lower Congo basin. *Mar. Pet. Geol.* 74, 59–70.
- Schmidt, J.S., Araujo, C.V., Souza, I.V.A.F., Chagas, R.B.A., 2015. Hydrous pyrolysis maturation of vitrinite-like and humic vitrinite macerals: implications for thermal maturity analysis. *Int. J. Coal Geol.* 144–145, 5–14.
- Schoenherr, J., Littke, R., Urai, J.L., Kukla, P.A., Rawahi, Z., 2007. Polyphase thermal evolution in the Infra-Cambrian Ara Group (South Oman Salt Basin) as deduced by maturity of solid reservoir bitumen. *Org. Geochem.* 38, 1293–1318.
- Scott, A.C., 2010. Charcoal recognition, taphonomy and uses in paleoenvironmental analysis. *Palaeogeogr. Palaeoclimatol. Palaeoecol.* 291, 11–39.
- Scott, A.C., Glasspool, I.J., 2007. Observations and experiments on the origin and formation of inertinite group macerals. *Int. J. Coal Geol.* 70, 53–66.
- Scott, A.R., Hussain, M., 1988. Organic geochemistry, source rock potential, and oil-source rock correlation of the Permian Spraberry Formation, northern Midland Basin, Jo Mill field, Borden County, Texas. In: Cunningham, B.K. (Ed.), *Permian and Pennsylvanian stratigraphy, Midland Basin, West Texas: studies to aid hydrocarbon exploration*. Society of Economic Paleontologists and Mineralogists, Permian Basin Section, Publication No. 88–28, pp. 33–51.
- Seeley, R., 2014. Monterey proves more complex than average shale play. *Unconv. Oil Gas Rep.* 2 (4) <http://www.ogj.com/articles/uogr/print/volume-2/issue-4/monterey-proves-more-complex-than-average-shale-play.html> (Accessed February 29, 2016).
- Seewald, J.S., Eglinton, L.B., Ong, Y.L., 2000. An experimental study of organic-inorganic interactions during vitrinite maturation. *Geochim. Cosmochim. Acta* 64, 1577–1591.
- Senftle, J.T., Landis, C.R., 1991. Vitrinite reflectance as a tool to assess thermal maturity. In: Merrill, R.K. (Ed.), *Source and Migration Processes and Evaluation Techniques*. American Association of Petroleum Geologists Treatise of Petroleum Geology, Handbook of Petroleum Geology, pp. 119–125.
- Slatt, R.M., O'Brien, O.R., 2011. Pore types in the Barnett and Woodford gas shales: contribution to understanding gas storage and migration pathways in fine-grained rocks. *Am. Assoc. Pet. Geol. Bull.* 95, 2017–2030.
- Smith, M.G., Bustin, R.M., 1998. Production and preservation of organic matter during deposition of the Bakken Formation (Late Devonian and Early Mississippian), Williston Basin. *Palaeogeogr. Palaeoclimatol. Palaeoecol.* 142, 185–200.
- Smith, G.C., Cook, A.C., 1980. Coalification paths of exinite, vitrinite and inertinite. *Fuel* 59, 641–647.
- Sokol, E., Kozmenko, O., Smirnov, S., Sokol, I., Novikova, S., Tomilenko, A., Kokh, S., Ryazanova, T., Reutsky, V., Bul'bak, T., Vapnik, Y., Deyak, M., 2014. Geochemical assessment of hydrocarbon migration phenomena: case studies from the southwestern margin of the Dead Sea Basin. *J. Asian Earth Sci.* 93, 211–228.
- Sondergeld, C.H., Ambrose, R.J., Rai, C.S., 2010. Micro-structural studies of gas shales. *Society of Petroleum Engineers Paper 131771*, SPE Unconventional Gas Conference, 23–25 February, USA, Pittsburgh, Pennsylvania (17 p.).
- Sonnenberg, S.A., 2011. The Niobrara petroleum system: a new resource play in the Rocky Mountain region. In: Estes-Jackson, J.E., Anderson, D.S. (Eds.), *Revisiting and revitalizing the Niobrara in the Central Rockies*, pp. 13–32.
- Spackman, W., 1958. The maceral concept and the study of modern environments as a means of understanding the nature of coal. *Trans. N. Y. Acad. Sci. Series II* 20 (5), 411–423.
- Spain, D.R., McLin, R., 2013. SEM characterization of shale gas reservoirs using combined secondary and backscatter electron methods: an example from the Haynesville Shale, Texas and Louisiana. In: Camp, W., Diaz, E., Wawak, B. (Eds.), *Electron Microscopy of Shale Hydrocarbon Reservoirs* Vol. 102. AAPG Memoir, pp. 45–52.
- Stach, E., Mackowsky, M.-T., Teichmüller, M., Taylor, G.H., Chandra, D., Teichmüller, R., 1982. *Stach's Textbook of Coal Petrology*, third Revised and Enlarged Edition. Berlin-Stuttgart, Gebrüder Borntraeger (535 pp).
- Stankiewicz, A., Ionkina, N., Motherwell, B., Bennett, B., Wint, O., Mastalerz, M., 2015. Kerogen density revisited: lessons from the Duvernay Shale. *Unconventional Resources Technology Conference Paper URTeC 2157904* (11 p.).
- Staplin, F.L., 1969. Sedimentary organic matter, organic metamorphism and oil and gas occurrence. *Bull. Can. Petrol. Geol.* 17, 47–66.
- Staplin, F.L., 1982. Determination of thermal alteration index from color of exinite (pollen, spores). In: Staplin, F.L., et al. (Eds.), *How to Assess Maturation and Paleotemperatures*. SEPM Short Course Vol. 7, pp. 7–11.
- Stasiuk, L.D., 1993. Algal bloom episodes and the formation of bituminite and micrinite in hydrocarbon source rocks: evidence from the Devonian and Mississippian, northern Williston Basin, Canada. *Int. J. Coal Geol.* 24, 195–210.
- Stasiuk, L.D., 1994. Fluorescence properties of Palaeozoic oil-prone alginite in relation to hydrocarbon generation, Williston Basin, Saskatchewan, Canada. *Mar. Pet. Geol.* 11, 219–231.
- Stasiuk, L.D., 1999a. Microscopic studies of sedimentary organic matter: key to understanding organic-rich strata, with Paleozoic examples from Western Canada. *Geosci. Can.* 26, 149–172.
- Stasiuk, L.D., 1999b. Confocal laser scanning fluorescence microscopy of Botryococcus alginite from boghead oil shale Boltysk, Ukraine: selective preservation of various microalgal components. *Org. Geochem.* 30, 1021–1026.
- Stasiuk, L.D., Burgess, J., Thompson-Rizer, C., Hutton, A., Cardott, B., 2002. Status report on TSOP-ICCP dispersed organic matter classification working group. *The Society for Organic Petrology Newsletter*, p. 14 19(3) http://tsop.org/newsletters/1999_2002.pdf (Accessed December 21, 2015).
- Stasiuk, L.D., Fowler, M.G., 2004. Organic facies in Devonian and Mississippian strata of Western Canada Sedimentary Basin: relation to kerogen type, paleoenvironment, and paleogeography. *Bull. Can. Petrol. Geol.* 52, 234–255.
- Stasiuk, L.D., Goodarzi, F., 1988. Organic petrology of Second White Speckled shale, Saskatchewan, Canada: a possible link between bituminite and biogenic gas? *Bull. Can. Petrol. Geol.* 36, 397–406.
- Stasiuk, L.D., Sanei, H., 2001. Characterisation of diatom-derived lipids and chlorophyll within Holocene laminites, Saanich Inlet, British Columbia, using conventional and laser scanning fluorescence microscopy. *Org. Geochem.* 32, 1417–1428.
- Steinhoff, I., Cicero, A.D., Koepke, K., Dezelle, J., McClain, T., Gillett, C., 2011. Understanding the regional Haynesville and Bossier shale depositional systems in east Texas and northern Louisiana: an integrated structural/stratigraphic approach. *American Association of Petroleum Geologists Search and Discovery Article No. 50379* 12 p. http://www.searchanddiscovery.com/documents/2011/50379steinhoff/ndx_steinhoff.pdf (Accessed February 29, 2016).
- Strapoč, D., Mastalerz, M., Schimmelmann, A., Drobnik, A., Hasenmueller, N.R., 2010. Geochemical constraints on the origin and volume of gas in the New Albany Shale (Devonian-Mississippian), eastern Illinois Basin. *Am. Assoc. Pet. Geol. Bull.* 94, 1713–1740.
- Streib, D.L., 1981. Distribution of gas, organic carbon, and vitrinite reflectance in the eastern Devonian gas shales and their relationship to the geologic framework. U.S. Department of Energy, Morgantown Energy Technology Center, Report METC/08216-1276 (262 p.).
- Suárez-Ruiz, I., Flores, D., Graciano Mendonça Filho, J., Hackley, P.C., 2012. Review and update of the applications of organic petrology: Part 1, geological applications. *Int. J. Coal Geol.* 99, 54–112.
- Switzer, S.B., Holland, W.G., Christie, D.S., Graf, G.C., Hedinger, A.S., McAuley, R.J., Wierzbicki, R.A., Packard, J.J., 1994. Devonian Woodbend-Winterburn strata of the Western Canada sedimentary basin (Compilers) In: Mossop, G.D., Shetsen, I. (Eds.), *Geological atlas of the Western Canada Sedimentary Basin*. Canadian Society of Petroleum Geologists and Alberta Research Council, Special Report 4 http://www.ags.gov.ab.ca/publications/wcsb_atlas/a_ch12/ch_12.html#ref (Accessed January 22, 2016).
- Taulbee, D.N., Seibert, E.D., Barron, L.S., Robl, T.L., 1990. Comparison of maceral group chemistries for a New Albany and an Ohio oil shale kerogen. *Energy Fuel* 4, 254–263.
- Taylor, G.H., Teichmüller, M., Davis, A., Diessel, C.F.K., Littke, R., Robert, P., 1998. *Organic Petrology*. Berlin and Stuttgart, Gebrüder Borntraeger (704 pp).
- Teichmüller, M., 1958. *Métamorphisme du charbon et prospection du Pétrole*. *Rev. Ind. Minér. Num. Spéc.* 99–113.
- Teichmüller, M., 1971. Anwendung kohlenpetrographischer methoden bei der erdöl und erdgasprospektion. *Erdöl, Kohle, Erdgas, Petrochem.* 24, 69–76.
- Teichmüller, M., Durand, B., 1983. Fluorescence microscopical rank studies on liptinites and vitrinites in peat and coals, and comparison with results of the Rock-Eval pyrolysis. *Int. J. Coal Geol.* 2, 197–230.
- Teichmüller, M., Ottenjann, K., 1977. Art und diagenese von liptiniten und lipoiden stoffen in einem erdölmuttergestein auf grund fluoroessenzmikroskopischer untersuchungen. *Erdöl und Kohle* 30, 387–398.
- Tessin, A., Hendy, I., Sheldon, N., Sageman, B., 2015. Redox-controlled preservation of organic matter during "OAE 3" within the Western Interior Seaway. *Paleoceanography* 30, 702–717.
- Tissot, B.P., Welte, D.H., 1984. *Petroleum Formation and Occurrence*. second ed. Berlin, Springer-Verlag (699 pp).

- Tissot, B.P., Pelet, R., Ungerer, P.H., 1987. Thermal history of sedimentary basins, maturation indices, and kinetics of oil and gas generation. *Am. Assoc. Pet. Geol. Bull.* 71, 1445–1466.
- Tribouillard, N., Algeo, T.J., Lyons, T., Riboulleau, A., 2006. Trace metals as paleoredox and paleoproductivity proxies: an update. *Chem. Geol.* 232, 12–32.
- Tricker, P.M., Marshall, J.E.A., Badman, T.D., 1992. Chitinozoan reflectance: a lower Palaeozoic thermal maturity indicator. *Mar. Pet. Geol.* 9, 302–307.
- Tyson, R.V., 1995. *Sedimentary Organic Matter: Organic Facies and Palynofacies*. Chapman and Hall, London (615 pp).
- Ujiié, Y., Sherwood, N., Faiz, M., Wilkins, R.W.T., 2004. Maturity and suppressed vitrinite reflectance for Neogene petroleum source rocks of Japan. *Am. Assoc. Pet. Geol. Bull.* 88, 1335–1356.
- Unconventional Oil & Gas Report, 2014a. Goodrich ramps up Tuscaloosa activity. *Unconventional Oil & Gas Report*. 2 (4), 14.
- Unconventional Oil & Gas Report, 2014b. Goodrich seeks to optimize drilling, completion recipe in complex Tuscaloosa marine shale. *Unconv. Oil Gas Rep.* 2 (3), 18–19.
- Unconventional Oil & Gas Report, 2015. Tuscaloosa marine shale pinched by low oil prices. *Unconv. Oil Gas Rep.* 3 (1), 25.
- Uguna, C.N., Carr, A.D., Snape, C.E., Meredith, W., Scotchman, I.C., Murray, A., Vane, C.H., 2016. Impact of high water pressure on oil generation and maturation in Kimmeridge Clay and Monterey source rocks: implications for petroleum retention and gas generation in shale gas systems. *Mar. Pet. Geol.* 73, 72–85.
- Utting, J., Zonneveld, J.P., MacNaughton, R.B., Fallas, K.M., 2005. Palynostratigraphy, lithostratigraphy and thermal maturity of the Lower Triassic Toad and Grayling, and Montney Formations of western Canada, and comparisons with coeval rocks of the Sverdrup Basin, Nunavut. *Bull. Can. Petrol. Geol.* 53, 5–24.
- Valentine, B.J., Hackley, P.C., Enomoto, C.B., Bove, A.M., Dulong, F.T., Lohr, C.D., Scott, K.R., 2014. Organic petrology of the Aptian section in the downip Mississippi Interior Salt Basin, Mississippi, USA: observations and preliminary implications for thermal maturation history. *Int. J. Coal Geol.* 131, 378–391.
- Valentine, B.J., Hackley, P.C., Enomoto, C.B., Scholl, O.D., Lohr, C.D., 2015. Preliminary thermal maturity and organic petrology of the Upper Cretaceous Tuscaloosa Marine Shale, Mississippi, USA. *Geological Society of America Abstracts with Programs*, Baltimore, Maryland, November 1–4, 2015, v. 47, no. 7, p. 455 <https://gsa.confex.com/gsa/2015AM/webprogram/Paper265264.html> (Accessed January 26, 2015).
- Valentine, B.J., Morrissey, E.A., Park, A.J., Reidy, M.E., Hackley, P.C., 2013. Development of web-based organic petrology photomicrograph atlases and internet resources for professionals and students. *Int. J. Coal Geol.* 111, 106–111.
- Valenza, J.J., Drenek, N., Marques, F., Pagels, M., Mastalerz, M., 2013. Geochemical controls on shale microstructure. *Geology* 41, 611–614.
- Vandenbroucke, M., Largeau, C., 2007. Kerogen origin, evolution and structure. *Org. Geochem.* 38, 719–833.
- Van de Wetering, N., Mayer, B., Sanei, H., 2015. Chemostratigraphic associations between trace elements and organic parameters within the Duvernay Formation, Western Canada Sedimentary Basin. *Unconventional Resources Technology Conference Paper URTeC 2153955* (11 p).
- Van de Wetering, N., Sanei, H., Mayer, B., 2016. Organic matter characterization in mixed hydrocarbon producing areas within the Duvernay Formation, Western Canada Sedimentary Basin. *Int. J. Coal Geol.* 156, 1–11.
- van Gijzel, P., 1981. Applications of the geomicrophotometry of kerogen, solid hydrocarbons and crude oils to petroleum exploration. In: Brooks, J. (Ed.), *Organic Maturation Studies and Fossil Fuel Exploration*. Academic Press, London, pp. 351–377.
- van Krevelen, D.W., 1993. *Coal: Typology, Physics, Chemistry, Constitution*. third ed. Elsevier, Amsterdam (979 pp).
- Varol, Ö.N., Demirel, I.H., Rickards, R.B., Günay, Y., 2006. Source rock characteristics and biostratigraphy of the Lower Silurian (Telychian) organic-rich shales at Akyaka, central Taurus region, Turkey. *Mar. Pet. Geol.* 23, 901–911.
- Walls, J.D., Morcote, A., 2015. Quantifying variability of reservoir properties from a Wolfcamp Formation core. *Unconv. Res. Technol. Conf. URTeC 2154633* (9 p).
- Walls, J.D., Sinclair, S.W., 2011. Eagle Ford shale reservoir properties from digital rock physics. *First Break* 29, 97–101 http://www.ingrainrocks.com/media/files/None/FB_EagleRock_June2011.pdf (accessed August 9, 2015).
- Wang, F.P., Gale, J.F.W., 2009. Screening Criteria for Shale–Gas Systems: Gulf Coast Association of Geological Societies Transactions 59, pp. 779–793.
- Wang, Y., Zhu, Y., Liu, S., Zhang, R., 2016. Methane adsorption measurements and modeling for organic-rich marine shale samples. *Fuel* 172, 301–309.
- Ward, C.R., Li, Z., Gurba, L.W., 2007. Variations in elemental composition of macerals with vitrinite reflectance and organic sulfur in the Greta Coal Measures, New South Wales, Australia. *Int. J. Coal Geol.* 69, 205–219.
- Wei, L., Mastalerz, M., Schimmelmann, A., Chen, Y., 2014. Influence of Soxhlet-extractable bitumen and oil on porosity in thermally maturing organic-rich shales. *Int. J. Coal Geol.* 132, 38–50.
- Wenger, L.M., Baker, D.R., 1987. Variations in vitrinite reflectance with organic facies—examples from Pennsylvanian cyclothem of the midcontinent, U.S.A. *Org. Geochem.* 11, 411–416.
- Wilkins, R.W.T., Boudou, R., Sherwood, N., Xiao, X., 2014. Thermal maturity evaluation from inertinites by Raman spectroscopy: the RaMM technique. *Int. J. Coal Geol.* 128–129, 143–152.
- Wilkins, R.W.T., Diessel, C.F.K., Buckingham, C.P., 2002. Comparison of two petrographic methods for determining the degree of anomalous vitrinite reflectance. *Int. J. Coal Geol.* 52, 45–62.
- Wilkins, R.W.T., Wang, M., Gan, H., Li, Z., 2015. A RaMM study of thermal maturity of dispersed organic matter in marine source rocks. *Int. J. Coal Geol.* 150–151, 252–264.
- Wilkins, R.W.T., Wilmhurst, J.R., Russell, N.J., Hladky, G., Ellacott, M.V., Buckingham, C., 1992. Fluorescence alteration and the suppression of vitrinite reflectance. *Org. Geochem.* 18, 629–640.
- Wood, J.M., Sanei, H., Curtis, M.E., Clarkson, C.R., 2015. Solid bitumen as a determinant of reservoir quality in an unconventional tight gas siltstone play. *Int. J. Coal Geol.* 150–151, 287–295.
- Wrightstone, G., 2009. Marcellus shale: geologic controls on production. *American Association of Petroleum Geologists Search and Discovery Article No. 10206* (10 p.) <http://www.searchanddiscovery.com/documents/2009/10206wrightstone/images/wrightstone.pdf> (Accessed May 22, 2016).
- Wüst, R.A., Hackley, P.C., Nassichuk, B.R., Willment, N., Brezovski, R., 2013a. Vitrinite reflectance versus pyrolysis T_{max} data: assessing thermal maturity in shale plays with special reference to the Duvernay shale play of the Western Canadian Sedimentary Basin, Alberta, Canada. *Society of Petroleum Engineers Unconventional Resources Conference and Exhibition Paper 167013*, Asia Pacific, Brisbane, Australia, 11–13 November 2013 (11 p).
- Wüst, R.A., Nassichuk, B.R., Bustin, R.M., 2013b. Porosity characterization of various organic-rich shales from the Western Canadian Sedimentary Basin, Alberta and British Columbia, Canada. In: Camp, W., Diaz, E., Wawak, B. (Eds.), *Electron Microscopy of Shale Hydrocarbon Reservoirs Vol. 102*. AAPG Memoir, pp. 81–100.
- Wüst, R.A.J., Willment, N., Nassichuk, B., 2015. Unconventional shale play stand-off in Alberta: Duvernay Formation versus Nordegg Member: stratigraphy, rock properties, depositional settings. *GeoConvention 2015: Geoscience New Horizons* (abs), Calgary, Alberta, May 4–8, 2015 http://www.geoconvention.com/archives/2015/267_GC2015_Unconventional_Shale_Play_Stand-Off_in_Alberta.pdf (Accessed February 29, 2016).
- Xiao, X., Wilkins, R.W.T., Liu, D., Liu, Z., Fu, J., 2000. Investigation of thermal maturity of lower Paleozoic hydrocarbon source rocks by means of vitrinite-like maceral reflectance: a Tarim Basin case study. *Org. Geochem.* 31, 1041–1052.
- Xiao, X., Wilkins, R.W.T., Liu, D., Liu, Z., Shen, J., 2002. Laser-induced fluorescence microscopy-application to possible high rank and carbonate source rocks. *Int. J. Coal Geol.* 51, 129–141.
- Xiong, F., Jian, Z., Chen, J., Wang, X., Huang, Z., Liu, G., Chen, F., Li, Y., Chen, L., Zhang, L., 2016. The role of the residual bitumen in the gas storage capacity of mature lacustrine shale: a case study of the Triassic Yanchang shale, Ordos Basin, China. *Mar. Pet. Geol.* 69, 205–215.
- Zargari, S., Canter, K.L., Prasad, M., 2015. Porosity evolution in oil-prone source rocks. *Fuel* 153, 110–117.
- Zdanaviciūtė, O., Lazauskienė, J., 2009. Organic matter of Early Silurian succession: the potential source of unconventional gas in the Baltic Basin (Lithuania). *Baltica* 22, 89–99.
- Zhang, T., Ellis, G.S., Ruppel, S.C., Milliken, K., Yang, R., 2012. Effect of organic-matter type and thermal maturity on methane adsorption in shale-gas systems. *Org. Geochem.* 47, 120–131.
- Zhou, Q., Xiao, X., Pan, L., Tian, H., 2014. The relationship between micro-Raman spectral parameters and reflectance of solid bitumen. *Int. J. Coal Geol.* 121, 19–25.
- Zielinski, R.E., McIver, R.D., 1982. Resource and exploration assessment of the oil and gas potential in the Devonian gas shales of the Appalachian Basin MLM-MU-82-61-0002, DOE/DP/0053-1125, 1982. (326 p).
- Zuckerman, G., 2013. *The Frackers: The Outrageous Inside Story of the New Billionaire Wildcatters*. Penguin (432 p).